VOLUMETRIC ANALYSIS OF THE ALVEOLAR HOUSING AROUND THE MANDIBULAR INCISORS IN RESPONSE TO CLASS II ORTHODONTIC CORRECTION

by

Kevin Chen

A thesis submitted in partial fulfillment of the requirements for the degree of

Master of Science

Medical Sciences - Orthodontics
University of Alberta

Abstract

Introduction: The use of Cone-Beam Computed Tomography (CBCT) in clinical practice has seen a rise in recent years. Its usefulness as a diagnostic adjunct to traditional imaging modalities is undeniable, especially in orthognathic surgery planning, temporomandibular joint imaging, and in locating ectopically positioned teeth. CBCTs have also been used in the literature to study changes in response to growth and treatment. The primary objective of this study was to evaluate the volumetric response of the bony alveolus around the mandibular incisors to orthodontic camouflage in growing patients with mild to moderate Class II Division 1 malocclusions. Prognostic factors including vertical face height, lower incisor proclination, and appliance type were used to predict alveolar response. The secondary objective was to determine changes in incisor inclination as a result of Forsus™ and Xbow® application.

Methods: The sample consisted of 43 growing patients with mild to moderate Class II Division 1 malocclusions (17 males and 26 females, mean age 13.53 $\pm$ 1.18 years). Each participant was randomly assigned to either Forsus™ group (N = 23) or the Xbow® group (N = 20). Pre-treatment (T_1) and post-treatment (T_2) records were collected in both groups including a full FOV CBCT scan, dental casts, intra- and extra-oral photos. Teeth 3.3-4.3 were segmented along with the anterior half of the bony mandible, and virtual models generated using ITK-SNAP, version 3.6. Based on landmarks which included the left and right mental foramen and B-point, 2 sagittal and 1 axial plane were created in SlicerCMF. These were used to define the boundaries of the region of interest, and the volumes were subsequently quantified. Mandibular incisor inclination (pitch) was also measured with respect to the defined axial plane. Six patients from the sample pool were randomly selected to validate and determine the reliability of the method using Intra-class Correlation Coefficient (ICC).

Results: Intra-rater and inter-rater reliability was good (ICC>0.75). The median increase of the alveolar housing was 4.55% ($p<0.05$) which was similar to the mean, 4.89%. There was some evidence that incisor proclination was predictive of the alveolar response ($p<0.05$). An inverse linear relationship was noted ($R^2 = 0.11$) based on a simplified multiple linear regression model.

Proclination of incisors >10.93° increased the likelihood of alveolar bone loss (95% confidence interval). Appliance type and vertical face height were not predictive of alveolar response. The average proclination of all of the mandibular incisors was $9.01° \pm 8.74°$ ($p < 0.05$). There was no difference in average proclination between treatment groups, and all incisors proclined a similar amount ($p > 0.05$).

Conclusions: In response to Class II correction, the overall volume of the alveolar bone increased in both treatment groups. Increasing incisor proclination was associated with decreasing alveolar volumes. Both Xbow® and Forsus™ appliances caused a similar proclination of the lower incisors. This study presented with significant limitations that may limit the clinical applicability of its conclusions.

"Besides being complicated,
reality, in my experience, is usually odd.
It is not neat, not obvious, not what you expect."
-C. S. Lewis

Acknowledgements

My sincerest gratitude to Dr. Carlos Flores-Mir, the conceiver of this project and my supervisor. His guidance, insight, patience, and flexibility were instrumental to the completion of this thesis. Despite his vast wealth of knowledge in the subject area, his humility and compassion were apparent throughout the three short years we spent together. Thank you, Dr. Carlos, for your kind instruction and generosity. You are a person of great character, and a benchmark that I hope to follow both personally and professionally. It is with honour I call you my teacher, mentor, and friend.

To my committee members Dr. Manuel Lagravere-Vich and Dr. Neel Kaipatur, many thanks for continually steering me in the right direction, and for providing me with constructive comments and feedback from a multidisciplinary perspective. I really appreciated both of your guidance, especially during times when I was truly lost. I am grateful to my external examiner Dr. Husniye Demirturk for your impartiality and kindness during my thesis examination. Your feedback and expertise was greatly appreciated, and without any doubt improved the quality of my work.

Without the instruction and mentorship of Dr. Giseon Heo, the monumental task of making sense of my data would have been impossible. I have gained a newfound appreciation for the intricacies and complexities of research methodology from a statistical perspective. Despite the monumental task of conveying the basic concepts of statistics to clinicians who perhaps have little affinity for it, Dr. Heo was able to break down difficult concepts into palatable components even if it meant sacrificing her personal time.

I am indebted to the clinical faculty for their generous instruction and dedication towards the future of orthodontics. I thank them for not only the hours of mentorship during seminar and clinic, but also for the personal time they have invested in us, some commuting monthly from as far away as Calgary. I also thank Dr. Paul Major and Dr. Tarek El-Bialy for their mentorship and instruction; for challenging us to be better and more competent clinicians. Thank you to the clinical support staff as well for their guidance and help, especially during long and challenging days, and for fostering a safe and friendly environment for learning. Deserving of particular mention is the radiology staff, and much appreciation to them for their work in collecting and preparing the DICOM images from the patient database.

Among my colleagues and friends, I want to particularly acknowledge my classmates Dr. Anthony Rossi and Dr. Gaston Coutsiers Morell. I could not have asked to be part of a better class. Thank you both for allowing me to learn from you and for your support through these challenging but rewarding three years.

I cannot thank my friends and family enough for their support over the last three years. To Dr. Francisco Plaza Villegas, my friend and mentor, my journey in orthodontics could not have been possible without your support. From my time as a dental student at the University of Detroit Mercy, to the time we spent in California together, and to the countless reference letters you have written for me, I owe you an enormous debt of gratitude for all you have done. To my supportive and wonderful parents, words cannot express how much I love you both and appreciate your support in all my endeavours. I am proud to be your son. To my loving and always supportive wife, Didi. There were many days, especially at the start of this program where I wanted to give up. Yet, your unconditional love, support and encouragement saw me through many sleepless nights. My heart is warmer and fuller, and my life more complete with you by my side.

Contents

List of Figures

Appendix B

List of Tables

Nomenclature

Acronyms

$\%\Delta V_{alv}$	Percentage change in the alveolar volume pre- to post- treatment. Refer to Equation (4.2)
$\overline{\Delta IC}$	The average change in inclination of all mandibular incisors from pre- to post-treatment. Refer to Equation (4.1)
$\overline{IC}$	Average inclination of all four mandibular incisors as measured in 3-dimensions relative to a reference plane defined by B-point and the left and right mental foramen
T_1	Initial Time Point, pre-treatment during initial records
T_2	Final Time Point, post-treatment at deband
V_{alv}	The measured alveolar volume around the mandibular incisors as defined by the region of interest (refer to Section 2.2.5)
AAOMR	American Academy of Oral and Maxillofacial Radiology
AJO-DO	American Journal of Orthodontics and Dentofacial Orthopedics
ALARA	As Low As Reasonably Achievable
ANOVA	Analysis of Variance
App	Appliance Type (i.e. Forsus™ and Xbow®)
CAD-CAM	Computer Aided Design, Computer Aided, Manufacturing
CBCT	Cone-beam Computed Tomography
CONSORT	Consolidated Standards of Reporting Trials
DICOM	Digital Imaging and Communications in Medicine
FMA	Frankfort-Mandibular Plane Angle
FOV	Field of view

Full FOV	Full Field of View Scan, defined as 16.0cm in diameter and a height of 13.3cm
ICC	Intraclass Correlation Coefficient
IMPA	Lower Incisor Mandibular Plane Angle
LiA	Lower Incisor Root Apex
LiT	Lower Incisor Crown Tip
MANOVA	Multivariate Analysis of Variance
MF	Mental Foramen
MLR	Multiple Linear Regression
PDL	Periodontal Ligament
ptB	B-point
ROI	Region of Interest
SN-MP	Sella-Nasion to Mandibular Plane Angle
TMD	Temporomandibular Joint Disorders
Xbow	Also known as the Higgins' Crossbow®

Chapter 1

Introduction

1.1 Introduction

The primary goal of orthodontics is to achieve a harmonious occlusion along with an esthetic balance from a facial and dental standpoint. Malocclusion can therefore result from skeletal or dental discrepancies, or a combination of both. Class II malocclusions manifest from a mismatch between maxillary and mandibular dentitions. In Class II malocclusions of skeletal etiology, the maxilla is positioned more anteriorly compared to the mandible resulting in a relative mandibular retrognathism. On the basis of facial esthetics, it is important to determine the relationship of both upper and lower jaws relative to the cranial base. Traditionally, clinicians have used a lateral cephalogram as well as extra-oral and intra-oral photography to optimize the treatment approach and prevent unwanted side-effects.

Regardless of the type of Class II correction, whether it be growth modification through the use of functional appliances or dental camouflage, some tooth movement will always be necessary to correct the molar relationship [7]. In patients with reasonable jaw relationships, such as those with mild to moderate Class II maxillo-mandibular relationships, tooth movement to compensate for the deficiency is reasonable provided that there will be very little impact esthetically. In general, dental correction of a mild to moderate Class II malocclusion occurs by distalization of the maxillary dentition, mesialization of the mandibular dentition, and often times a combination of both. This can be achieved by differential movement of the maxillary and mandibular dentition using extraction spaces, or it can proceed non-extraction by using intermaxillary Class II elastics or fixed Class II correctors [7].

Extraction versus non-extraction is a controversial topic in the field of orthodontics, and the debate has existed as long as the profession itself. Contemporary practitioners of orthodontics have been exposed to philosophies which favour a non-extractionist approach. Through transverse expansion and interproximal reduction as well as molar distalization approaches, some advocate for the avoidance of premolar extractions [8]. Nevertheless,

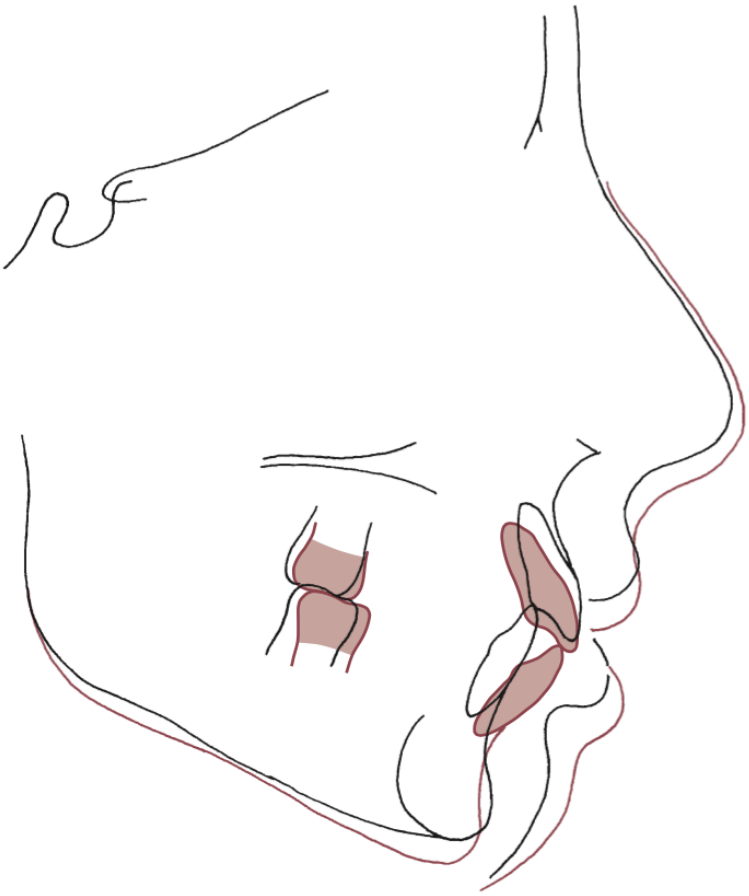

Figure 1.1: Cephalometric superimposition pre- to post- correction of Class II malocclusion. The black tracing represents pre-treatment and the red tracing, post-treatment. Note the significant amount of lower incisor proclination and protrusion along with mandibular and occlusal plane clockwise rotation post-correction. Figure 16.25 from Proffit et al. [7]

the decision to pursue non-extraction requires careful judgement regarding the extent of the anatomical limits set forth by the periodontal tissues [9]. All Class II correctors move the lower dentition anteriorly to some degree, thus proclining and protruding mandibular incisors potentially beyond boundaries set forth by the periodontium [7, 9]. Figure 1.1 is a superimposition of the effects of Class II correction. There has been much controversy regarding the relationship between certain orthodontic movements and the development of gingival recession given the low to moderate levels of evidence currently available in literature [10].

With wide availability and access to 3-dimensional CBCT imaging modalities, clinicians have employed this technology to their advantage. It has aided in the diagnosis and treatment planning of many clinical orthodontic conditions [7, 9, 11]. CBCT imaging

should provide a clear advantage over traditional radiographic techniques such as a panoramic and lateral cephalograms. There have been studies that have explored the use of CBCT in temporomandibular joint imaging, airway and its relationship to sleep disordered breathing, and tooth development and its relative position in alveolar bone. However, in the position statement by the American Academy of Oral and Maxillofacial Radiology (AAOMR), which is based on the "As Low As Reasonably Acceptable" (ALARA) principle, the use of CBCT is justified on a case by case basis and only in situations where this imaging modality provides a justifiable benefit over traditional radiographic modalities [12]. This is to reduce ionizing radiation burden to the patient, especially in the prototypical demographic of orthodontics patients. It is now recognized that young children and early adolescents demonstrate an increased susceptibility to ionizing radiation due to the rate of cellular growth and organ development [12]. Therefore, when considering which radiographic modality to use, the clinician must weigh the benefits of CBCT imaging modalities over lateral cephalograms and panoramic radiographs at the cost of potential increased radiation dose to the patient. In addition, the significant time and financial investment associated with CBCT implementation should not be understated.

Therefore, the motivation behind this study was to contribute to the discussion around indications for CBCT use in orthodontic diagnosis, and specifically on the topic of the alveolar response relative to mandibular incisor positioning. Previous studies have found justifiable scenarios for the use of small field of view (FOV) CBCT imaging in cases of ectopically erupting canines [13], dental impactions [14], orthognathic surgery [15], and temporomandibular joint disorders [16]. The use of CBCT imaging has seen a recent increase in use, and some have advocated for it as part of routine comprehensive diagnostic records. This is based on the fact that CBCT use can provide significantly more diagnostic information than a combination of traditional panoramic and lateral cephalograms [17]. One of the justifications for routine CBCT use is the detection of periodontal bone levels prior to the start of treatment in order to avoid unwanted recession. However, there have been few *in-vivo* studies on the ability of CBCT to detect bone levels, with most of the cited studies using *in-vitro* protocols [18–20]. Refer to Section 1.4 for further discussion on the role CBCT imaging modalities have played on the current understanding of the alveolar response to orthodontic movement of the mandibular incisors.

1.2 Review of Cone-Beam Computed Tomography (CBCT)

1.2.1 Fan-Beam Multi-Detector CT and CBCT [1, 2]

There are two types of computed tomography available for clinical use: fan-beam and cone-beam. As its name suggests, in fan-beam computed tomography (also known as axial CT) a narrow slice-based beam passes through the subject along the axial plane producing multiple two-dimensional axial slices, which are then stacked together to

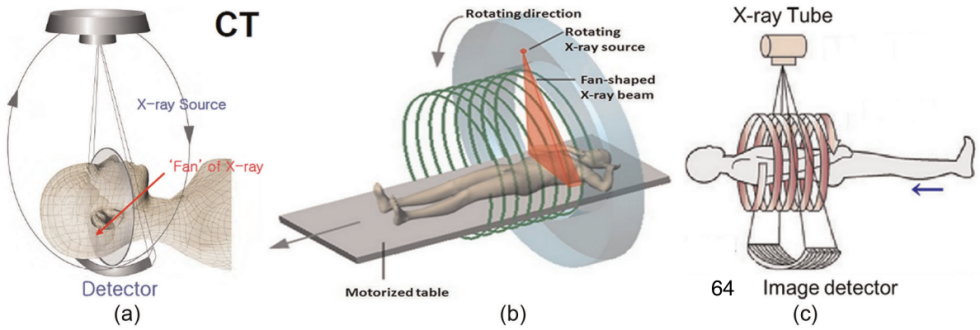

Figure 1.2: A schematic diagram of a multi-detector helical CT. (a) Schematic of a single slice CT detector. (b) A motorized table allows the patient to translate cephalo-caudally as the x-ray source continuously rotates around the target. (c) In the most advance fan-based system, 64 2D slices can be captured in one pass. Image taken and modified courtesy of Chen et al. [21].

produce three-dimensional representations. The most advanced fan-based systems employ helical multi-detectors which can allow capture of 64 2D slices in one pass of the fan beam. Therefore, this decreases exposure time and radiation dose. In the medical community, this has been the gold standard technique for obtaining 3D images; however, at increased imaging costs and radiation dose to the patient (Figure 1.2). Given that orthodontics is elective treatment, the use of high-resolution medical CT imaging may not be advisable.

With the advent of cone-beam computed tomography (CBCT), the cost of obtaining a 3D diagnostic image, especially for dental applications, has been reduced and the use of this imaging modality has thus become more pervasive in the dental community. A cone-beam or pyramidal-shaped divergent beam is directed through the area of interest and onto a detector on the opposite side. Both the detector and the source are mounted on a rotating mechanism, and in one rotation of the gantry is able to capture enough data for 3D image reconstruction (Figure 1.3).

1.2.2 Image Acquisition and Reconstruction [3, 4]

The construction of the final three-dimensional CBCT image can be broken down into two phases: image acquisition and image reconstruction. Image acquisition occurs similarly to conventional radiography, where the cathode is heated by a large current. This generates electrons which are attracted to a focal spot on the anode. The high energy bombardment at the anode, which is dependent on the potential difference between the cathode and the anode, causes the bombarding electrons to slow down due to collisions with the orbital electrons in the anode. With these collisions, there is excess energy released mainly as heat, with relatively small amounts of electromagnetic radiation (i.e. x-rays). X-radiation is scattered about with most being absorbed by shielding around the x-ray tube or by collimators. Only the beams directed at the aperture and towards the detector are ejected toward the subject (Figure 1.4).

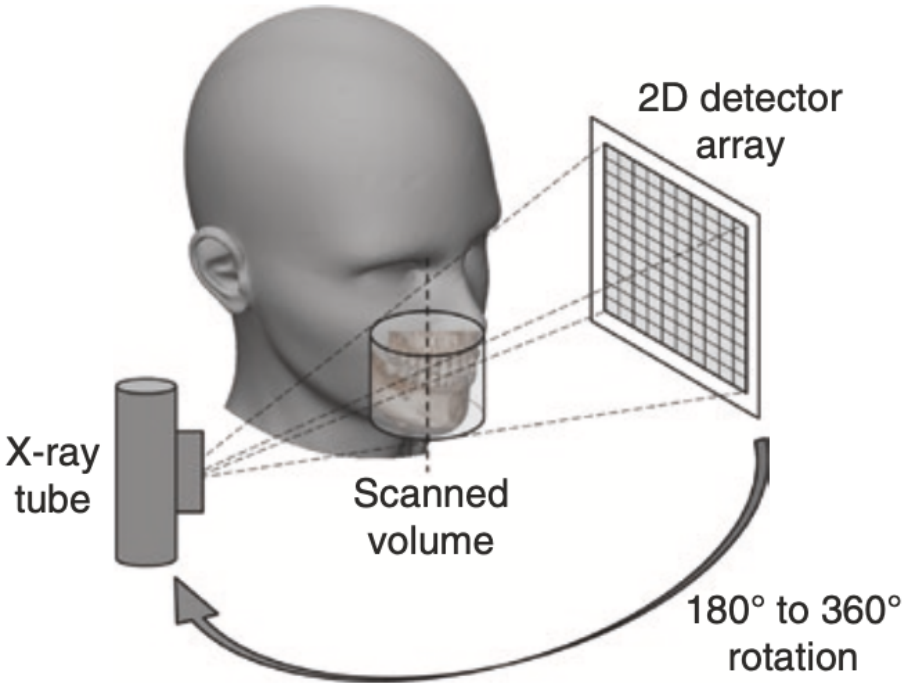

Figure 1.3: A schematic representation of CBCT image acquisition [3]. The dimension of the FOV is determined by the region of interest. A cone-beam or pyramidal shaped divergent beam is directed through the area of interest and onto a detector opposite to the source. During a single 180° to 360° rotation of the gantry, hundreds of static 2-dimensional images of the region of interest (ROI) is captured onto a flat 2D detector array.

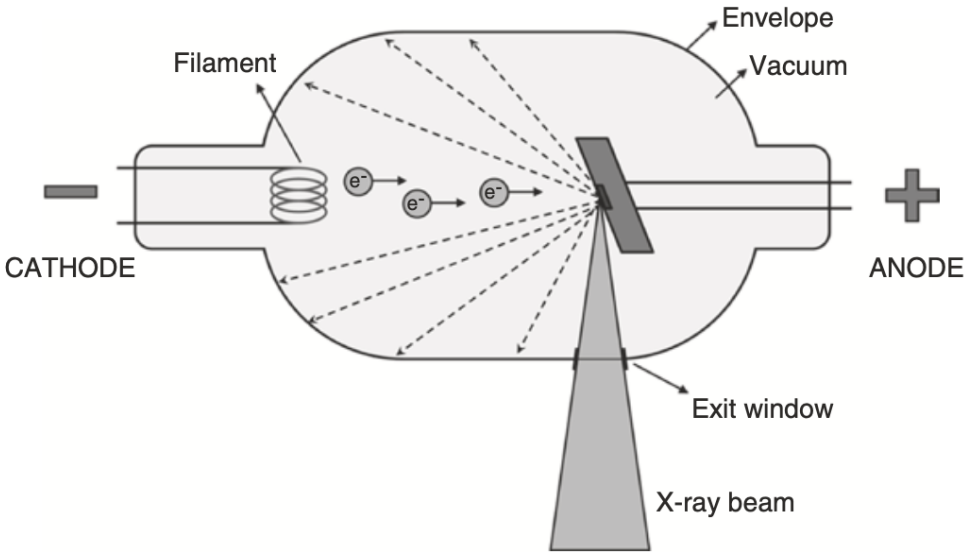

Figure 1.4: A schematic representation of the x-ray tube components [3]. Electrons are released from filaments in the cathode and ejected towards the focal spot in the anode. Part of the energy released are in the form of x-radiation (x-rays).

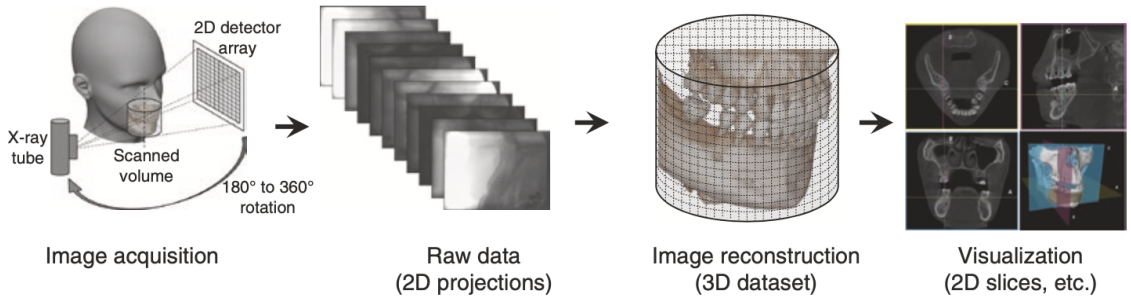

Figure 1.5: A schematic of the image acquisition and reconstruction process according to Pauwels et al. [3]. Multiple 2-dimensional projections are acquired which are known as basis projections (raw data). The raw data is then processed into 3-dimensional volumes composed of voxels. This is known as *primary reconstruction*. This is subsequently reformatted into orthogonal axial, sagittal and coronal slices (*secondary reconstruction*).

The field of view (FOV) is determined by physical collimation of the x-ray beam. During a single 180°-360°rotation of the gantry, hundreds of static 2-dimensional images of the region of interest (ROI) are produced at various horizontal angles. The detectors collect a charge proportional to the intensity of the x-ray beam it receives. Soft tissues which allow radiation to pass through appears more intense and darker than hard tissue which tends to block or scatter radiation. The physical pixel size of the detectors is an important property as it determines the detail and resolution of the CBCT image. Smaller detector pixel sizes lead to better spatial resolution but with increased noise. In addition, other factors such as voxel size of the final image can decrease spatial resolution as well.

Each raw projection, which are composed of pixels with assigned values according to the x-ray intensity, are together reconstructed into 3D volumetric data using software algorithms. The three-dimensional volumetric dataset is composed of cuboidal elements known as voxels. Slices in three planes of space, axial, coronal and sagittal are then created from the 3D dataset (refer to Figure 1.5). Image reconstruction is computationally demanding, and the amount of time required for processing is dependent on many factors including voxel size, FOV, and number of projections.

Finalized reconstructed CBCT images are composed of stacks of voxels, each assigned a grey value according to its estimated x-ray attenuation. Higher grey values represent greater estimated x-ray attenuation with a maximum value of 4096 (assuming a 12 bit scale). Unlike CBCT images, medical CT images using fan-shaped beams and multi-detectors can be calibrated to the Hounsfield units in which x-ray attenuation is compared to air and water. CBCT images cannot be calibrated to Hounsfield units due to a number of factors: high amounts of non-uniform x-ray scatter, beam hardening due to lower energy x-rays, distortion effects of tissue outside the field of view, and metal artifacts which are inherent to CBCT technique and maxillofacial imaging as a whole.

1.2.3 CBCT Image Quality [4, 5]

Overall, CBCT images provide good spatial resolution, owing to its use of small detector pixels and smaller image voxels. Unfortunately, CBCT images present with poor contrast resolution due to radiation scatter, smaller detector pixels, and lower tube output (kV) compared to medical CT. Therefore, CBCT are generally noisier than their medical counterpart.

Image quality can be defined by four parameters which include contrast resolution, spatial resolution, noise, and artifacts. CBCTs in general have good spatial resolution and poor contrast resolution, and are susceptible to noise and artifacts. Spatial resolution, also known as sharpness, is the ability to discern fine detail, or the ability to distinguish two objects that are close together in 3D space.

Spatial resolution is related to the voxel size, where the smaller the voxel size the greater the spatial resolution. According to the manufacturer's technical specifications, CBCTs can reconstruct voxel sizes anywhere from 0.07mm to 0.6mm. Realistically, the effective spatial resolution is always diminished due to technical limitations as well as inevitable patient motion during exposure. Theoretically, if computational resources were limitless, smaller voxel sizes can be calculated from large FOV scans. This in turn increases spatial resolution. However, computational limitations do not allow voxel sizes which are calculated from large FOV to be smaller than those calculated from smaller FOV. There is a maximum geometric resolution for a given projection geometry and FOV. A threshold exists where the voxel size matches the detector pixel size. Lowering the voxel size beyond this threshold is redundant and does not provide additional information. Apart from voxel sizes, the reconstructed spatial resolution is also strongly determined by pixel density at the detector, and fill factor. The fill factor is the area of radiosensitive elements to the total pixel area. Other factors that can affect spatial resolution include patient motion, focal spot size, beam geometry, scatter, and the reconstruction algorithm. According to Brullmann and Schulze [5], considering the presence of patient motion, a true spatial resolution between 0.3mm and 0.5mm is realistic.

Contrast resolution refers to the ability to discern two objects based on differences in attenuation and thus differences in radiodensity. It also depends on the ability for the difference in attenuation to be displayed with different grey levels. Contrast resolution in CBCT imaging is limited compared to medical CT modalities. This is due to the inherent geometric limitations of CBCT, which results in higher amounts of radiation scatter because of short object to detector distance, and low tube output (i.e kV and mAs).

Noise is defined as the variation in grey values in an object that is of uniform density, and is the result of relatively low tube output, x-ray scatter, and random x-ray interaction with the detector. The detector itself also causes electronic noise during signal transmission which further exacerbates noise.

Artifacts can be generally defined as a mismatch between the grey values as represented

on the acquired image and the true attenuation values of the subject in question [22]. In other words, it can be any discrepancy that appear in an acquired image that is unrelated to the subject. Artifacts occur due to inaccuracies with the physical properties of the CBCT unit itself, and the mechanism by which images are generated. For the example, the circular orbit of the acquisition mechanism itself results in the generation of artifacts. According to Hsieh [22], artifacts can be classified based on their appearance in the image, or based on where they occur in the image acquisition chain. Based on their appearance, artifacts can include streaks, shadings and rings or bands. Patient-related artifacts include patient motion, which results in a "double contour" appearance. Subtle motion results in blurring or unsharpness of the image. Patient motion can be minimized by decreasing the exposure time, at the cost of resolution, or using physical restraints. Scanner-related artifacts usually presents as circular or concentric dark rings in the axial plane, centred around the axis of rotation. They can result from poor calibration of the CBCT machine or from beam-related artifacts as they pass through materials with varying densities (i.e. radiation scatter and beam hardening).

1.2.3.1 Partial Volume Averaging

Partial volume averaging is important in order to understanding how objects smaller than the size of a voxel can be inaccurately represented in the image [23]. A voxel is discreet and represents one grey value. Any object that is less than its dimensions will have its grey value averaged with the adjacent material. That voxel will not accurately represent the grey value of the object in question, making boundaries between densities harder to discern, and effectively decreasing spatial resolution. Figure 1.6 is an example where partial volume averaging has created the false appearance of a communication between the anterior cranial fossa and the maxillary sinus [24]. The effect of partial volume averaging is more pronounced in areas of thin bone and has been well documented in conventional CT modalities [25].

1.3 Position of the Mandibular Incisors in Bone and the Response of the Surrounding Periodontium to Tooth Movements

Gingival recession results in increased root sensitivity, root caries, and inadequate periodontal support. This leads to eventual tooth mobility and loss. Recession also results in unacceptable esthetics. Repair of these defects are often difficult and unpredictable. [26, 27]. The subsequent sections aim to provide a brief survey of the literature regarding the relationship between orthodontic movement and the response of the periodontium, with a particular focus on the bony housing adjacent to the mandibular incisors. As previously mentioned, all Class II correctors procline and bodily move mandibular incisors anteriorly [7, 9]. To this end, the rest of the chapter will highlight the effects of the

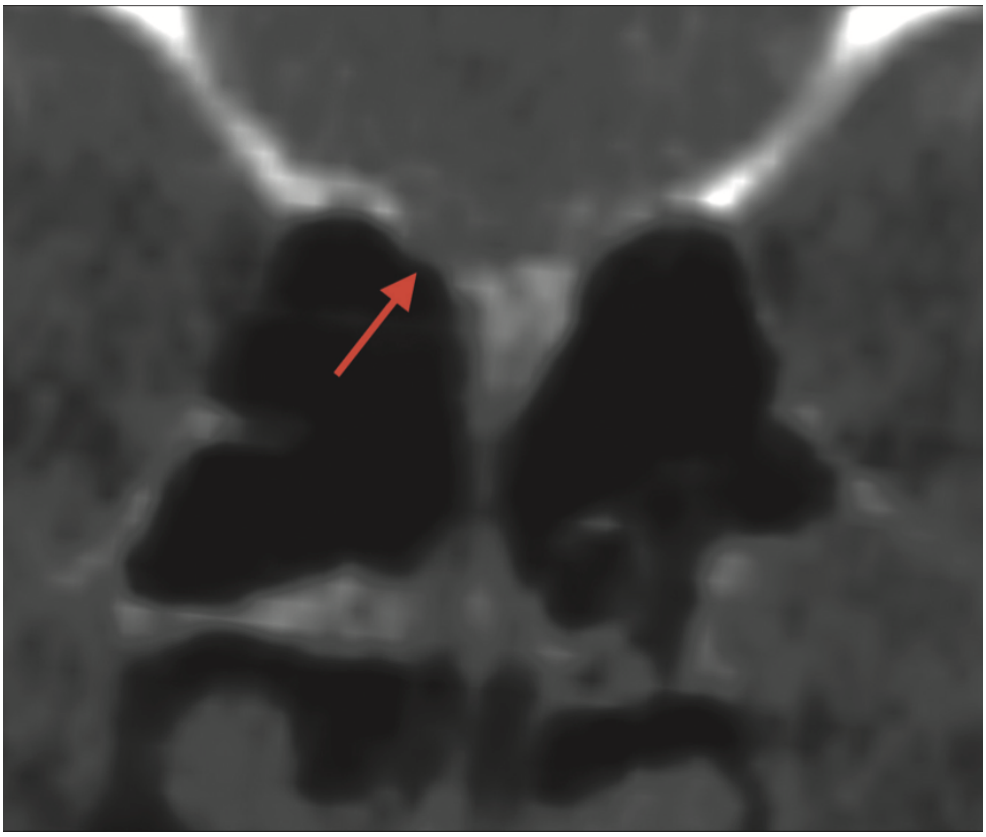

Figure 1.6: Example of partial volume averaging on thin cortical bone [24]. There is a false communication between the anterior cranial fossa and the maxillary sinus (red arrow) due to the partial volume averaging effect.

periodontal response around the mandibular incisors.

1.3.1 Early Animal Studies

Iatrogenically-induced gingival recession associated with orthodontic movement has been controversial in the literature; specifically, whether the movement of mandibular incisors beyond the anatomical boundaries leads to this unwanted result. Early animal studies by Wennström et al. [28], Thilander et al. [29] showed that bony dehiscences and fenestrations occurred when teeth were moved beyond the alveolar bone, but the connective tissue attachment was not necessarily lost. In a later study by the same authors, they concluded that the rate of connective tissue destruction may be enhanced by orthodontic movement, especially into an infrabony defect at sites with plaque-induced gingival inflammation [30]. In a study on monkeys, Batenhorst et al. [31] found the development of bony dehiscences when incisors were tipped facially and extruded. This was accompanied by apical migration of the connective tissue and subsequent gingival recession. Steiner et al. [32] confirmed these findings in their study on monkeys. When they moved maxillary and mandibular central incisors bodily through labial bone, significant gingival recession, connective tissue attachment loss, and loss of crestal bone integrity occurred. However, Wingard and Bowers [33] found no dehiscences or bone loss in monkeys when incisors were moved facially. Similarly, Ericsson and Thilander [34] study with beagle dogs found no detrimental effects in sites lacking gingival inflammation, even in areas with remarkable loss of periodontal support.

1.3.2 Human Studies

Contradictory results have been presented in the literature associating the forward movement of incisors and apical displacement of periodontal tissues. In one of the early studies on this matter, Dorfman [26] suggested that in a small percentage of his sample (1.8%), there was decreased attached keratinized tissue even with minimal change to the incisors. He concluded that inadequate initial width of keratinized tissue, between 0 to 2mm, could compromise periodontal health overtime with the movement of lower incisors. In a small adolescent cohort with Class II division 1 malocclusion, Hollender et al. [35] showed that there was significant reduction in marginal bone height in the maxilla, but not in the mandible. Interestingly, there was no difference in clinical crown height in the upper, but an increase in clinical crown height in the lower. The author suggested that the clinical crown height increase was due to natural growth, and the contradictory result in the maxilla could be explained by gingival hypertrophy which occurred as part of fixed appliance therapy. An important point to note was that the marginal bone loss was only shown to be 0.3mm, which may not have any significant clinical implications [35]. Årtun and Krogstad [36] looked at changes in clinical crown height as well as visual classification of gingival recession using coloured slides between pre- and post-treatment.

They found significant increases in clinical crown heights and gingival recession in patients with significant incisor proclination.

More recent clinical studies have shown that this relationship may not exist; at least, the relationship between incisor movement and gingival recession may not be a simple cause and effect relationship. Ruf et al. [37] surveyed 98 children undergoing therapy with a Herbst appliance. In total 392 lower incisors were studied, and incisor proclination post-treatment was confirmed (mean=8.9°). 97% of the enrollees developed no recession or no worsening recession. Therefore no relationship was seen between lower incisor inclination and the development of recession. In a retrospective study, Djeu et al. [38] looked at the records of 67 patients pre- to post-treatment and found no correlation between incisor proclination and gingival recession. In another similar study, Årtun and Grobéty [39] found no evidence of increased gingival recession in dento-alveolar mandibular retrusive patients. Melsen and Allais [40] looked at a clinical sample of 150 adult patients treated with fixed appliances. 2.8% of the patients developed recession greater than 2mm. In 5% of the participants, their pre-existing recession actually improved. The study concluded that there was no link between orthodontic factors, such as incisor inclination, and the development of recession in a biomechanically and periodontally controlled environment. However, the presence of plaque induced gingival inflammation, thin width of attached gingiva, and thin gingival biotype could not be ruled out as risk factors for development of dehiscences. Renkema et al. [41] looked at 117 subjects retrospectively and divided them into two groups based on the final incisor inclination, <95°and >100.5°. Clinical crown heights as well as plaster models were analyzed to determine the presence of gingival recession. It was found that the proclination of mandibular incisors did not increase the risk of developing gingival recession.

1.3.3 Review of the Current Understanding of the Periodontal Response

In a recent systematic review of the relationship between appliance-induced labial movement of mandibular incisors and gingival recession [42], ten retrospective studies were selected that fit the inclusion criteria. None of the studies randomized patients to treatment or control. Six of the ten studies found no relationship between labial movement of mandibular incisors and gingival recession. The review concluded that most of the studies had methodological limitations in their outcome measures. This included assessing clinical crown heights from dental casts, a questionable method as it assumes no extrusion or eruption of teeth, or absence of dental restorations. In another systematic review [43] which included both retrospective human and animal studies, no significant correlation was reported between the development of gingival recession and the amount of incisor proclination, width of attached gingival tissue, oral hygiene, periodontal condition, or the thickness of the symphysis. They pointed out that the included studies were considered low level of evidence. More randomized clinical trials looking at gingival and periodontal

conditions before, during, and after treatment were needed in order to clarify associations between incisor proclination and gingival recession.

Kapila et al. [44] defined the term *alveolar boundary conditions* as the depth, height, and morphology of the alveolar bone relative to tooth root dimensions, angulations, and spatial conditions. They are not only defined by their parameters pre-treatment, but also their adaptability during orthodontic treatment, and the morphology of the dentoalveolar complex post-treatment. Alveolar boundary conditions are dynamic, as the alveolus is allowed to remodel in response to tooth movement. Without this mechanism, orthodontic treatment would not be possible. Conversely, applying inappropriate forces can affect it negatively resulting in dehiscences and fenestrations [27].

1.3.4 Response to Fixed Class II Correctors

A non-extraction orthodontic treatment plan for Class II camouflage may include the distal movement of the upper dentition. However, the clinical predictability of this option has been called into question. This is especially the case without the use of temporary skeletal anchorage devices, or extraction of the distal most tooth in the dentition [7].

A second non-extraction option consists primarily of forward movement of the lower dentition. According to Proffit et al. [7], this comes at a cost of potential significant mandibular incisor protrusion. This may not necessarily be associated with gingival recession (Section 1.3.3). Two popular fixed Class II corrector appliances used are currently the Forsus™ springs (3M, Saint Paul, MN) and Xbow® appliance (Duncan Higgins, Delta, BC, Canada).

Xbow® is often used as phase 1 treatment in late mixed to early permanent dentition with the goal of early antero-posterior and maxillary transverse correction before the use of full fixed appliances (Figure 1.7a). Flores-Mir et al. [45] found that the lower incisors proclined an average of 3.6° compared with a matched control group. Similarly, lower incisor protrusion relative to pogonion was found to be 1.4mm greater than control. When comparing Forsus™(Figure 1.7b) to Xbow®, both appliances produced similar effects on the lower incisors, proclining them an average of 3.4° and 4.8° respectively [46]. Given similar dental effects between Xbow® and Forsus™, the advantages of one over the other seems to be time spent in active full fixed appliances and potential total treatment time. Miller et al. [46] suggested that when comparing Xbow® and Forsus™, mean treatment time was on average approximately 6 months less ($p < 0.05$) when using Xbow®, and also averaged 10 fewer months in full fixed appliances than Forsus™. It appears that functional appliances, such as the Herbst, also result in significant proclination and protrusion of the mandibular anterior dentition [45, 47, 48].

A functional appliance is any appliance that holds the mandible forwards in cases of mandibular deficiency. This stimulates the growth of the mandible and forward remodelling of the glenoid fossa, resulting in improved facial esthetics. The profile is

less convex resulting in an improved subjective perception of beauty [7]. The Herbst appliance tends to be popular in clinical use given its fixed design, as it removes the need for good patient compliance. A telescoping mechanism connecting the maxillary molar to a soldered arm in the area of the mandibular premolar keeps the mandible in a continuously protruded position. However, this compliance-free mechanism comes at the cost of potential appliance breakage and increased emergency appointments [49]. Pancherz and Fackel [50] conducted a long-term study of Class II malocclusions treated with Herbst appliances. Interestingly, a temporary acceleration of growth was noted. Compared to the control group, the final size of the mandible remained roughly the same as the untreated group. Momentary acceleration of growth occurred during the use of functional appliances. However, decreased growth compared to control was observed once the functional appliance was removed. This resulted in no net improvement in mandibular body length [7]. In a randomized control trial conducted by the University of North Carolina, early pre-adolescent treatment with headgear or functional appliance was compared with one phase treatment, commencing near the peak of adolescent growth [7, 51]. The authors concluded that skeletal changes produced by early treatment was negated by subsequent growth in phase 2 treatment. At the end of phase 2, alignment and occlusion was similar in patients who received early treatment compared with those that did not. Therefore ,the skeletal effect achieved in early treatment contributed very little to the overall result. Early treatment did not reduce the need for extractions or surgery. The duration of phase 2 treatment was the same for both groups. The authors' conclusion was that for most patients, there was little advantage to treat early. A survey of literature concluded that all Class II correctors, regardless of orthopedic effect, correct Class II malocclusions by varying degrees of dental movement. This includes combinations of maxillary distalization and molar distal tipping, mandibular mesialization, incisor protrusion, as well as rotation of the occlusal plane clockwise [7, 45, 49, 52]. Given the minute perceived skeletal gain of functional appliances, and similar dental mechanisms by which Class II malocclusions are corrected, the choice of which class II corrector to prescribe is due to clinician and patient preference.

1.4 The Role of CBCT in the Study of Alveolar Response

Attempts to validate linear and volumetric accuracy and precision of 3-dimensional measurements using CBCT imaging have been successful *in-vitro*. Lagravère et al. [53] showed that CBCT imaging was able to detect and accurately locate landmarks on a 3-dimensional coordinate system. When markers were placed on a synthetic mandible, the precision between CBCT images and the coordinate measuring machine was nearly perfect, with no detectable differences between the two methods ($p > 0.05$). Another comparison of linear measurements between on mandibular casts and CBCT images found no statistical difference between the two methods. No measurements that deviated more

(a) An example of a Xbow® appliance taken from Flores-Mir et al. [45]. The appliance consists of an upper expander and a lower holding arch with a labial bow. Forsus™ springs are attached bilaterally for antero-posterior correction. The use of Gurin locks along the labial bow allow for reactivation of the appliance without the need for longer push rods or shims.

(b) An example of a Forsus™ appliance. It is used in conjunction with fixed appliances to aid in the correction of a Class II malocclusion.

Figure 1.7: Examples of Xbow® and Forsus™ appliances

than 0.59mm $\pm$ 0.38mm [54]. Naji et al. [55] used 30 CBCT images to demonstrate that landmarking using clinical CBCT records were reliable within and between examiners using a Cartesian coordinate system. The most reliable mandibular landmarks were the mental foramen, as well as the medial and lateral poles of the condyle. An *in-vitro* study conducted by Misch et al. [18], created artificial periodontal defects on dry skull. Linear measurements on CBCT, periapical intraoral radiographs, and periodontal probing were accurate compared to physical caliper measurements. These results were supported by another study which also looked at dry skulls. Metal markers were used to measure the linear distance between the cemento-enamel junction and the alveolar crest [19]. It was concluded that CBCT imaging was more accurate than traditional full mouth series radiographs. However, Leung et al. [56] demonstrated that examiners falsely identified the presence of an alveolar bone defect 3 times more than when directly examining dry skulls. Sun et al. [57] found that CBCTs underestimated the buccal bone height by as much as 1.2mm at a thickness of 0.4mm. An interesting study was conducted by Timock et al. [58], who used embalmed cadavers. CBCT measurements of alveolar bone height demonstrated good inter- and intra-rater reliability around posterior and anterior teeth (ICC$\geq$ 0.97) in comparison to direct physical measurements. However, measurements of alveolar width was slightly less reliable (ICC=0.90).

Relatively few studies have attempted to quantify bone volumes using CBCT images. An *in-vitro* study artificially created defects of known dimensions using a dry human mandible, after which a CBCT scan was taken. Volumetric measurements using image visualization software was compared to physical measurements. Volumetric measurements were shown to be highly accurate (-6.9mm^3 $\pm$ 4) [59]. Chaison et al. [60] designed a clinical study that involved recruiting patients who already had CBCTs taken as part of routine orthodontic records as well as dental cast records. CBCT scans were taken of the casts of patients who demonstrated no relapse, and relapse 10 years post-treatment. in patients who presented with relapse, an increase in alveolar volume was noted compared with T_1. The proposed explanation was significant changes of the inter-canine width resulting in an increased measured volume. A recent study published in AJO-DO looked at volumetric changes of the alveolar housing in response to twin-block and modified twin-block therapy using 3-dimensional segmented virtual models derived from CBCT imaging [61]. The authors used the left and right mental foramen, the mandibular trigone, and the genial tubercles to superimpose pre-treatment and post-treatment models. The mandibular left central incisor of 26 treated patients were chosen, and linear measurements and volumes around that tooth characterized. This study found that the bone height and volume on the labial side of the incisors significantly decreased after treatment. Lingual crestal bone height, lingual alveolar volume, total alveolar volume, and labial and lingual thickness from the root apex remained unchanged.

Beyond clinical factors such as observable gingival inflammation and apical migration of connective tissue, there are limited studies documenting conditions of the bony housing

pre-, mid-, and post-treatment. Cone-beam computed tomography provides further insight into pre-treatment conditions of the alveolar housing, which may be used to identify potential prognostic factors for gingival recession. Cadaver and dry skull studies have shown that bony dehiscences and fenestrations are present in the anterior alveolus prior to the start of any treatment [56, 62]. Evangelista et al. [62] found dehiscences were associated with about 50% of all teeth, and fenestrations with 36% of all teeth in a sample of 4319 teeth. Interestingly, Class I malocclusions had greater prevalences of dehiscences, a 35% increase over Class II division 1 malocclusions.

1.4.1 Relationship of Vertical Facial Growth Patterns to Symphyseal Width

Using methods described by Handelman [63], studies that looked at pre-treatment dehiscences and fenestrations also found varying thickness of labial crestal bone (refer to Figure 4.2). Wehrbein et al. [64], in a case study on a cadaver with a history of orthodontic treatment, noticed a potential relationship between symphysis shape and the presence of dehiscences and fenestrations. The study concluded that in cases of narrow and high mandibular symphyses, pronounced sagittal and rotational movements of incisor teeth may lead to progressive loss of bony support. Gracco et al. [65] explored the relationship between various facial types and the morphology of the mandibular symphysis using CBCT techniques. With a sample size of 80 patients, they found that the total symphyseal width was greater in short face individuals than in long face individuals. However, the total area of the symphysis was not significant between different facial types. They concluded that there was a statistical difference between facial types and the total thickness labio-lingually of the mandibular symphysis (refer to Figure 1.8). In another paper, it was shown that skeletal Class III patients with high mandibular plane angles had thinner alveolar bone widths compared to low and normal angle patients [66]. In a large sample, Enhos et al. [67] looked at 1872 teeth in 26 hyperdivergent, 25 normodivergent, and 27 hypodivergent participants who did not have previous orthodontic treatment. Axial and coronal views were used to assess whether dehiscences or fenestrations were present. The results suggested that there were significant differences in the prevalence of dehiscences between different facial patterns. There was a lower prevalence of dehiscences in the hypodivergent group compared with the normal and hyperdivergent groups.

Looking at differences between pre- and post-treatment CBCT images, Hoang et al. [68] studied 75 non-growing individuals who were categorized into low, average, and high angle groups depending on the sella-nasion to mandibular plane angles (SN-MP). Bucco-lingual widths of the right mandibular central incisor were measured at the root apex, mid root, and at alveolar crest. These individuals were then followed through treatment where post-treatment CBCT records were taken. The authors found that low angle patients tended to have a significantly increased alveolar width at the apex of tooth 4.1 than in average and high angle individuals ($p < 0.001$). High-angle subjects were more

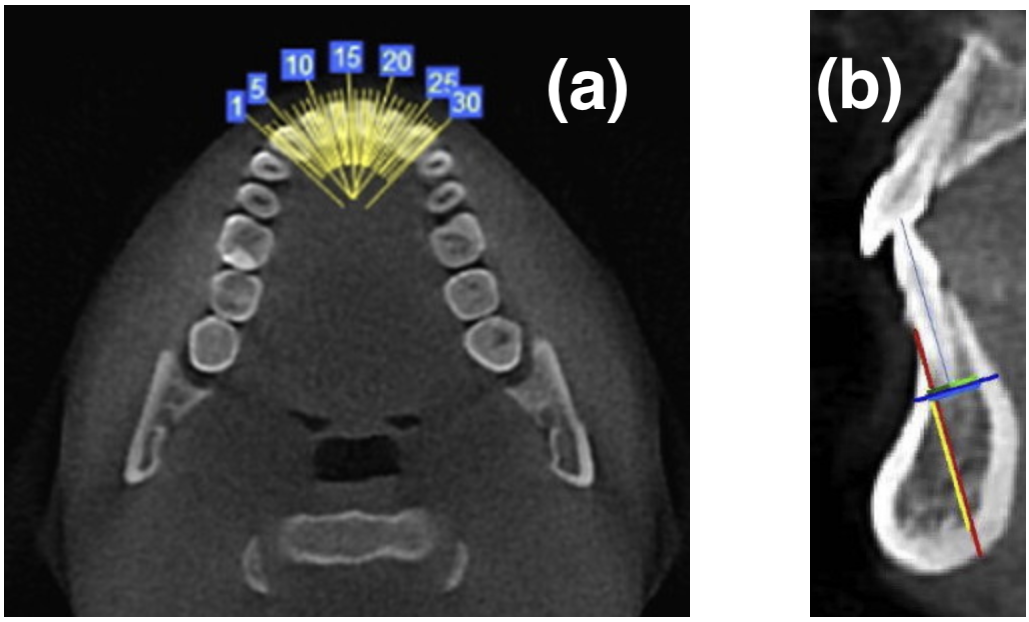

Figure 1.8: Characterization of symphyseal morphology according to Gracco et al. [65]. (a): Of the multiple sections taken perpendicular to the dental arch, only the sections taken through the central axis of the mandibular lateral and central incisors were chosen. (b): In each of the chosen sagittal sections, measurements were taken to characterize the morphology of the symphysis. The red line represented the total height of the symphysis, and the yellow, only the cancellous bone height. The blue line represented the total alveolar width, with the green line representing the cancellous bone width.

prone to root resorption beyond that of expected routine orthodontic treatment, and the overall degree of labio-lingual bone loss in all 3 facial patterns were minimal.

Mazurova et al. [69] studied a cohort of 177 individuals from pre-treatment through to the end of treatment, and followed up with them for 5 years post-treatment using traditional lateral cephalograms. The participants were categorized into 3 groups depending on the width of their dentoalveolus at B-point: narrow, average, and wide (refer to Figure 1.9, *W2*). All groups at 5 years post-treatment had similar changes to the incisor inclination with no differences in gingival labial recession. Similarly, different vertical facial patterns were not found to be a predictor of gingival recession [70].

1.4.2 Other Patient-Specific Factors Predictive of the Mandibular Alveolar Response

The occlusal classification has been thought to be predictive for the alveolar bone response. Evangelista et al. [62] showed that approximately 51% of all teeth in a sample of 79 Class I and 80 Class II patients with no previous orthodontic treatment presented with dehiscences, and 36% were associated with fenestrations. Of these teeth, most of the dehiscences presented in the lower arch (57%). Yagci et al. [71] found that in normal vertical facial patterns, a similar prevalence of dehiscences were found in all three occlusal

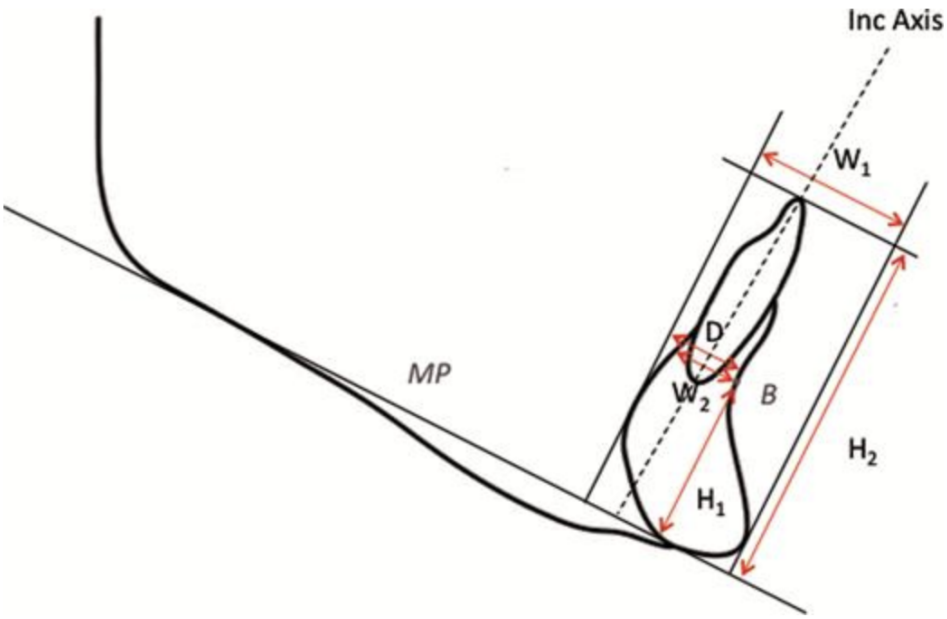

Figure 1.9: Characterization of the mandibular symphysis used by Mazurova et al. [69]. In order to measure the width of the dentoalveolus, *W2*, a line parallel to the mandibular plane extending from B-point to the lingual contour of the symphysis was measured.

classifications (Class I, II, III). More dehiscences were found in the mandibular arch, and more fenestrations were found in the maxilla. When considering only the mandible, dehiscences and fenestrations were found more in Class II (41%) and Class III (45%) individuals.

1.5 Purpose and Objectives

There is no clear consensus regarding the periodontal response of the anterior mandibular symphysis to orthodontic treatment. Early animal studies had found that protruding teeth outside of the bony envelop resulted in gingival recession, especially in the presence of gingival inflammation. However, this conclusion was not supported in more recent human studies. No clear relationship was found between the labial movement of mandibular incisors and gingival recession [42, 43]. However, this does not mean that a relationship does not exist. The level of evidence presented in literature has been questionable due to methodological limitations. For example, no studies have control comparisons, and the outcome measures evaluated present objectionable relationships with gingival recession [42, 43].

Studies that used lateral cephalograms to study bony response presented with significant limitations. This is due to overlap of adjacent tissues, and errors related to patient positioning. In addition, there are technological limitations associated with inadequate resolution to resolve the labial bone. More recent investigations using CBCT imaging

analyzed bony response on a slice-by-slice basis, usually selecting the slice that best represented the position of greatest defect (Figure 1.9). The use of one slice or tooth to represent the entire mandibular symphysis may have been too presumptive.

The purpose of this study was to apply techniques developed by Yushkevich et al. [72] and Cevidanes et al. [11, 73–76] at the University of Michigan, with the objective of studying bony volume changes of the mandibular alveolus in response to Class II correction using Forsus™ and Xbow® appliances. Recent advances in computed imaging quantification developed by Fedorov et al. [77] were also employed in this study. The novel method developed was tested on a pilot sample of patients undergoing orthodontic treatment for Class II correction. This study aimed to clarify the usefulness of CBCT imaging, with the goal of contributing to the current discussion centred around the periodontal response to orthodontic correction. Volumetric quantification was chosen over linear measurements as it better characterized 3-dimensional reality.

1.5.1 Research Questions

This thesis aimed to address the following questions:

1. In adolescent patients presenting with a mild to moderate Class II malocclusion, does the volume of the alveolar housing around the mandibular incisors change in response to orthodontic correction? If so, by how much?

2. Can the type of fixed Class II corrector (i.e. Forsus™, Xbow®), the degree of incisor proclination, and/or vertical face type be used to predict its response?

3. Secondary measure: In adolescent patients presenting with a mild to moderate Class II malocclusion, how does the incisor inclinaton change in response to Forsus™ vs. Xbow®?

Chapter 2

Method Development

2.1 Introduction

The framework for method development was as follows:

1. **Sample selection** and retrieval of the DICOM images for analysis.
2. **Segmentation** of the mandibular incisors using an automatic segmentation method with manual human refinement, similar to the protocol described by Forst et al. [78].
3. **Segmentation** of the anterior mandibular body to include the left and right mental foramen (MF), and exclude the segmented mandibular incisors.
4. **Conversion of the segmentation to 3D virtual models and landmarking** using 3DSlicer to define sagittal and axial reference planes.
5. **Measurement of incisor inclination** in 3D relative to a stable axial reference plane.
6. **Measurement of the alveolar volume** around the mandibular incisors.
7. **Validation** of the method using statistical analysis.

2.2 Methods

2.2.1 Sample Selection

Data collection for this study was taken from a prospective clinical trial started in October 2012 and completed by June 2018 (refer to Chapter 3 for the trial design). Of the 43 participants remaining in the study, six patients were randomly selected in order to validate the method using computerized randomization. For each of the these samples, time points were randomized selecting either T_1 or T_2, and the data analyzed. Participant demographics are presented in Table 2.1. All participants at the start of their treatment were between 11-15 years old, had mild to moderate Class II Division 1 malocclusions, and

Table 2.1: Participant demographics for method validation. Patients were chosen at random from a pool of 43 participants. Time points were chosen based on computer randomization.

Patient Number	Time point	Sex	Treatment Appliance
1	T1	Female	Forsus
2	T1	Male	Forsus
3	T2	Male	XBow
4	T2	Female	Forsus
5	T2	Female	XBow
6	T2	Male	XBow

presented in the late mixed to early permanent dentition. Syndromic and severe vertical growth tendencies were excluded from this study.

CBCT scans were taken at the University of Alberta Graduate Orthodontic Clinic using iCat (Imaging Sciences Intarnational, Hatfield, PA). The full FOV scans were taken at $0.3mm^3$ over 8.9 seconds (120kVp, 5mA). Image files were then converted into DICOM format using the iCAT software (Visualization Sciences Group, Burlington, MA).

2.2.2 Segmentation

The construction of a 3-dimensional volume map of the CBCT image, also known as volumetric segmentation, was performed using open source software ITK-SNAP, version 3.6 [72]. The DICOM files were first converted into "gipl.gz" files using ITK-SNAP for convenience and file portability. A semi-automatic segmentation method was employed (Figure 2.1). Active contour algorithms allowed for regions of interest to be computed in 3-dimensions using CBCT grey level intensities and boundaries [76, 79]. Thresholds for grey level intensities were defined on an image-by-image basis, which provided the automated segmentation algorithm with user-defined limits. ITK-SNAP included a tool which provided visualization of automatic segmentation boundaries as defined by grey level thresholds (Figure 2.1b). Seed points were placed within the boundaries of the ROI, and automatic segmentation commenced via active contouring. Seed points continued to expand until the region of interest was completely highlighted, at which point the user terminated the process. Slice-by-slice inspection and manual refinement by the user was necessary to add to regions missed by the algorithm and remove from regions which leaked past the ROI (Figure 2.1d).

Once all of the mandibular incisors were segmented, the volume map for the anterior mandibular body was generated making sure to include the right and left mental foramen (Section 2.2.3.2). Although the entire corpus and dentition was included during automated segmentation, the incisors previously segmented was ignored by ITK-SNAP. This is because different volume labels were assigned to the teeth and the bone (refer to Figure 2.2).

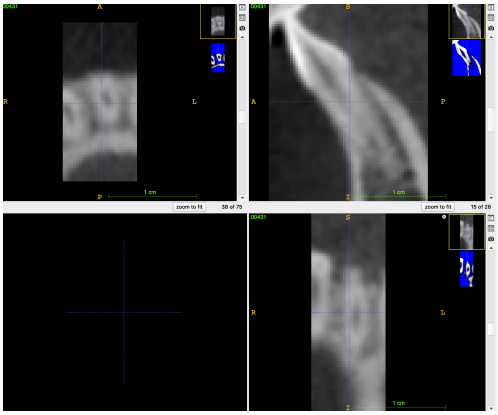

(a) Image cropped to leave only the ROI.

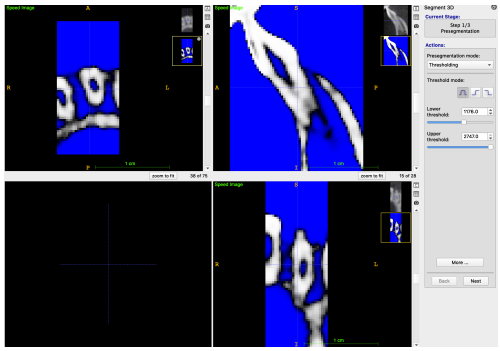

(b) Visual interface of user-defined boundaries based on grey value thresholds. Automatic segmentation via active contouring ignored blue shaded areas and highlighted regions in white. [72].

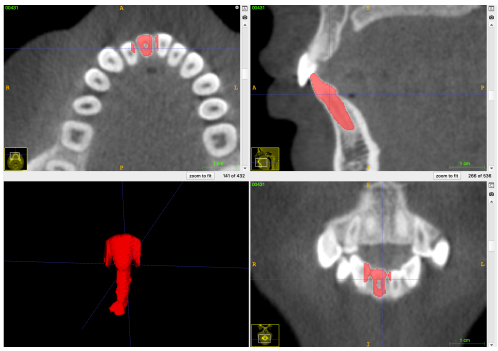

(c) Result of fully automatic segmentation. Note the extraneous areas mesial and distal to the incisor crown, as well as apical to the root apex.

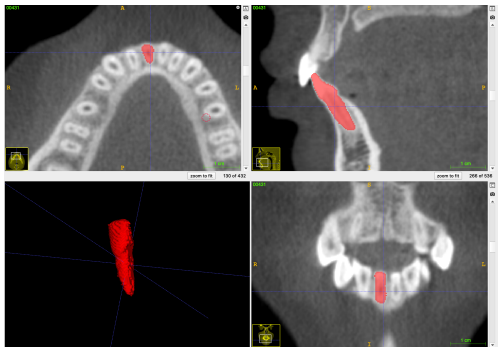

(d) Result after manual refinement using the brush tool. Areas outside the ROI, as highlighted in (c), were removed on a slice-by-slice basis.

Figure 2.1: Steps for semi-automatic segmentation of the ROI using ITK-SNAP. As an example, tooth 4.1 has been segmented from the rest of the image.

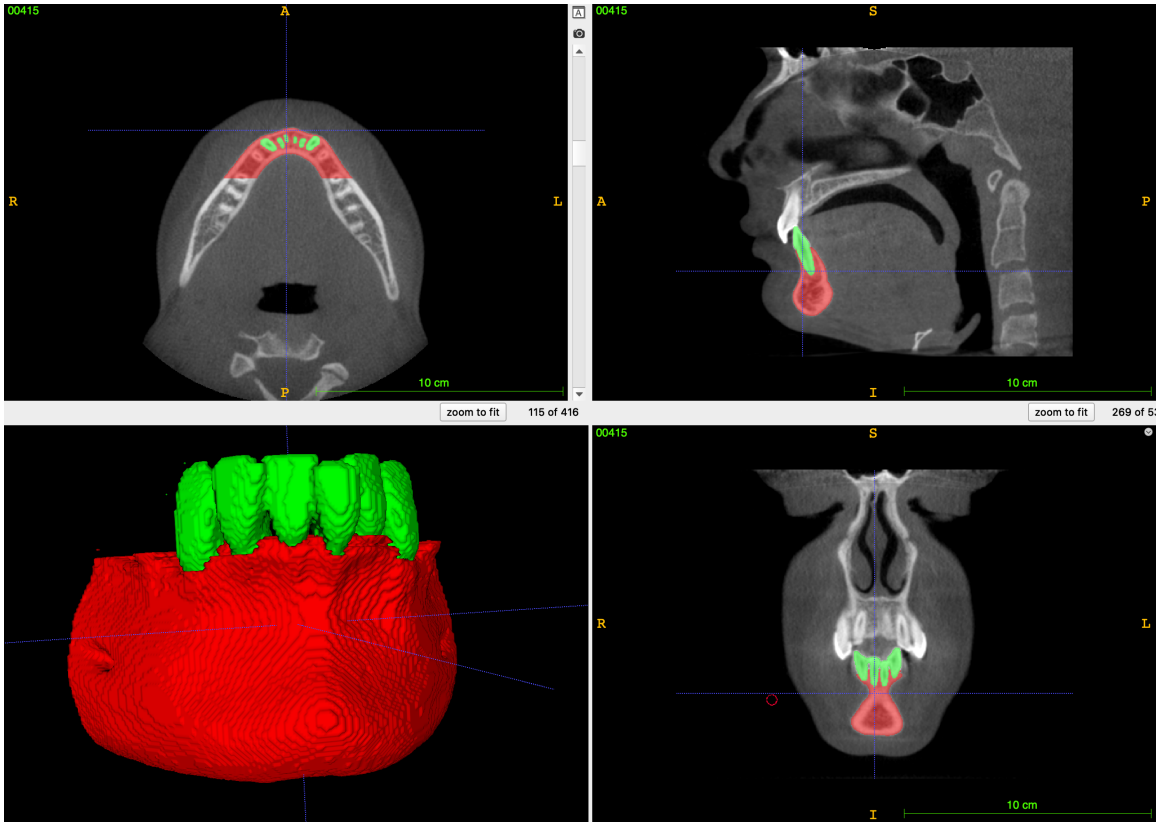

Figure 2.2: Example of semi-automatic segmentation for the anterior corpus of the mandible using ITK-SNAP. The dentition was first segmented and assigned a coloured label (green). A different label (red) was used to segment the mandible. This differentiation instructed the software to ignore the dentition during segmentation. The anatomy of the left and right mental foramen were preserved for landmarking. Manual refinement was completed after automatic segmentation.

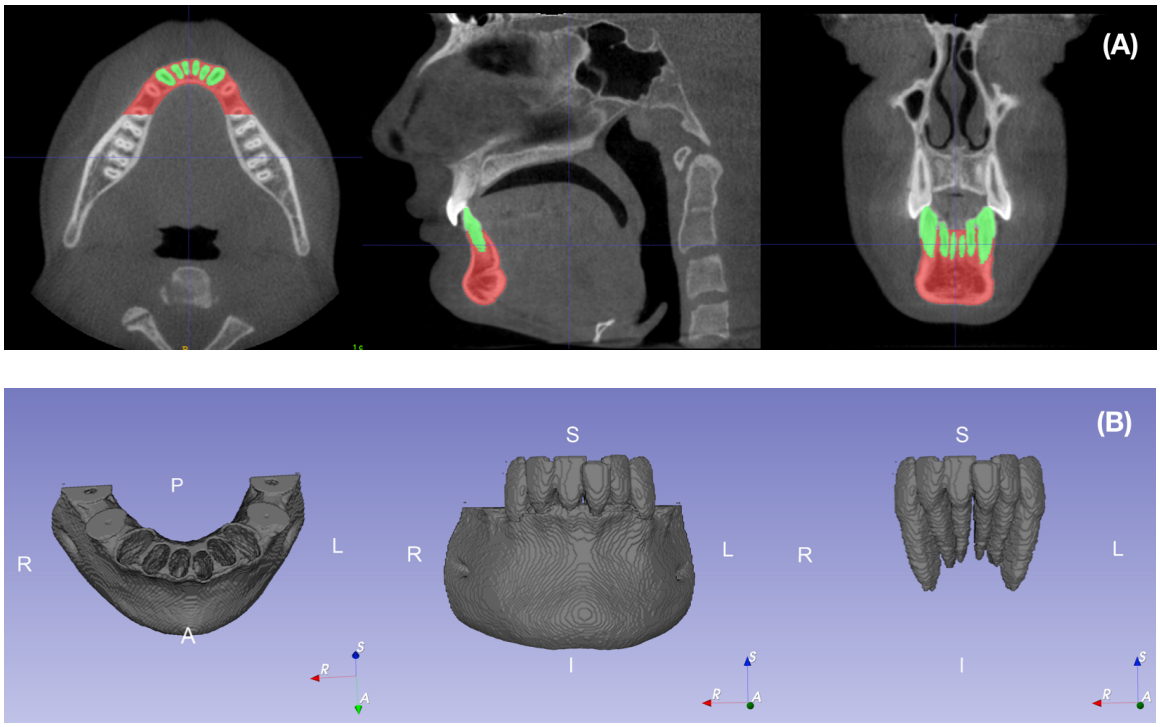

Figure 2.3: (a) Completed 2D volume map using semi-automated segmentation method. The sagittal, coronal, and axial views are shown. (b) Surface mesh (3D model) output as viewed from 3DSlicer. As the models for the teeth and the mandible were generated separately, the models could be visualized together or apart.

2.2.3 3D Model Rendering and Landmarking

2.2.3.1 Volume Map to Surface Mesh

In order to visualize and manipulate the regions of interest (ROIs) in 3-dimensions, the volume maps were converted to ".vtk" virtual models using the "Export as Surface Mesh" feature in ITK-SNAP. This allowed for manipulation and quantitative analysis in 3DSlicer (www.slicer.org) via the SlicerCMF project (version 4.10.2, revision 28257) (cmf.slicer.org) [80, 81]. All smoothing algorithms were turned off during conversion of volumetric segmentations to ".vtk" models. Figure 2.3 demonstrates the process from completed volumetric segmentation to 3-dimensional surface mesh or models. As models of the teeth were created separate from the mandible, analysis could be performed on the teeth, the mandible, or together at the same time (Figure 2.3b).

2.2.3.2 Landmarking

Table 2.2 summarizes the landmarks used to develop this method. Using the "markups" module in 3DSlicer, fiducial points were placed at the anterior rim of the right and left MF, and at ptB. The "Q3DC" module, as part of the slicerCMF package, calculated the fiducial at

Table 2.2: Definition of landmarks. Refer to Figure 2.4 for a visual representation of these landmark locations.

Landmark	Description	Definition
Skeletal Landmarks		
L.MF	Left Mental Foramen	The most anterior point on the rim of the left mental foramen
R.MF	Right Mental Foramen	The most anterior point on the rim of the right mental foramen
ptB	B-point	The most concave point of the mandibular symphysis, on the mid-sagittal plane
Calculated Fiducials		
H.MFD	Half the Mental Foramen Distance	The calculated halfway point on the vector traced from the left and right mental foramen landmarks
1Q.MFD	One Quarter the Mental Foramen Distance	The calculated point exactly 1/4 the distance along the vector traced from right to left mental foramen
3Q.MFD	Three Quarter the Mental Foramen Distance	The calculated point exactly 3/4 the distance along the vector traced from the right to left mental foramen
Dental Landmarks		
LiA	Lower Incisor Apex	The most apical point on the root of the mandibular incisors
LiT	Lower Incisor Incisal Crown Tip	The centre of the labio-incisal line angle of the mandibular incisors

1/2 (H.MFD), 1/4 (1Q.MFD), and 3/4 (3Q.MFD) the distance, along the vector joining the right and left MF. Based on the Cartesian coordinate system, these points were calculated automatically using the following formulas $\left(\frac{x_1+x_2}{2}, \frac{y_1+y_2}{2}, \frac{z_1+z_2}{2}\right)$, $\left(\frac{x_1+3x_2}{4}, \frac{y_1+3y_2}{4}, \frac{z_1+3z_2}{4}\right)$, $\left(\frac{3x_1+x_2}{4}, \frac{3y_1+y_2}{4}, \frac{3z_1+z_2}{4}\right)$ respectively, where (x_1, y_1, z_1) are the coordinates for the R.MF and (x_2, y_2, z_2) for the L.MF. User-positioned landmarks were also placed at the most apical point along the root of the central and lateral mandibular incisors (LiA), and at the centre of the facio-incisal line angle (LiT). Refer to Figure 2.4 for a visual example of landmark placements.

2.2.4 Measurement of Incisor Inclination

The Q3DC module in 3DSlicer also allowed for measurement of angles between two lines. In 3-dimensional space, the angular relationship between two lines can be described by three angles: pitch, yaw, and roll. The Q3DC module provided tools to calculate these angles based on user-defined fiducials. This study only considered the pitch angle, which

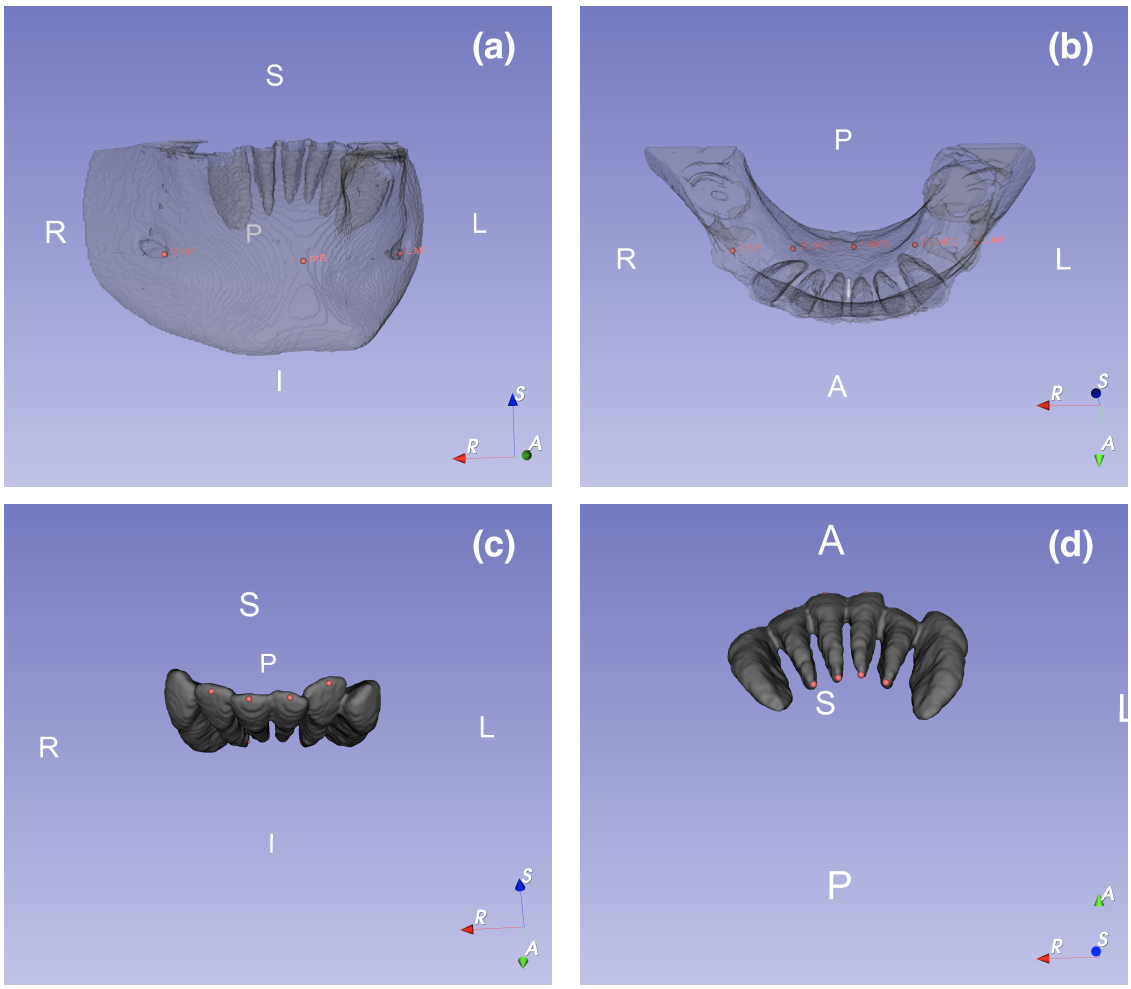

Figure 2.4: (a) User-positioned landmarks which were placed on the anterior rim of the left and right MF (L.MF/R.MF) and at B-point (ptB). (b) Calculated fiducials using the Q3DC package (cmf.slicer.org). Points were calculated at 1/2, 1/4, and 3/4 the distance along a line connecting the left and right MF. (c) User-defined fiducials placed along the incisal-facial line angle, halfway between the most mesial and distal. (d) User-defined fiducials placed on the root apex.

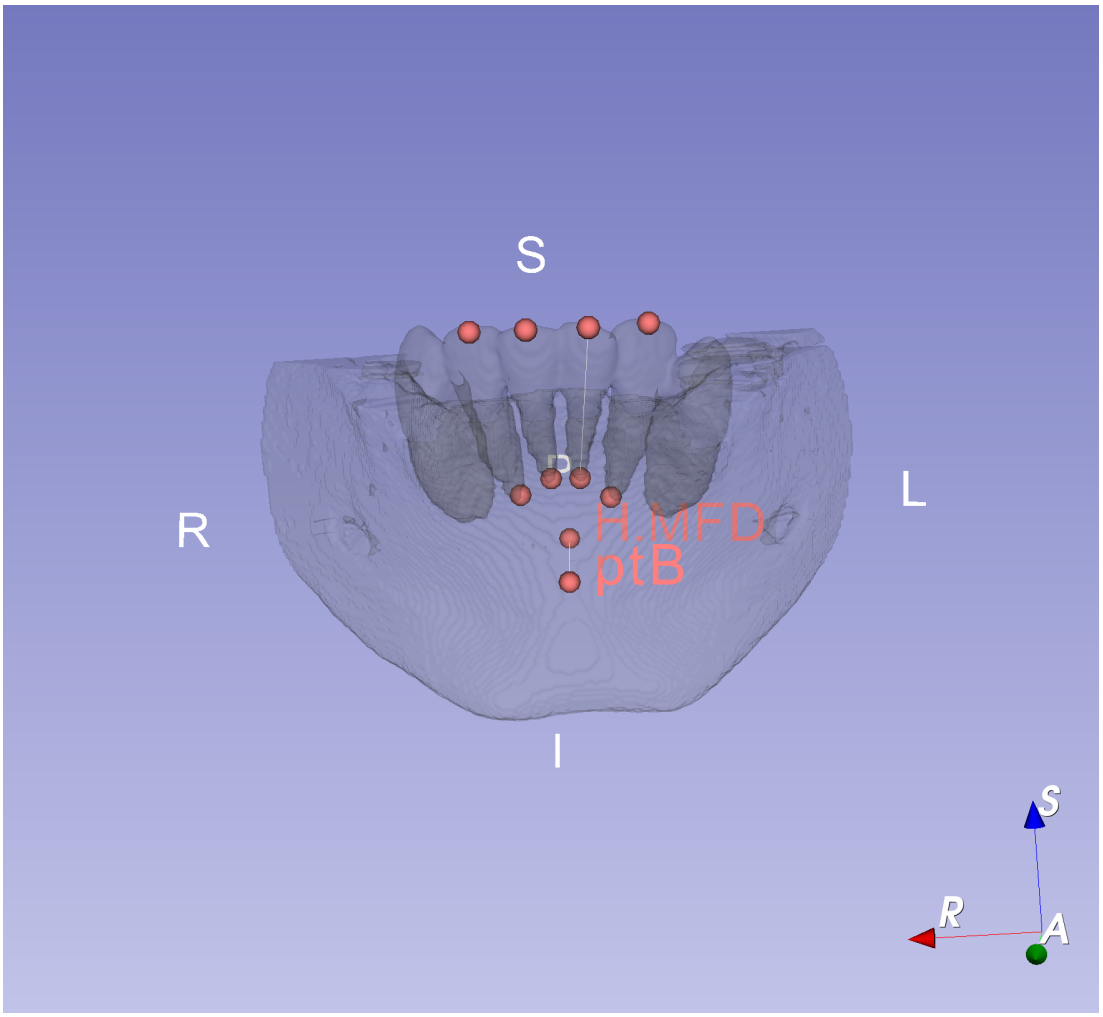

Figure 2.5: Incisor inclination quantification of Tooth 3.1 using the Q3DC module (cmf.slicer.org). Vectors are drawn; $\overrightarrow{H.MF}, \overrightarrow{ptB}$ and $\overrightarrow{LiA}, \overrightarrow{LiT}$ as shown by the white line, and the pitch, yaw, and roll angles computed. Only the pitch angles were recorded and used in this study. The pitch angle of tooth 3.1 was calculated to be 114.15°.

is analogous to the incisor-mandibular plane angle (IMPA) in 2-dimensions.

The reference line chosen was defined by a vector drawn from H.MFD to ptB. The long axis of each mandibular incisor was represented by a vector originating at LiA to LiT, and the pitch angle was generated and recorded on a spreadsheet (refer to Figure 2.5). For each subject, the individual incisor pitch angle from tooth 3.2 to 4.2 was averaged to determine one average value.

2.2.5 Measurement of the Alveolar Volume

Once the mandible was segmented and landmarked, a method for isolating the ROI while clipping out the rest of the mandible was needed. In order to determine the alveolar bone volume surrounding the mandibular incisors, two sagittal and one axial plane were

defined based on the landmarks described in Section 2.2.3.2.

2.2.5.1 Defining the Clipping Planes

The lateral boundaries of the ROI were defined by two clipping planes perpendicular to the vector $\overrightarrow{R.MF, L.MF}$, intersecting at the calculated points 1Q.HMD and 3Q.HMD (Table 2.2). The axial plane was defined by three points: L.MF, R.MF and ptB as shown in Figure 2.6. The "Easy Clip" module (cmf.slicer.org) provided the tools necessary to visualize the clipping planes, make adjustments manually, and crop the ROI.

2.2.5.2 Quantification of the Alveolar Housing

Using the models module in 3DSlicer, the volume of the resultant clipped model was computed. As shown in Figure 2.7, the ROI was the bony housing supporting the mandibular incisors. Also note a portion of the bone mesial to each lower canine had been included.

2.2.6 Statistical Validation

Six patients were randomly selected from the pool of 43 participants as part of the Forsus™ vs. Xbow® study in order to determine method reliability for alveolar volume measurement and mean incisor inclination. For each subject selected, either T_1 or T_2 was randomly chosen. Consistency (intra-rater) and absolute agreement (inter-rater) were measured using intra-class correlation coefficient (ICC) under a single measures two-way mixed model (Sections 2.2.4, 2.2.5). Measurements were repeated 3 times in a blinded fashion 1 week apart by the same examiner (KC), and repeated once by a trained second examiner (GCM). Good reliability of the measured alveolar volume implied the individual steps of segmentation, anatomical landmarking, and definition of the clipping planes were also reliable.

The percent error was calculated using the following formula:

$$\%error = \left| \frac{\sum_{i=1}^{n} (x_i - \overline{x})}{n\overline{x}} \right| \times 100\% \tag{2.1}$$

where n is the number of measurements, and $\overline{x}$ is the sample mean.

The significance level was set to $\alpha = 0.05$ for all statistical analyses used.

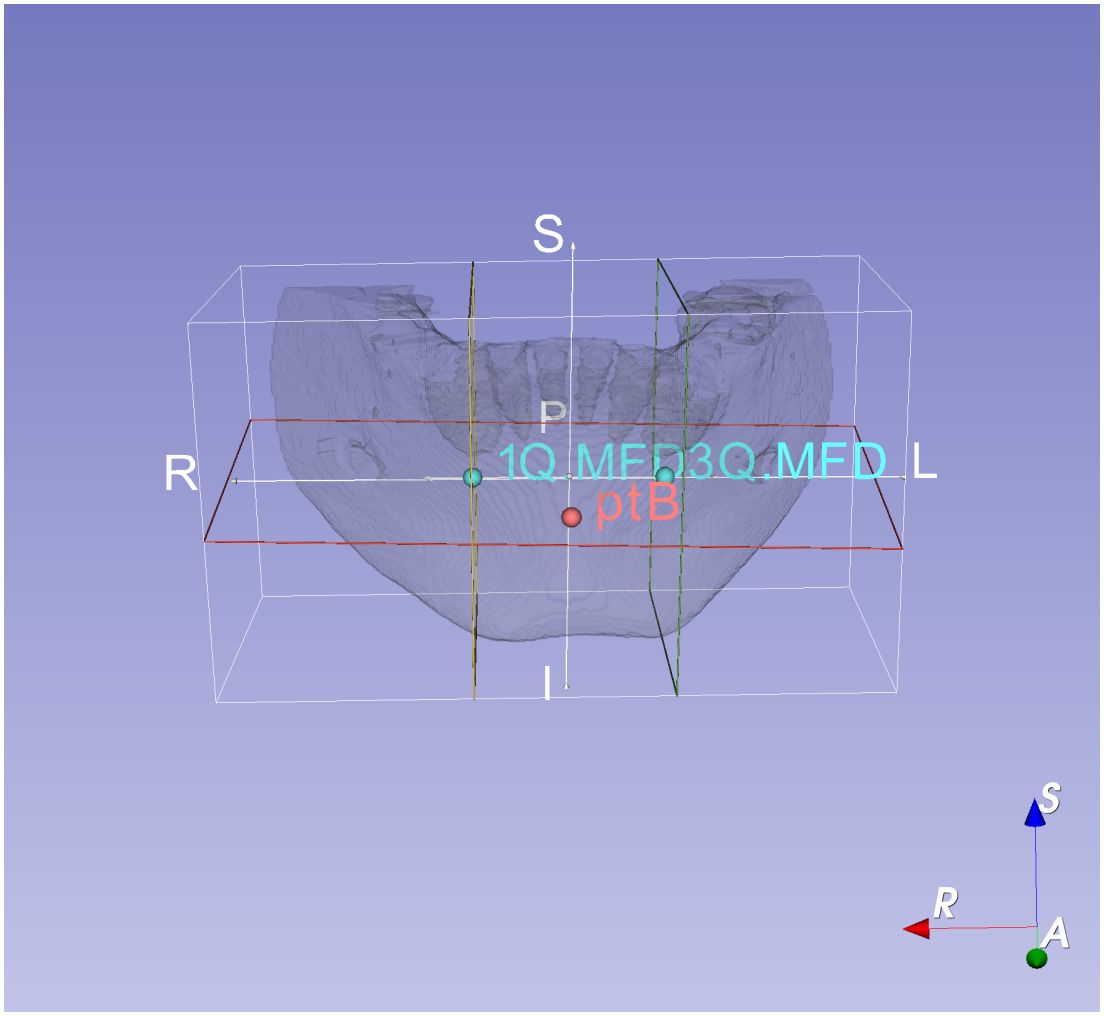

Figure 2.6: Using the "Easy Clip" module, as part of the SlicerCMF distribution of 3D slicer, two sagittal (yellow and green) and one axial (red) clipping planes were used to define the boundaries of the ROI based on the computed fiducials 1Q.HMD, 3Q.HMD (cyan) and user-positioned ptB (red) (Table 2.2). Note the white arrows that represent vectors perpendicular to their corresponding planes; these were used to help orient the clipping planes.

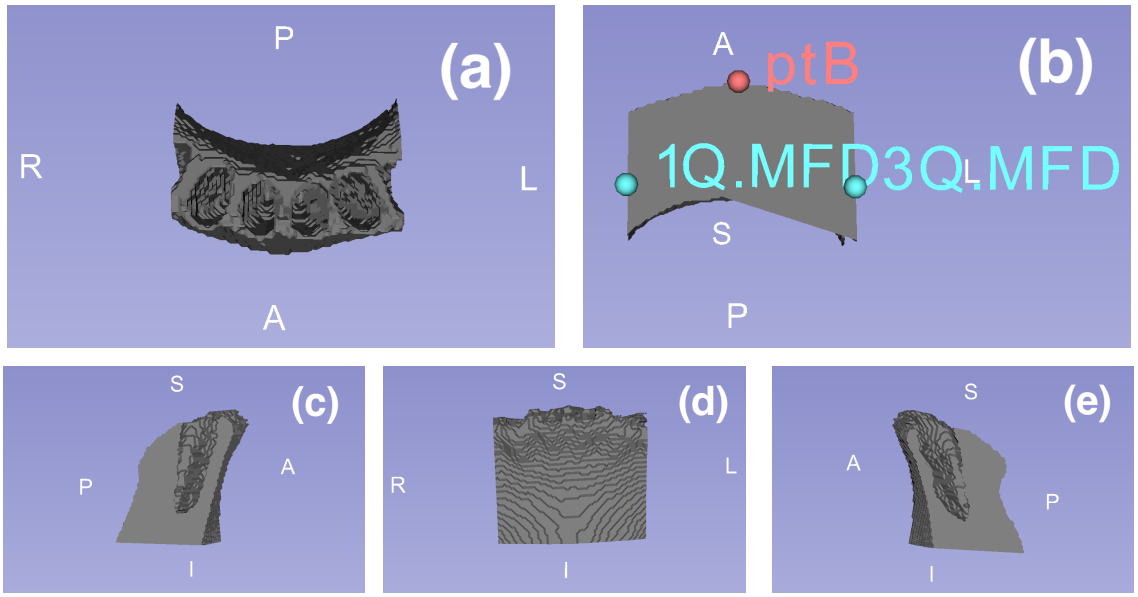

Figure 2.7: Model of the alveolar housing after the mandible was cropped with clipping planes based on reference fiducials 1Q.MFD, 3Q.MFD, and ptB. (a) Superior View, (b) Inferior View, (c) Right Sagittal View, (d) Centre View, (e) Left Sagittal View. Volume quantification was computed using the "Models" module as part of the 3DSlicer platform.

Table 2.3: Descriptive statistics of the average incisor inclination and alveolar volume. For each patient, the pitch inclination of all four incisors were measured individually and then averaged.*N* = Number of subjects.

	Average Incisor Inclination (°)			Alveolar Volume (mm^3)		
	N	Mean	Std.Dev.	*N*	Mean	Std.Dev.
Measurement 1	6	123.19	8.90	6	1948.00	436.86
Measurement 2	6	123.28	9.99	6	1985.78	501.84
Measurement 3	6	122.87	10.97	6	1903.59	429.80

2.3 Results

2.3.1 Consistency

The ICC for the average incisor inclination ($\overline{IC}$) was **0.981 [0.922,0.997]** and **0.941 [0.778, 0.991]** for the alveolar volume (V_{alv}). Descriptive statistics are presented in Table 2.3 along with the results of intra-examiner consistency (Table 2.4). Figure 2.8 presents pictorial representations of the results.

The percent measurement error, as calculated using Equation (2.1), varied between 1.50% to 11.98% for V_{alv} and between 0.07% and 5.31% for incisor inclination (Table 2.5).

Table 2.4: Calculated intra-examiner ICC values for average incisor inclination ($\overline{IC}$) and Alveolar Volume (V_{alv}). Measurements were repeated 3 times, 1 week apart.

		95% Confidence Interval		
	ICC	Lower Bound	Upper Bound	*p*-value
$\overline{IC}$	0.981	0.922	0.997	<0.001
V_{alv}	0.941	0.778	0.991	<0.001

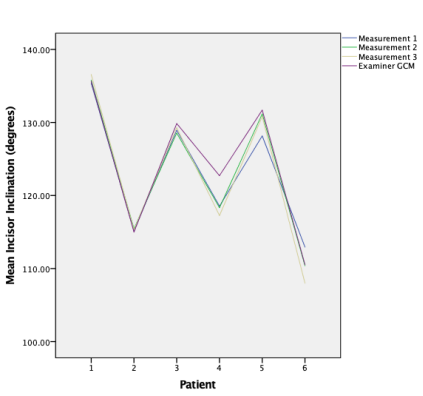

(a) Line plot of the mean incisor inclination. Measurements are in degrees (°).

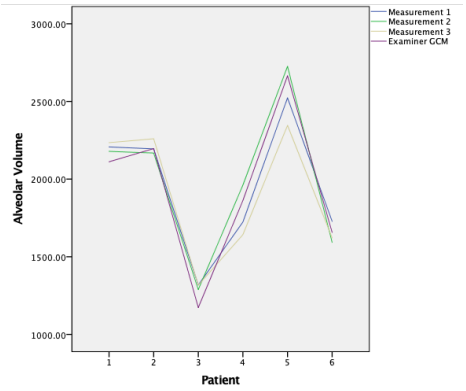

(b) Line plot of the alveolar volume. Measurements are in mm^3.

Figure 2.8: Line plot of the intra- and inter-examiner results. Measurements of both the mean incisor inclination (a) and alveolar volume (b) were repeated 3 times by the same examiner (KC), and repeated once by a second trained examiner (GCM).

2.3.2 Absolute Agreement

The ICC value for method reliability between two examiners was **0.982 [0.892, 0.997]** for the average incisor inclination and **0.972 [0.814, 0.996]** for alveolar volume measurement (Table 2.6). Figure 2.8 also includes the second investigator (GCM) measurements, as depicted with the purple line, compared with the three measurements of the primary investigator (KC). The agreement in measurements between the two investigators could also be plotted against a 45° line (Figure 2.9). The measurement error for V_{alv} ranged from 0.09% to 11.68%. The $\overline{IC}$ error ranged from 0.00% to 8.25%. Refer to Table 2.7 for complete results.

2.4 Discussion

CBCT imaging has provided the field of dentistry with tools for three-dimensional visualization of hard tissue structures. Applications include diagnostic information on the size and shape of the mandibular condylar heads [73, 82], presence of root resorption [83, 84], and in surgical treatment planning [74, 75, 85, 86]. It can also be used to reconstruct

Table 2.5: Percent error of repeated intra-examiner measurements. Tooth numbers represent the measurement error of the individual incisor in 3D space.

	Method	% Measurement Error
Patient 1	V_{alv}	1.70
	3.2	0.57
	3.1	0.07
	4.1	0.80
	4.2	1.08
Patient 2	V_{alv}	2.78
	3.2	0.42
	3.1	0.63
	4.1	0.34
	4.2	0.70
Patient 3	V_{alv}	1.50
	3.2	1.03
	3.1	0.31
	4.1	0.42
	4.2	0.78
Patient 4	V_{alv}	11.98
	3.2	5.25
	3.1	4.23
	4.1	4.60
	4.2	5.31
Patient 5	V_{alv}	10.01
	3.2	2.28
	3.1	1.37
	4.1	0.85
	4.2	1.84
Patient 6	V_{alv}	5.47
	3.2	3.28
	3.1	3.35
	4.1	2.36
	4.2	2.95

Table 2.6: Calculated inter-examiner ICC values for average incisor inclination ($\overline{IC}$) and alveolar volume (V_{alv}). Measurements between the two examiners were blinded from one another.

		95% Confidence Interval		
	ICC	Lower Bound	Upper Bound	p-value
$\overline{IC}$	0.982	0.892	0.997	<0.001
V_{alv}	0.972	0.814	0.996	<0.001

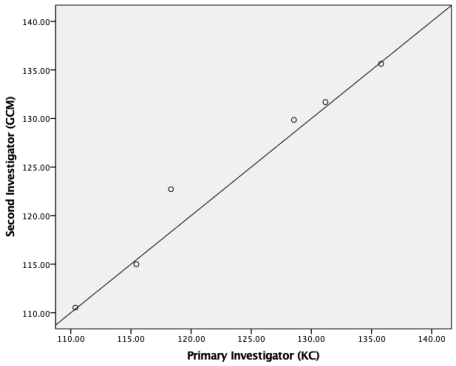

(a) Scatter plot of average incisor inclination measurements between both investigators plotted to the reference line $y = x$. Measurements on both axes are in degrees (°).

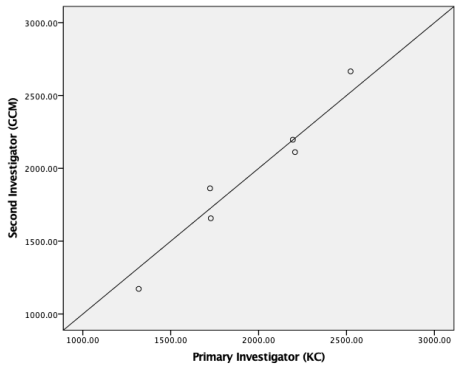

(b) Scatter plot of alveolar volume measurements between both investigators plotted against the reference line $y = x$. Measurements on both axes are in mm^3.

Figure 2.9: Scatter plot of measurements between two examiners plotted against line $y = x$. (a) represents $\overline{IC}$ and (b) represents V_{alv}.

Table 2.7: Percent error between two investigators.

	Method	% Measurement Error
Patient 1	V_{alv}	4.43
	3.2	0.24
	3.1	0.68
	4.1	0.19
	4.2	0.68
Patient 2	V_{alv}	0.09
	3.2	0.19
	3.1	0.68
	4.1	0.00
	4.2	0.74
Patient 3	V_{alv}	11.68
	3.2	2.18
	3.1	0.98
	4.1	0.97
	4.2	0.08
Patient 4	V_{alv}	7.74
	3.2	7.36
	3.1	7.24
	4.1	7.02
	4.2	8.25
Patient 5	V_{alv}	5.49
	3.2	1.23
	3.1	1.18
	4.1	1.43
	4.2	0.11
Patient 6	V_{alv}	4.20
	3.2	0.89
	3.1	1.02
	4.1	0.65
	4.2	1.08

traditional 2-dimensional images such as lateral cephalograms and panoramics [82]. The diagnostic value of orthogonal visualization in axial, coronal, and sagittal views as afforded by 3D tomographic modalities is undisputed. However, landmarking and image analysis in each of the three orthogonal planes can be quite daunting and tedious, especially when employing full FOV images which may exceed 200 axial slices.

Image segmentation refers to the process of highlighting ROIs visible in cross-sections of the DICOM data [74, 75, 82, 83, 85, 86]. The result is a volumetric label map. 3D rendering software can then be used to create models that can be navigated on a voxel-by-voxel basis and allow for panning, rotation, and zooming. More sophisticated Image processing software can also enable distance, surface area, and volumetric quantification, fiducial landmarking, and shape analysis [83]. Recent papers involving CBCT image analysis studied post-treatment changes using voxel-based registrations. This allowed for sub-voxel accuracy [87]. New registration methods may be more accurate because they are largely automated, dependent on computer tools, and are not subjugated to human error and biases [74].

Although voxel-based registration methods were not used for this study, the importance of automated segmentation tools cannot be understated. Forst et al. [78] showed that compared to full manual slice-by-slice tracing of a maxillary molar, automated segmentation with manual refinement was similarly reliable and precise. The distinct advantage with a semi-automated method was convenience and efficiency, significantly reducing the time required while maintaining precision and reliability through manual refinement. Yushkevich et al. [72] developed ITK-SNAP to allow users with little or no mathematical expertise to take advantage of methodological advancements in segmentation; specifically, using the active-contour method. ITK-SNAP provided a user-friendly interface in which complex segmentation algorithms could be applied. Padala et al. [88] suggested that CBCT grey values are useful in identifying the height of the alveolar crest, especially in large voxel size and large FOV images. Therefore, the method this study employed made use of differential grey values of dentin, cementum, bone, and soft tissue to set boundaries for automatic segmentation. The details regarding the math behind active contouring methods falls outside the scope of this dissertation; however, the Yushkevich et al. [72] paper does an excellent job in explaining the algorithm which ITK-SNAP is based. Automatic segmentation using active contouring methods essentially allows for user-guided inputs on ROI boundaries, based on differential grey values of adjacent tissues of varying radiodensities. The user places seed points within the boundaries, and once the algorithm within ITK-SNAP is invoked, the seed continues to expand until a boundary is met. At this point, expansion of the seed slows or stops altogether. However, given the inherent limitations associated with CBCT technology (i.e. artifacts, partial volume averaging, and low resolution), and in order to reduce the radiation burden to the patient, boundaries may be hard to distinguish based on grey values alone. It is inevitable for automatic segmentation to either expand beyond the ROI, or significantly fall short of it if stopped

early. Manual refinement relies on user experience and interpretation to precisely define the ROI [78]. Nevertheless, automated active contouring allows for efficient segmentation, saving significant time and reducing user error compared with a slice-by-slice full manual methods.

The alveolar housing supporting the mandibular incisors were best represented by a grey value intensity ranging from 300-600, whereas more radiodense dental structures were best represented by grey values >750-900. Unlike CT images, CBCT greyscale values are not standardized according to Hounsfield units [89]. The lack of standardization explained the range and inconsistency of threshold greyscale values. Manual refinement was necessary to verify and improve delineation between different tissues sharing similar grey values, or to fill in areas that were missed by automated segmentation due to radiographic artifacts. In order to ensure fidelity of the resultant model, smoothing was turned off during conversion of the segmented volume label maps to surface mesh models. Liu et al. [90] found a 3-12% reduction in computed tooth volumes if smoothing algorithms were used.

Choice of Landmarks

Naji et al. [55] identified eight mandibular reference landmarks based on CBCT images. These included the mental foramen; the lingula; the mandibular canal at the furcation of the first molar; the medial and lateral poles of the condyle; and the anterior, superior, and posterior most points of the condyle. All of these landmarks demonstrated good intra- and inter-rater reliability with deviation not exceeding 1mm. These results were further supported and verified by another *in-vitro* study [91]. In addition to these landmarks, Lagravère et al. [92] looked at the consistency and absolute agreement of identifying ptB, L1T, and L1A on CBCT images within and between examiners. All of these landmarks exhibited an ICC > 0.9, proving that they could be consistently identified on CBCT images.

In order to demarcate the area of interest, one axial and two sagittal planes were defined based upon previously mentioned landmarks (Table 2.2). Specifically, the left and right MF as well as ptB were selected to define the lateral and inferior boundaries respectively. According to Bjorn and Skieller's studies, the mandibular canals and the symphysis demonstrate relative stability in the sagittal dimension [93]. 3D studies also supported the stability of the mandibular canal and the anterior superior border of the chin in the sagittal dimension [94, 95]; however, Krarup et al. [94] showed that there may be some transverse changes during growth. The Burlington and Bolton growth studies demonstrated minimal transverse change of the body of the mandible in adolescence. Interestingly, Wagner and Chung [96] demonstrated that the antegonial width increased approximately 1.6mm per year until the age of 14, at which point growth started to taper off. Ricketts [97] supported this finding and showed an increase in antegonial width of 1.4mm per year until the age of 16. Using Bjorn's metallic implant method and 2D posterior-anterior cephalographs, Gandini Jr and Buschang [98] found an average increase

Figure 2.10: Mandibular mask, highlighted in yellow, was used for voxel-based 3D registration. de Oliveira Ruellas et al. [76] demonstrated that the entire body of the mandible was reliable to use in 3-dimensional registrations.

of 0.5mm per year of the mandibular corpus width in participants at the peak of growth. However, the sample size was quite small. de Oliveira Ruellas et al. [76] concluded that the use of the mandibular body mask was reliable to use as a 3D voxel-based reference in growing patients when comparing two time points. They defined the mandibular body mask as the corpus of the mandible without teeth, alveolar bone, rami, and condyle (refer to Figure 2.10). Bjorn showed that within the body of the mandible, the mandibular canal as well as the inner cortical surface of the symphysis and the anterior superior surface of the chin were stable [93]. The mental foramen, the site at which the mandibular nerve exits the bony canal and becomes the mental nerve, had been shown to be reliable and repeatable on 3-dimensional imaging [55, 92]. The mental foramen was also included in the mandibular body mask as laid out in the study by de Oliveira Ruellas et al. [76]. Finally, Lagravère et al. [99] followed adolescent patients (initially 12-14 years of age) for approximately 12 months. They found that there was a maximum mean increase of 0.5mm between the centre of the left and right mental foramen on 3-dimensional CBCT images. This agreed with the study by Gandini Jr and Buschang [98]. From the aforementioned studies, it was concluded that the transverse dimension between the left and right mental foramen are stable throughout an average orthodontic treatment duration of 24 months.

The stability of B-point during adolescent growth was an important consideration prior to its inclusion in this study. Lagravère et al. [92] demonstrated reliability of B-point identification on CBCT images, but the study did not describe its positional changes during growth. Buschang et al. [100] looked at serial lateral cephalograms of 75 patients from ages 6 to 15 years old to determine growth changes of the symphysis. It was found that ptB in males migrated superiorly at a rate of 0.5mm per year, and lingually at 0.3mm per year during the pubertal growth spurt. The magnitude of ptB change in females was less; however, the direction of migration in the superior-lingual direction was the same. A diagram of the change in symphyseal morphology in male children and adolescents is presented in Figure 2.11. A similar study was repeated by the same authors approximately 10 years later with more patient participants [101]. ptB was found to migrate superiorly by 2.37mm from ages 10-15. Interestingly, there was negligible change in ptB in the sagittal

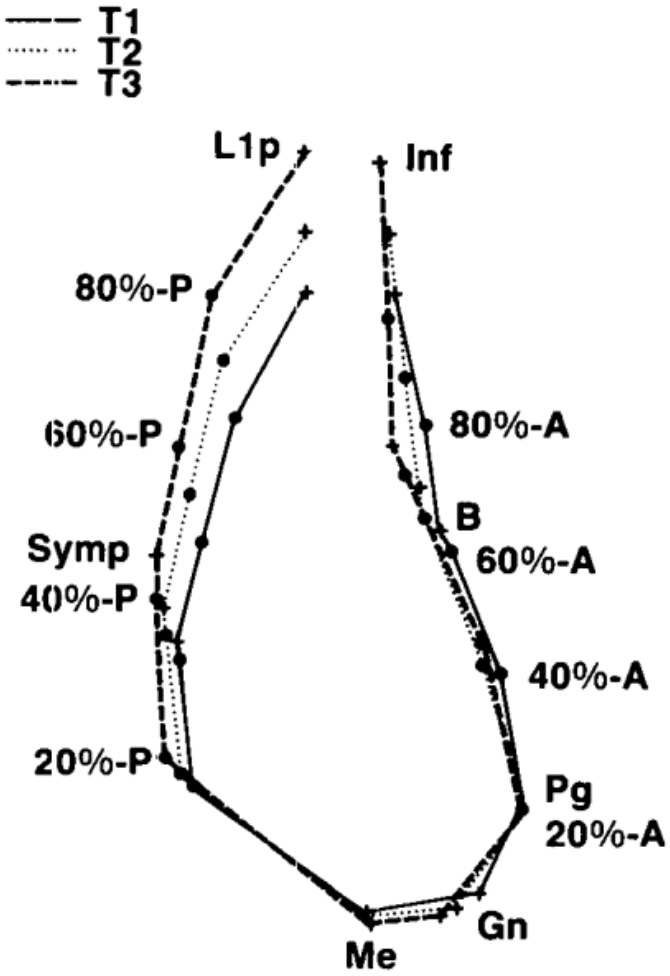

Figure 2.11: Changes in symphyseal morphology in males from childhood to adolescence. Derived from Buschang et al. [100], Figure 2A.

dimension. Aki et al. [102] studied the morphology of the mandibular symphysis and used ptB as the most superior limit of the bony mandibular symphysis. Therefore, hard tissues superior to ptB was considered part of the dento-alveolar apparatus for the purpose of this study.

The expected result from the incisal migration of ptB over the course of treatment is a decrease in alveolar volume. This is apparent from the aforementioned studies [100–102]; however, over the course of a 2-year treatment, this migration is minimal and likely insignificant, especially compared to the error presented in this method (Table 2.5 and Table 2.7). Intuitively, it can be deduced that ptB migrates occlusally as the lower incisors continue to erupt with continued vertical growth. If this is the case, then there is minimal change in alveolar volume due to compensatory eruption of the incisors. Al-Abdwani et al. [103] found an insignificant effect of incisor inclination on the position of ptB. However, there was a statistically significant but clinically irrelevant change in A point.

Table 2.8: Guidelines according to Portney and Watkin [104] for method reliability using Intra-class Correlation Coefficient (ICC).

ICC > 0.90	Excellent Agreement
0.75 > ICC > 0.89	Good Agreement
0.51 > ICC > 0.74	Moderate Agreement
ICC < 0.50	Poor Agreement

From literature, it appears that any effects on ptB and its stability through orthodontic treatment is not due to dental positional changes, but due to natural growth over time. Future consideration to determine the effects of altering ptB on alveolar volume will be warranted.

Study of the ICC values (refer to Table 2.4 and 2.6) revealed good intra-examiner consistency and inter-examiner agreement. According to Portney and Watkins [104], both results demonstrated good agreement when the lower bound of the 95% confidence interval was considered (Table 2.8).

Figure 2.8a illustrates that most consistency issues associated with the measurement of $\overline{IC}$ occurred with patient 4. This was also evident when considering the percent error in the measurements (Table 2.5 and 2.7). However, percentage error associated with V_{alv} was sometimes as high as 12% (Table 2.7, patient 4) which was approximately twice as high as the $\overline{IC}$ within the same patient. In patient 3, the percentage error of V_{alv} was almost 6 times greater than the $\overline{IC}$ (Table 2.7). The primary reason for this apparent discrepancy between the two developed methods, alveolar volume (V_{alv}) and the average incisor inclination ($\overline{IC}$) determination, can be explained by the ambiguous identification of the alveolar housing. This is due to its close proximity with the cementum, which has similar grey values to bone [88]. Many studies have shown that full FOV, large voxel-size CBCT images (0.3-0.4mm^3), typically taken for orthodontic records, are susceptible to unreliable and inaccurate alveolar bone height measurements. This is because of factors attributed to image quality, which include condition of the soft tissues [105], the dimensions of the target tissue [57, 106], scanning parameters such as geometry and rotational distance [107], and the inherent limitations associated with artifacts and noise [89, 108]. Rater experience and subjective visual interpretation of the ROI during segmentation must also be accounted for in the context of large measurement error. An interesting study by Ballrick et al. [109] showed that at 0.4mm^3 voxel size, an interline distance of 0.86mm was necessary to distinguish four lines. The width of the periodontal ligament (PDL) has been shown to be approximately 0.3-0.5mm. Thus, it could not be distinguished at 0.3 voxels and full FOV due to the partial volume averaging phenomenon. Practically, this made it hard to distinguish cementum from alveolar bone. There are also physical limitations associated with human vision. For example, according to Kimpe and Tuytschaever [110], CBCT images can contain a minimum of 12 bits per pixel, corresponding to to 2^{12}=4096 shades of grey. At its best, the

human eye can only distinguish 700-900 shades of grey, which may contribute to within and between rater variability. It should be noted that most studies examining reliability and accuracy of linear measurements on CBCT images have been performed *in-vitro*. These studies do not take into account patient motion, which introduces significant artifacts and degradation of image quality [89, 108].

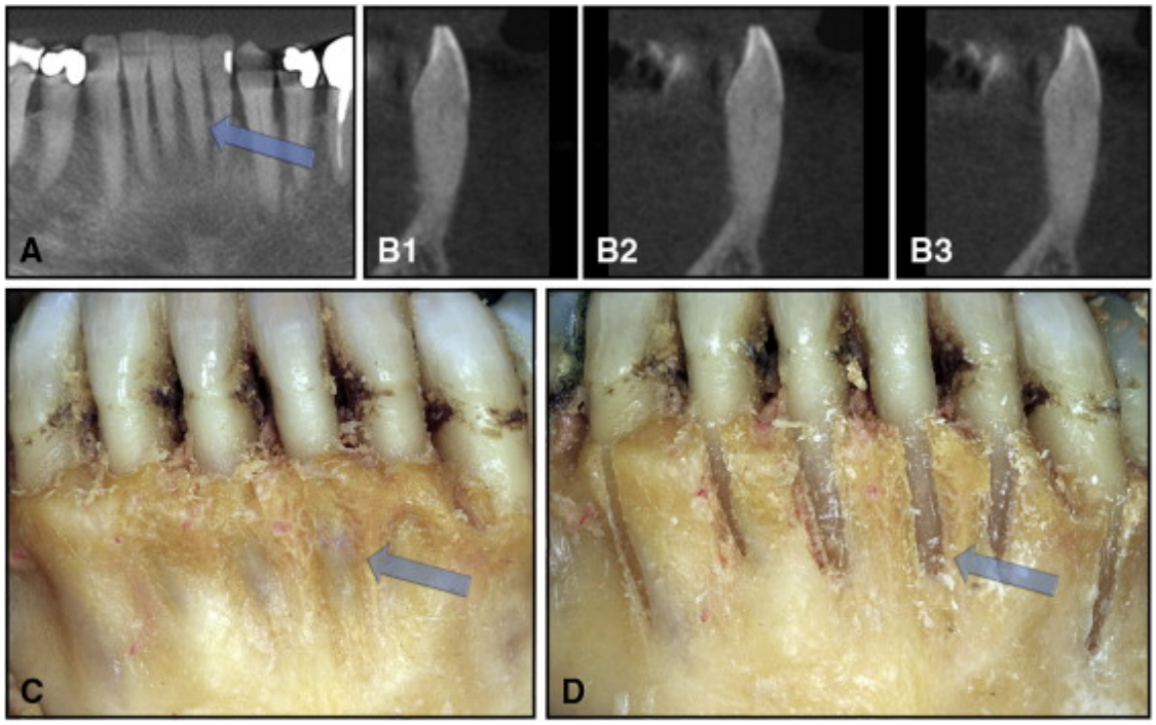

Figure 2.12: Example of the difference between clinical and radiographic finding using CBCT images. The reconstructed orthopantomogram (**A**) draws attention to tooth 3.1. **B1-B3** are 3 slices in sagittal view demonstrating no detectable bone covering. **C** represents the clinical views after gingival tissues were removed. In contrast to **C**, **D** presents the specimen with bone completely removed to create a dehiscence. 0.4mm voxel size. Figure taken from Patcas et al. [106].

Both Patcas et al. [106] and Sun et al. [57] highlighted important factors that cannot be understated. Some studies that demonstrate good linear measurement accuracy associated with low resolution CBCT images did not account for bony thickness. Both papers supported the finding that CBCT images at a voxel size of 0.4mm can overestimate marginal bone loss by as much as 2mm compared with clinical reality (i.e. cadavers) if the bone was $\leq$1mm thick. Leung et al. [56] showed that CBCT images tend to overestimate fenestrations by a factor of 3 compared with dry skull examination. It was apparent that CBCT could not detect bone less than 0.6mm thick, and at voxel size=0.38mm. Patcas et al. [106] showed that the alveolar bone over the anterior symphysis can be as thin as 0.14mm on a cadaver specimen. They also concluded the inability of CBCT images to discern the presence of bone in these areas (refer to Figure 2.12). Wood et al. [105] showed that decreasing the voxel size from 0.4mm to 0.2mm may provide better measurement accuracy

in the molar region; however, only if the gingival tissues are intact. Understandably, this cadaver study does not account for artifacts introduced by patient motion.

2.5 Conclusion

The method presented in this dissertation, used to define the boundaries of the alveolar housing around the lower incisors using the mental foramen and ptB, has been shown to be reliable. Of the six patients observed, only one patient showed a measurement error in alveolar volume as high as 12%. Reasons for this potential inaccuracy was presented. The main sources of error were attributed to the quality and resolution of the CBCT image, and the ambiguous identification of anatomical boundaries. In patients with thin biotype, there may be clinically significant ambiguity in its visual identification on CBCT images. Three-dimensional measurements of incisor pitch, or incisor proclination, was shown to be reliable both within and between examiners. Low measurement error was also demonstrated using this method.

Chapter 3

Trial Design

3.1 Introduction

This chapter presents the clinical trial conceived by Dr. Carlos Flores-Mir (CFM). The trial involved adolescent patients with mild to moderate Class II malocclusions treated with either Xbow® or Forsus™ appliances. In order to aid in transparent and accurate reporting of this randomized control trial, the CONSORT guidelines will be used as a framework for the rest of this chapter [111–113]. CONSORT, the Conslidated Standards of Reporting Trials, was developed to provide guidance to researchers in reporting their randomized clinical trials. It was adopted by the American Journal of Orthodontics and Dentofacial Orthopedics (AJO-DO) in 2004, and its use has been encouraged since 2011. Introduction of CONSORT guidelines led to improved reporting quality and facilitated successful interactions between the authors, reviewers, and editors [113].

This short chapter will introduce the design of the randomized trial, including the original objectives and randomization protocols as set by Dr. Carlos Flores-Mir (CFM). More information can be found on the ClinicalTrials.gov website (Identifier: NCT01530516).

3.2 Title

The title of the trial as registered on clinicaltrials.gov:

Crossbow® Versus Forsus™ Springs in Mild to Moderate Class II Malocclusion Cases

3.3 Objectives

Primary Outcome Measure

1. Facial soft tissue, dental and skeletal changes [Time Frame: 24 months]

   Pre- and post-treatment changes were measured from CBCT data and dental casts.

Secondary Outcome Measure

1. Root resorption [Time Frame: 24 months]

   Evaluation of the magnitude of external root resorption as quantified/qualified from the CBCT data.

2. Treatment Efficiency [Time Frame: 24 months]

   As measured by treatment outcome specifics such as total time in treatment, number and frequency of appointments, number of emergencies, and survey of patient satisfaction.

3.4 Methods

Trial Design

The trial was a single centre randomized trial consisting of two treatment groups: Forsus™ and Xbow®. The trial was conducted in Edmonton, Alberta, Canada at the University of Alberta's Graduate Orthodontic Clinic. Treatment was performed by a single-blinded investigator (CFM). Pre- and post-treatment records, which included full FOV CBCT images, were also collected. True blinding during clinical treatment was not possible because of the difference in physical design of the Xbow® and Forsus® appliances (Figure 1.7).

Changes to Trial Design

There were no changes or deviations from the original trial design.

Participants

A total of 56 adolescent participants were enrolled in this trial, which representing both sexes.

Inclusion Criteria

1. Male and female adolescent patients between ages eleven and fifteen years old.
2. Mild to Moderate Class II Division 1 malocclusion.
3. Late mixed to permanent dentitions.

Exclusion Criteria

1. Individuals with underlying syndromes.
2. Severe vertical growth patterns.

3. Individuals with craniofacial growth completed.

4. Treatment plan requiring dental extractions.

Study Settings

All trials were completed at the University of Alberta's Graduate Orthodontic Clinic in the Kaye Edmonton Clinic. Data collection began in October 2012 and orthodontic treatment was completed for the last patient by June 2018. Approximately one-fifth of the total number of patients are still within 2 years of debond (retention phase).

Interventions and Protocol

Participants were randomly assigned to one of two intervention groups:

1. **Crossbow®**, followed by full fixed edgewise appliances (refer to Figure 1.7a).

2. **Forsus™**, used in conjunction with full fixed edgewise appliances (refer to Figure 1.7b).

Both treatment groups utilized the 3M™ Unitek™ bracket system with a 0.022" slot size. Archwire sequences were as follows: 0.014", 0.018", 0.016"x0.022" nickel titanium; 0.018"x0.025" stainless steel (as needed); and 0.017"x0.025" β-titanium alloy.

Esthetic and occlusal objectives achieved for all patients followed reasonable care standards.

Consecutively treated patients meeting the inclusion criteria were assigned randomly to either the Forsus™ or Xbow® group. Extra- and intra-oral records were taken after a thorough clinical examination was completed. These included photos, impressions for dental casts, and a full FOV CBCT scan at T_1. These same records were taken again at deband (T_2).

The following exposure settings for CBCT image acquisition for both T_1 and T_2 were as follows:

Equipment: iCAT (Imaging Sciences International, Hatfield, PA)

Resolution: 0.3 voxels, 120kVp, 5mA, 8.9 seconds

FOV: Diameter 16.0cm, Height 13.3cm

Outcomes

Facial soft tissue, dental, and skeletal changes were assessed. Outcome variables were fixed at the commencement of the trial.

Sample Size

Sample size determination was based on calculations to detect 5° of inclination change of the mandibular incisors. Therefore, a minimum of 50 participants, 25 per treatment group, was required. This did not including those lost at follow-up. All in all, a total of 56 patients were enrolled in the trial.

Randomization and Blinding

None of the investigators (KC, CFM, and GCM) were involved in the randomization process. Once the participants met the inclusion criteria and provided informed consent to treatment, a third-party statistician randomly allocated patients to one of the two treatment groups using Microsoft Excel (Microsoft, Redmond, WA). A block randomization method was used to ensure equal sample size in the two groups. Assignments were concealed in a sealed envelope and numbered consecutively to ensure randomization order was followed appropriately.

3.5 Participant Flow

Figure 3.1 depicts the participant flow from initial eligibility determination, to those lost at follow-up, and finally to the number of participants that completed the trial for each group.

Of the 64 potential candidates, 8 were excluded based on ineligibility as determined during clinical screening. At follow-up, 5 patients were lost from the Forsus™ group due to the following reasons:

- One patient was not satisfied with treatment results and required extractions.
- Records could not be found for another patient post-treatment.
- The remaining 3 participants had minimal sagittal discrepancies such that Forsus™ was not required.

There were 8 patients that were lost in the Crossbow® groups due to the following reasons:

- The final CBCT image of one participant had significant distortions and could not be used.
- Two participants dropped out of the trial: one due to a potential but unconfirmed allergy, and the second patient moved away.
- The records of five other patients could not be found.

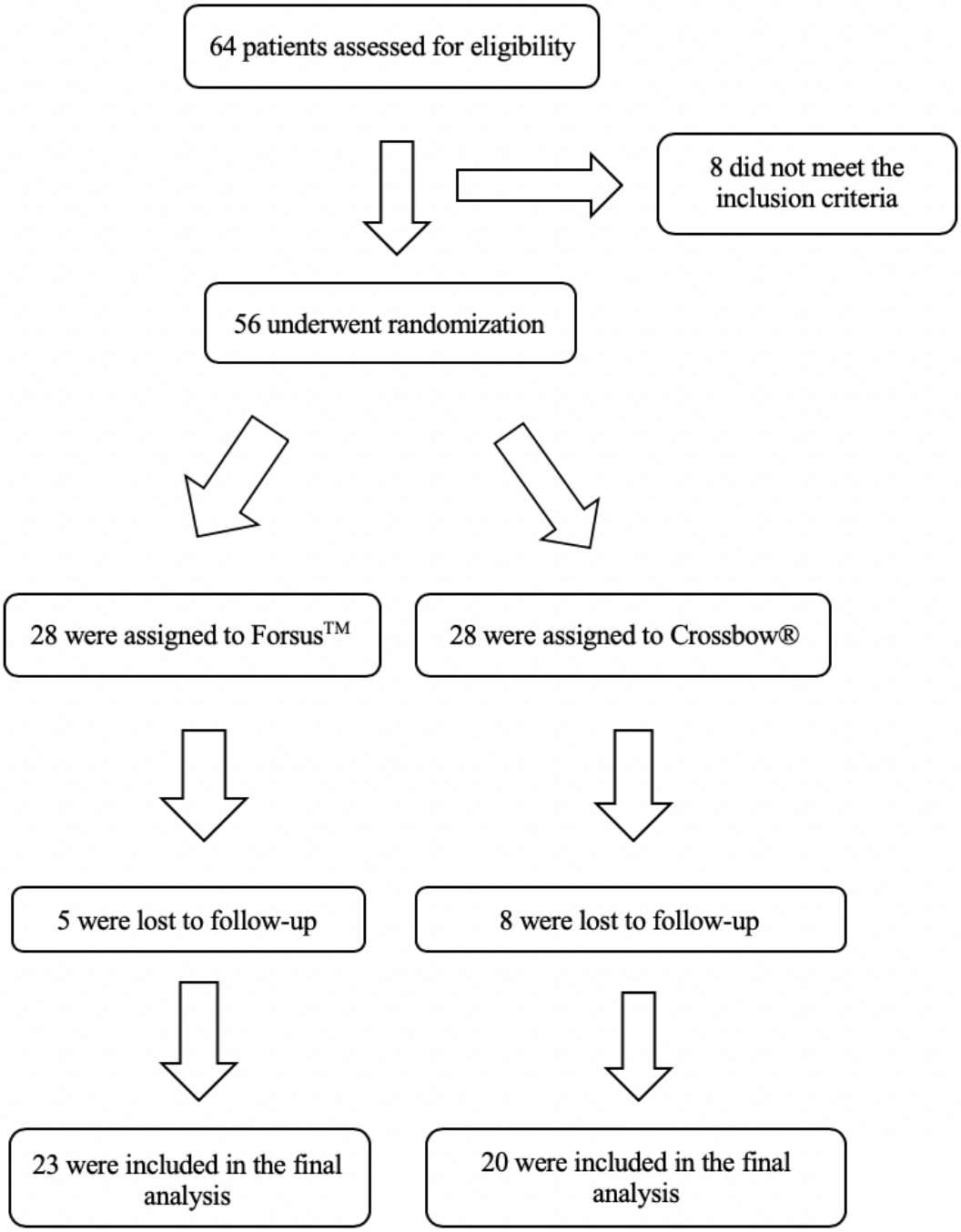

Figure 3.1: A flowchart representing participant flow in the clinical trial.

Baseline Comparisons

Both treatment groups were considered statistically equal when all the predictor variables were analyzed. These included sex, age, FMA, average incisor inclination, and alveolar volume. Descriptive statistics along with hypothesis testing at T_1 for all variables concerned can be found in Section 4.3.1 and Table 4.1.

3.6 Other Information

Registration

This trial was approved by the Human Ethics Research Office at the University of Alberta, Pro00023805.

Funding

No external funding was received.

Chapter 4

Clinical Study

4.1 Introduction

The primary objective of this study was to determine the response of the alveolar housing supporting the mandibular incisors as a result of orthodontic treatment. Volume was used as a proxy to describe changes in the alveolar bone quantity. Closely related was the secondary objective; to determine the change in lower incisor inclination in response to orthodontic treatment. CBCT offers an advantage over traditional imaging modalities because it allows for visualization of each individual incisor. The method developed to measure the change in inclination of each individual tooth in 3-dimensions was presented in Chapter 2. Because the lower incisors usually procline as an effect of fixed appliances [114], it was also prudent to study incisor proclination as not only a predictor of alveolar response, but also as an outcome measure.

A survey of literature did not reveal any studies examining proclination of each individual mandibular incisor in response to Class II orthodontic management. Most studies used traditional lateral cephalometry to determine incisor angulation despite superimposition of structures. Miller et al. [115] showed no differences in lower incisor to mandibular plane angle (IMPA) between Forsus™ and Xbow®. Flores-Mir et al. [45] showed that in patients where Xbow® was employed to correct a mild to moderate Class II malocclusion, there was a significant increase in IMPA by an average of 3.6° compared with control, and a significant reduction in overjet compared to baseline. Aziz et al. [116] showed that lower incisors proclined approximately 3° in response to Xbow® treatment. However, they could not show any clinically significant pre-treatment cephalometric measurements that could predict incisor response. Systematic reviews regarding Herbst appliances, a type of fixed Class II corrector, have been unanimous in concluding lower incisor proclination and protrusion as a response to treatment [47, 48]. D'Antò et al. [117] performed a comprehensive systematic review, looking at all functional Class II orthopedic appliances and found some evidence of consistent lower incisor proclination.

Given the limitations associated with a traditional 2-dimensional cephalogram, inclina-

tions of individual teeth cannot be measured accurately. This is due to superimposition of adjacent hard and soft tissues. Slice-by-slice analysis of lower incisors, which can be obtained from CBCT images, can provide additional insight into angulations of individual teeth. However, inclinations are still measured in views parallel to the patient's mid-sagittal plane, and not necessarily perpendicular to the curvature of the mandibular symphysis. The method, as outlined in Section 2.2.4, allowed the incisor inclination to be described using Euler's angles. Euler's angles allowed for inclination of an incisor to be described in 3-dimensional space relative to a reference plane as components of 3 angles: yaw, pitch, and roll. Of the three angles, the pitch angle is the 3-dimensional analogue to traditional inclination measurements, or movement in the 3rd order.

The discussion around orthodontic treatment, specifically labial movement of lower incisors and its relationship with gingival recession, has been controversial in the orthodontic literature [42]. Earlier studies have suggested an association between the two [28, 32]; however, this has been questioned by more recent studies. Some studies showed pre-existing fenestrations and dehiscences prior to the start of treatment [67]. Nevertheless, CBCT has been previously employed to study the buccal bone pre-, mid-, and post-orthodontic treatment.

The goals of this clinical study was twofold: firstly, to apply the method developed in Section 2.2 to quantify volumetric changes in the bony alveolar housing around the mandibular incisors; secondly, to determine the changes to incisor inclination after Class II correction using Forsus™ and Xbow® appliances. Instead of multiple linear measurement, the method employed volumetric measurements as a proxy for overall bony response.

4.2 Methods

Methods developed in Chapter 2 were applied to extract data from pre- and post-treatment CBCT records, which were collected as part of the study evaluating clinical effects of Xbow® and Forsus™ as detailed in Chapter 3.

4.2.1 Collection of Data

For each patient that participated and completed the study, the following parameters were collected:

1. Frankfort-Mandibular Plane Angle (FMA)
2. Appliance Type (App)
3. Average Incisor Inclination at T_1 ($\overline{IC}_{T_1}$)
4. Average Incisor Inclination at T_2 ($\overline{IC}_{T_2}$)
5. Alveolar volume at T_1 ($V_{alv_{T_1}}$)

6. Alveolar volume at $T_2 (V_{alv_{T_2}})$

4.2.2 Calculation of Variables

The average change in incisor inclination was calculated with the following formula:

$$\overline{\Delta IC} = \overline{IC}_{T_2} - \overline{IC}_{T_1} \tag{4.1}$$

where $\overline{IC}_{T_1}$ is the average incisor inclination of the mandibular incisors measured in 3-dimensional space pre-treatment, and $\overline{IC}_{T_2}$ is the average incisor inclination of the mandibular incisors post-treatment.

The percentage change in alveolar volume over the course of treatment was calculated with the following equation:

$$\%\Delta V_{alv} = \left(\frac{V_{alv_{T_2}} - V_{alv_{T_1}}}{V_{alv_{T_1}}} \right) 100\% \tag{4.2}$$

where $V_{alv_{T_1}}$ is the alveolar volume measured in 3-dimensions pre-treatment and $V_{alv_{T_2}}$ is the alveolar volume measured in 3-dimensional space post-treatment. Refer to Section 2.2 for the developed technique used to segment, define, and measure alveolar volumes.

4.2.3 Hypothesis Testing

The decision to use a specific statistical test was dependent on the question to be answered. The number of independent and dependent variables influenced the type of analysis chosen. The significance level for all tests were set to $\alpha = 0.05$.

Refer to Appendix A and Appendix B for complete data tables and specifics associated with hypothesis testing.

An omnibus multivariate analysis of variance (MANOVA) was used to determine differences in FMA, average incisor inclination, and alveolar volume prior to treatment in order to ensure homogeneity between intervention groups.

Given significant issues with multicollinearity, t-tests were used instead of MANOVA to determine whether there were significant changes to incisor inclination of teeth 3.1 and 4.1. A Wilcoxon Signed-Rank test had to be used for the mandibular lateral incisors due to violations in normality. A one-way ANOVA was used to determine whether changes between the incisors were different from each other. A Mann-Whitney U test was employed to determine differences between Forsus™ and Xbow® groups.

The second part of the study was to determine whether a difference existed between pre- and post-treatment alveolar volume. A non-parametric Wilcoxon Signed-Rank test was used to elucidate the overall bony response due to the unsuitability of a one sample t-test. Follow-up hypothesis testing using multiple linear regression was used to determine

Table 4.1: Descriptive statistics of the collected variables at baseline (T_1). FMA is the Frankfort-Mandibular plane angle, $\overline{IC}_{T_1}$ represents the average inclination of the mandibular incisors relative to a reference line defined in Section 2.2.4, and $V_{alv_{T_1}}$ is the volume of the alveolar housing pre-treatment.

	Forsus (N=23) Male=8 Female=15		Xbow (N=20) Male=9 Female=11		Total (N=43) Male=17 Female=26	
	Mean	SD	Mean	SD	Mean	SD
Baseline Factors						
Age (years)	13.90	1.26	13.10	0.92	13.53	1.18
FMA (°)	21.31	6.52	19.54	6.43	20.49	6.46
$\overline{IC}_{T_1}$ (°)	128.78	10.44	131.48	13.59	130.03	11.93
$V_{alv_{T_1}}$ (mm^3)	1936.82	815.51	1787.93	482.37	1867.57	677.70

if any factors such as appliance type, FMA, and $\overline{\Delta IC}$ could predict the response of the alveolar housing supporting the lower mandibular incisors (i.e. $\%\Delta V_{alv}$).

4.3 Results

The results were organized into two sections for clarity. The first section looked at changes in incisor inclination as the outcome measure, and the second studied the response of the alveolar housing to Class II orthodontic correction. For descriptive statistics of the collected data, refer to Table 4.2.

4.3.1 Pre-treatment Comparisons

Descriptive statistics for the clinical data at baseline are presented in Table 4.1. There were no differences between the Forsus™ and Xbow® groups in all the pre-treatment factors combined, $F(4, 38) = 2.46, p = 0.062 > 0.05; Wilks' \Lambda = 0.794; partial\eta^2 = 0.206$. A test of two proportions using the χ^2 test of homogeneity revealed no differences in gender between Forsus™ and Xbow® groups ($p = 0.494$). Therefore, the groups can be considered equal prior to the start of treatment. There were approximately 1.5 times the number of females enrolled in each group than males. The average age at the beginning of the study was 13.53 ± 1.18 years.

4.3.2 Response of the Mandibular Incisors

There was strong evidence that all four mandibular incisors experienced a significant change in response to orthodontic treatment ($p < 0.001$). Incisors 3.1 and 4.1 proclined an average of $8.18°(95\%CI, 5.28° - 11.08°), t(42) = 5.70, p < 0.001$ and $8.42°(95\%CI, 5.67° -$

Table 4.2: Descriptive statistics of the collected data. The mean, median, and standard deviations are summarized and grouped according to the appliance type.

	Forsus (N=23)			Xbow (N=20)			Total (N=43)		
	Mean	Median	SD	Mean	Median	SD	Mean	Median	SD
FMA (°)	21.31	19.70	6.52	19.54	19.70	6.43	20.49	19.70	6.46
$\overline{\Delta IC}$ (°)	10.51	11.51	8.64	7.28	6.98	8.75	9.01	7.29	8.74
$\%\Delta V_{alv}$	0.37	1.81	9.89	10.08	7.54	14.01	4.89	4.55	12.80

Table 4.3: Descriptive statistics of the changes in incisor inclination relative to the defined plane established in Section 2.2.4. ΔIC_x represents the change in incisor inclination where "x" is the tooth number. $\overline{\Delta IC_{32,31,41,42}}$ is the change in inclination of all four incisors averaged. All measurements are in °.

	Forsus (N=23)			Xbow (N=20)			Total (N=43)		
	Mean	Median	SD	Mean	Median	SD	Mean	Median	SD
ΔIC_{32}	10.74	11.57	8.61	8.26	7.82	9.08	9.58	8.63	8.82
ΔIC_{31}	9.85	11.63	9.85	6.26	6.43	8.73	8.18	7.77	9.41
ΔIC_{41}	9.39	10.24	8.75	7.30	6.49	9.27	8.42	7.57	8.95
ΔIC_{42}	12.08	11.81	9.37	7.31	7.48	8.72	9.86	8.59	9.28
$\overline{\Delta IC_{32,31,41,42}}$	10.51	11.51	8.64	7.28	6.98	8.75	9.01	7.29	8.74

$11.18°), t(42) = 6.17, p < 0.001$ respectively. A Wilcoxon Signed-Rank test revealed that tooth 3.2 and 4.2 presented with significant increases in median ΔIC. The median increase in inclination of tooth 3.2 and 4.2 were $8.63°, Z = -5.06, p < 0.001$, and $8.59°, Z = -.488, p < 0.001$, respectively. There was no evidence that the ΔIC between the lower four incisors were different from each other, $F(3, 168) = 0.360, p = 0.782$. When comparing Forsus™ and Xbow® appliances, there was no evidence that the medians of $\overline{\Delta IC}$ were different, $U = 281, p = 0.214$. Refer to Table 4.3 for the descriptive statistics.

4.3.3 Response of the Alveolar Housing

The median increase in the volume of the alveolar housing was 4.55%, $Z = -2.113, p = 0.035$ which was similar to the mean increase of 4.89% ± 12.80% (refer to Table 4.2). In order to determine how appliance type, face height (FMA) and incisor proclination ($\overline{\Delta IC}$) influenced the bony response, a mathematical model based on multiple linear regression analysis was developed. Refer to Equation (4.3). The change in incisor inclination ($\overline{\Delta IC}$) was the only factor studied that was predictive of alveolar volume ($p < 0.05$). Refer to Table 4.4 for the result of multiple linear regression analysis.

Table 4.4: Results of the Multiple Linear Regression Analysis using Equation (4.3) as the selected model.

			95% Confidence Interval	
Factor	Coefficient	p-value	Lower Bound	Upper Bound
(Constant)	5.982	0.520	-12.658	24.621
App	-6.372	0.612	-31.613	18.868
FMA	-0.035	0.928	-0.110	0.741
$\overline{\Delta IC}$	-0.463	0.037	0.897	-0.029
App x FMA	0.743	0.206	-0.425	1.912

$$\mu\{\%\Delta V_{alv}|App, FMA, \overline{\Delta IC}, AppxFMA\} = 5.982 - 6.372App - 0.035FMA - 0.463\overline{\Delta IC} + 0.743(AppxFMA) \quad (4.3)$$

Given that only one of the factors was significant, the model was further simplified, and is represented in Equation (4.4). A scatter plot of $\overline{\Delta IC}$ vs. $\%\Delta V_{alv}$ was created and a line of best fit drawn in order to study the linear relationship between the two (Figure 4.1).

Therefore, appliance type (Forsus™ or Xbow®) and face height were not shown to be predictive of alveolar volume changes, nor was their interaction. There was, however, an inverse relationship between incisor proclination and the alveolar response.

$$\mu\{\%\Delta V_{alv}|\overline{\Delta IC}\} = 9.25 - 0.48\overline{\Delta IC} \quad (4.4)$$

4.4 Discussion

The result of this study supported the findings of Miller et al. [115]: there were no differences in incisor proclination between Forsus™ and Xbow® treatments in mild to moderate Class II patients. Furthermore, the study also showed no differences in incisor proclination (ΔIC) between teeth 3.2, 3.1, 4.1, and 4.2. Therefore, further analysis using the average change in incisor inclination ($\overline{\Delta IC_{32,31,41,42}}$) was justified.

The primary outcome measure was to determine how alveolar volume changes in response to orthodontic Class II correction. Not only does the clinician have to consider whether orthodontic treatment will result in acceptable facial esthetics, determination of whether teeth can be moved within physiological limits without creating iatrogenic tissue loss is vital to treatment success. Determination of this boundary has been quite elusive, with no definitive guidelines; its importance in determining whether a case can be orthodontic camouflaged or surgery is required cannot be understated. One of the earlier

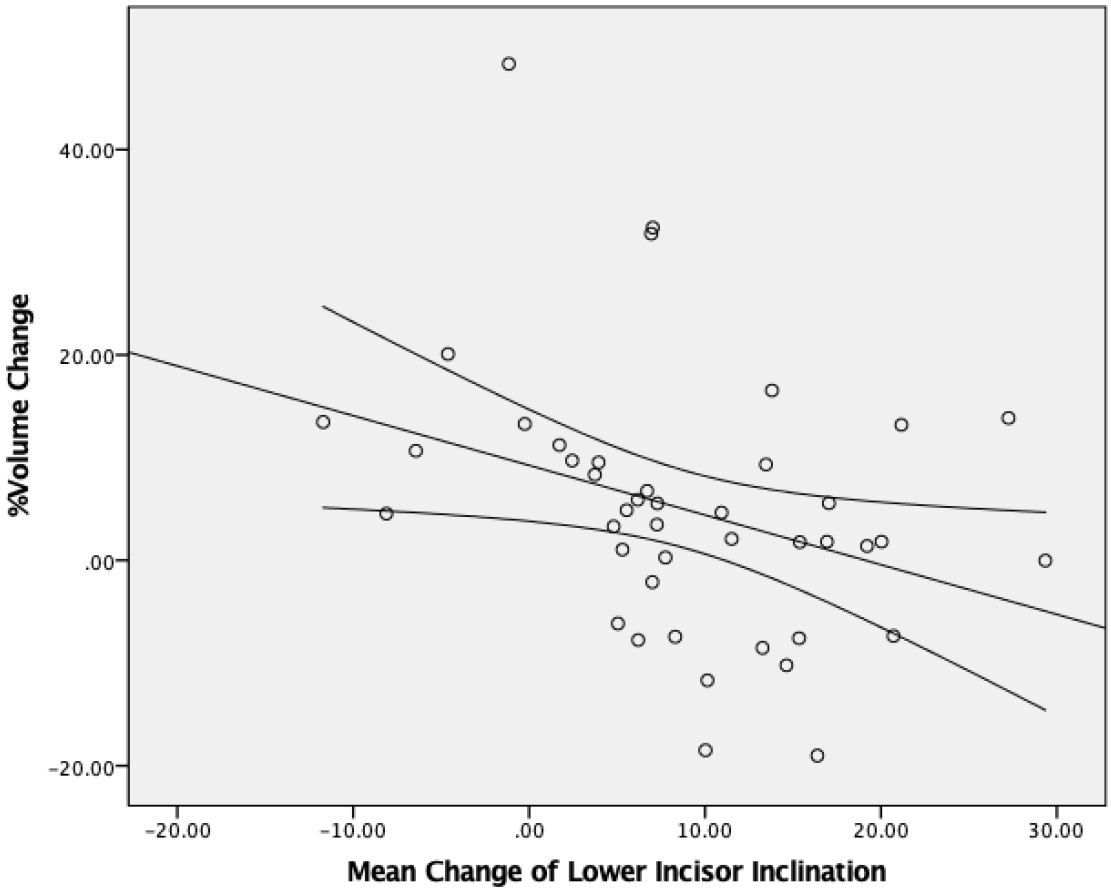

Figure 4.1: Scatter plot of $\overline{\Delta IC}$ vs. $\%\Delta V_{alv}$. The equation of the regression line, $\mu\{\%\Delta V_{alv}|\overline{\Delta IC}\} = 9.25 - 0.48\overline{\Delta IC}$, along with bands representing the upper and lower bounds of the 95% confidence interval is shown. R^2 linear = 0.11.

studies looking at the response of the maxillary anterior alveolus in bimaxillary protrusive patients suggested that the bony limits of tooth movement was the width of the bone at the apex (refer to Figure 4.3). The alveolus mid-root and the marginal ridge could remodel as teeth were retracted palatally [6]. Handelman [118] described a method to measure the width and height of the alveolar housing using lateral cephalograms. The width of the alveolus was divided into labial and lingual components based on the location of the incisor root apex (refer to example Figure 4.2).

It was also important to answer whether face height, type of appliance, incisor proclination, or any of these combinations could be used to predict the alveolar response [27]. Handelman [118] showed that the width of the alveolus could be related to the vertical facial height of the patient. In Class I, II, and III individuals, thin alveolar widths were found in high angle cases. However, this was rarely seen in patients with brachyfacial types and in Class I normofacial individuals. Enhos et al. [67] found that brachyfacial patients tended to have less dehiscences compared to normo- and hyperdivergent patients prior to the start of orthodontic treatment. There were no differences in fenestrations between different vertical facial types. It is important to point out that dehiscences nevertheless may exist in individuals prior to orthodontic treatment [62, 67]. Evangelista et al. [62] found no differences in alveolar defects among different facial types. None of the above mentioned studied looked at changes in alveolar dimension in response to orthodontic treatment. However, Mazurova and colleagues followed a cohort of 177 individuals through to the end of treatment, and until 5 years post-treatment [69, 70]. There was no evidence in their clinical data that suggested vertical facial types were predictive of the occurrence of gingival recession.

Due to the inherent limitations associated with conventional lateral cephalograms-namely superimposition of soft and hard tissues-a 2-dimensional representation of a 3-dimensional reality may not be accurate or suitable. More recent studies have used techniques similar to the one described by Handelman [118] to measure the width of the dento-alveolus using sagittal CBCT sections [66, 119–121]. Nevertheless, these studies employed selected slices to represent the condition of the entire volume. Linear measurements may not be the most appropriate measure to describe a 3-dimensional body. The idea of using volumetric measurements as a proxy for bone quantity stemmed from a previous *ex-vivo* study that compared volume of extraction sockets in the mandible. Volumes were measured using CBCT images and compared with physical measurement using a water displacement technique [122]. No difference in measurements were found between those obtained by CBCT and physical measurements. The evidence suggested that volumetric measurements could provide insight into the condition of the alveolar bone. For example, Agbaje et al. [122] concluded that if the volume of the bony socket decreased, this could be indicative of bone infill and healing. Interestingly, the variability between measurements in the Agbaje et al. [122] study was found to be between 0.27%-8%, which was similarly found in the previous chapter (Table 2.5).

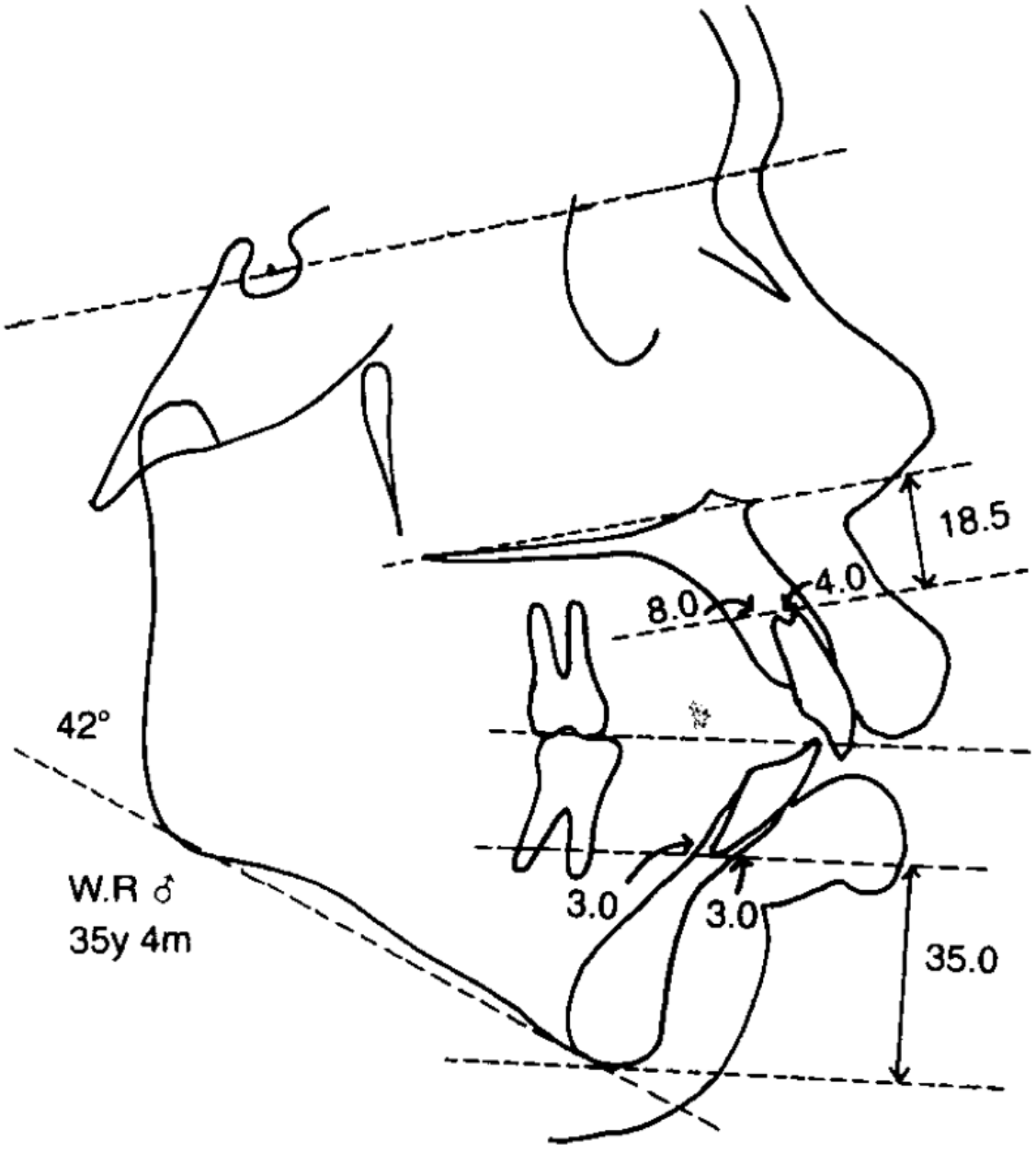

Figure 4.2: A common method cited by many studies in order to determine the width of the alveolar housing, as measured on a lateral cephalogram. The boundary of the labial and lingual components of the anterior alveolus is demarcated by the position of the root apex. Image taken from Handelman [118].

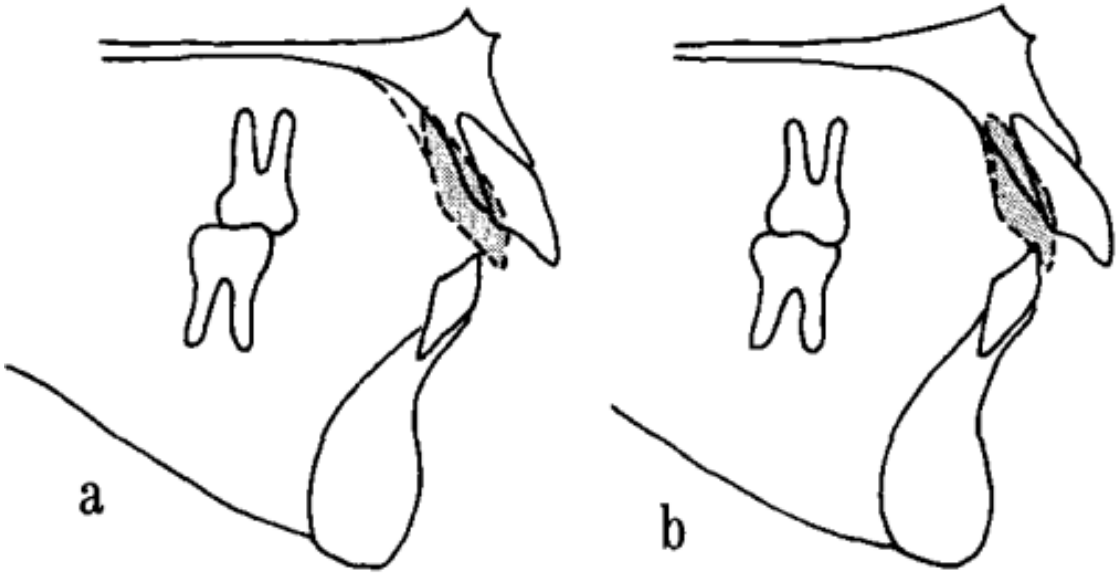

Figure 4.3: Two assumption of the remodelling of the dento-alveolar complex in response to orthodontic movement proposed by Edwards [6] . **A:** A false assumption where the entire alveolus can remodel around the new position of the incisor. **B:** Only the mid-root and marginal alveolus can remodel, while the bone at the level of the apex does not remodel and is the limit of orthodontic tooth movement. Images taken from Handelman [118].

The results presented found that the median change of the alveolar housing pre- to post-treatment was 4.55%, which was similar to the mean increase of 4.89% (Section 4.3.3). However, this result must be taken into context of the variability as seen by the large standard deviation of the mean (Table 4.2), and also the large measurement error (Tables 2.5, 2.7). There was evidence that an adaptive process may occur where bone labial to the proclining incisors remodel while the lingual contours of the bone remain unchanged. However, the ability of the alveolar bone to adapt to changes in arch length have not been sufficiently documented in literature [27]. Classic studies, such as those by Thilander et al. [29] and Wennström et al. [28], suggest the ability of connective tissue to regenerate, provided that teeth are moved back within the alveolar boundary and in the absence of gingival inflammation. However, these studies were performed in controlled environments with small sample sizes. The contemporary understanding of the bony response to movement of teeth outside the alveolar boundaries is that fenestrations and dehiscences can occur, but this does not always result in clinically significant changes such as gingival recession [27, 37, 123]. Other factors such as oral hygiene, traumatic occlusions, eccentric tooth positions, pre-existing fenestrations and dehiscences, and gingival biotype may contribute to clinically significant retraction of gingival tissues and exposure of the roots [124].

It was possible that the detected increase in alveolar volume was due to natural growth, which could have been accounted for had a control group been included. For example, Flores-Mir et al. [45] included age-matched samples from the Burlington Growth Centre. Also, a change of 4.55% may not be clinically significant given the uncertainty in measurement accuracy. The error was as high as 12% (Table 2.5) and, as previously mentioned in Section 2.4, was due to the ambiguity in interpreting the CBCT image itself. Figure 4.4 depicts two volumes of the mandibular symphysis constructed from the same post-treatment CBCT image. The segmentations were taken 1 week apart to allow an adequate washout period. Note the marked presence of dehiscences and fenestrations in Figure 4.4a compared to Figure 4.4b. The ambiguity in interpreting bony boundaries could have resulted in measurement imprecision. Scarfe and Angelopoulos [125] noted that artifacts such as partial volume averaging, patient motion, artifacts from surrounding soft tissue, and inherent artifacts caused by physical properties of beam attenuation may lead to imprecisions with interpretation. This could also have accounted for the low R^2 value observed in Figure 4.1, where the average change in incisor inclination $\overline{\Delta IC}$ accounted for approximately 11% of the variation in $\%\Delta V_{alv}$.

One approach to determine whether the imprecision of the method was due to ambiguity of image interpretation or systematic errors in the method itself, would be to determine a "gold standard" by which to compare repeated measurements. One way to minimize artifacts is to increase the energy of the beam by increasing kVp or mA, resulting in better resolution and minimized scatter. Smaller voxel sizes would result in increasing interpretation accuracy; however, this exposes patients to high levels of ionization radiation

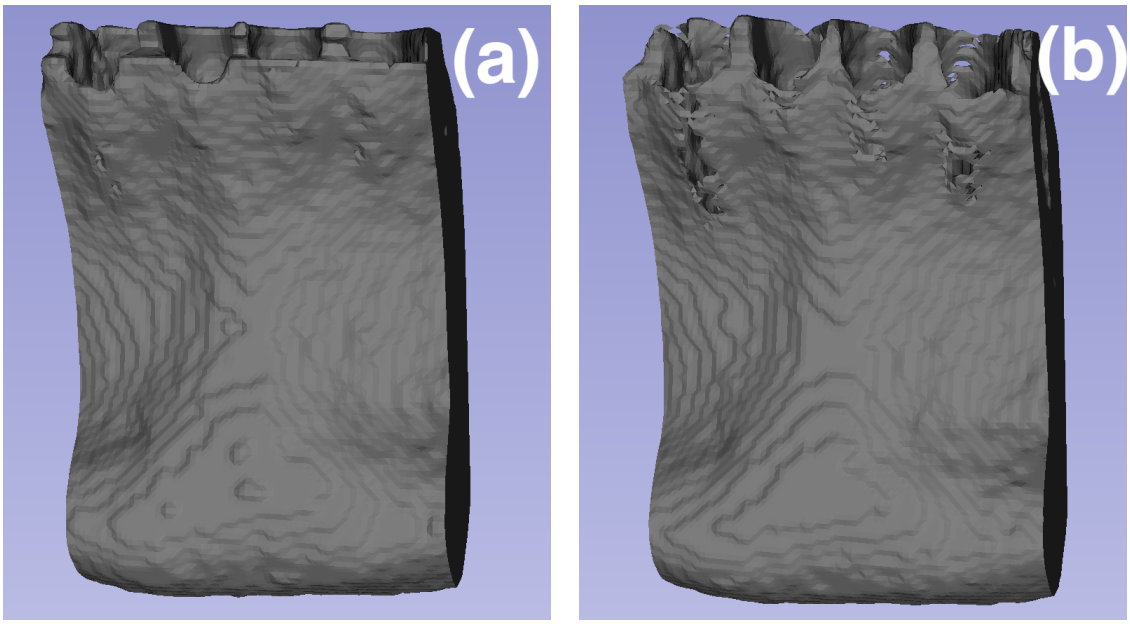

Figure 4.4: An example of repeated measurements on the same post-treatment CBCT image taken one week apart. The images represent the entire mandibular symphysis with boundaries clipped using the method defined in Section 2.2.5. (a): No fenestrations or dehiscences noted. (b): Fenestrations and dehiscences noted over the mandibular incisors. Remarkable fenestrations noted over teeth 3.2 and 4.2.

which could not be justified according to the ALARA principle [126–129]. Future ex-vivo studies on cadaver or animal models could be carried out to determine the clinical validity and accuracy of the method. There have been numerous studies that have compared volumetric measurements of CBCT images to the object in question using the water displacement technique. For example, Liu et al. [130] compared the volumes of extracted teeth to volumes obtained using CBCT images. García-Sanz et al. [131] and Bayram et al. [132] used the water displacement technique to compare mandibular condyles, and Agbaje et al. [122] looked at the volume of extraction sockets. All the above studies were *in-vitro* studies which demonstrated good accuracy compared to the gold standard. Given that there are additional artifacts seen in CBCT images taken *in-vivo*, such as those produced by patient motion and peri-oral soft tissues, the clinical applicability of the aforementioned studies are questionable [125].

The results of this study supported the conclusions drawn by Mazurova et al. [70] where vertical facial type, as represented by FMA, was not a predictor for alveolar bone response. There was moderate evidence that incisor proclination was predictitve of bony response: an inverse relationship was noted (Figure 4.1). This is supported by earlier animal studies by Batenhorst et al. [31] and Steiner et al. [32] that showed an increased incidence of gingival recession when incisor teeth were moved labially. Årtun and Krogstad [36] showed negative periodontal effects associated with incisor proclination. However, Ruf et al. [37] did not find any evidence of recession in their sample. Renkema et al. [41]

also found no gingival recession at 5-year follow-up compared with the control group. This study seemed to suggest that for every 10 degrees of incisor proclination, the volume of the alveolar housing was predicted to decrease by 4.45%.

If $\overline{\Delta IC} \leq 10.93^{\circ}$, then $\%\Delta V_{alv} > 0$ at the lower bound of the 95% confidence interval (Figure 4.1). In other words, there was evidence that if the incisor were to be proclined more than approximately 11°, loss of alveolar volume $\%\Delta V_{alv} < 0$, and thus bone loss was likely. This result supported a previous study by Årtun and Krogstad [36] that suggested incisor proclination of more than 10° resulted in gingival recession.

It is just as important to recognize that an increase in alveolar bone volume ($\%\Delta V_{alv} > 0$) did not necessarily equate to the absence of bone loss. It depended on where this new bone volume was distributed. For example, if bone was deposited lingually to the labially displaced incisors, or in the inter-radicular regions during arch width increases, labial bone loss would still have been likely despite bony volume gains. Perhaps, there was an adaptive process where the alveolus remodels around the labially displaced roots as proposed by Edwards [6]. As such, development of 3-dimensional shape analysis tools would be helpful to visualize distribution of bony volume. The use of high definition imaging modalities would also be helpful to precisely identify bony contours in thinner regions such as the mandibular alveolus.

Investigation into the relationship of volumetric changes to clinical relevance could be determined in the future. An experimental design could include a survey of periodontists and orthodontists to determine the threshold at which the percentage volume change is recognized to be clinically relevant. Establishing an association between $\%\Delta V_{alv}$ and clinical measurements may also test the validity of using measured volumes as a model for clinical realities.

Given the large amount of variation in measured volumes, and the fact that only 11% of it could be accounted for by $\overline{\Delta IC}$, the result of the multiple linear regression (Equation (4.4)) may not be useful to predict the response of the alveolar housing as a function of incisor proclination. In their systematic review, Aziz and Flores-Mir [42] found no association between appliance-induced labial movement of incisors and gingival recession. Other factors that may be considered for future studies could be gingival biotype, oral hygiene control, and alveolar width. The use of higher quality CBCT images should also help. Increases in measurement precision should result by improving image quality and decreasing ambiguity in determining bony boundaries,

4.5 Conclusion

The present study found that all mandibular incisors proclined in response to Forsus™ or Xbow®. However, there were no significant differences in incisor proclination among the incisors, and also between the two appliances in question. Therefore, using the mean proclination to represent all mandibular incisors was justified.

In response to Class II correction, the volume of the alveolar housing increased by a median of 4.55%. Given the uncertainty associated with the high measurement error, this result may not be clinically significant. The increase in volume may suggest an adaptive mechanism in which bone volume is maintained labial to orthodontically moved incisors. However, without a control group, this conclusion cannot be made definitively as volume increases due to natural growth - eruption of the incisors and increases in the transverse dimension - may account for this change.

Appliance type and vertical face height (FMA) could not be used as predictors of bony response. However, there was moderate evidence that there was a linear relationship between the average change in incisor inclination and percent alveolar volume change. For every 10° of proclination, the volume of the alveolus decreased by 4.45%. The data also suggested that the lower incisors should be proclined no more than 10.93° to avoid bony volume loss.

Prospective follow-up studies may include control groups to determine the amount of volume change contributed by natural growth alone. Other predictive factors which may be studied include oral hygiene, gingival biotype, and probing depths. Employing smaller FOV CBCT images or other imaging technologies for future studies should improve image quality, while keeping ionizing radiation exposure to a minimum in order to reduce error in image segmentations.

Chapter 5

Overall Discussion and Conclusions

5.1 Introduction

The prominent role that technology plays in orthodontics is undeniable. Prime examples include clear aligner therapy based on CAD-CAM systems, as well as diagnostic modalities that include CBCT imaging, 3-dimensional modelling, and manipulation techniques used for orthodontic and surgical predictions [44, 74, 133]. The fascination and appeal with employing these new tools in clinical practice has clear advantages. However, a thorough understanding of its effectiveness, limitations, and potential to do harm - especially over traditional standard of care - should not be understated.

Proponents for the routine use of CBCT imaging modalities as part of comprehensive orthodontic care argue that significantly more diagnostic information can be obtained than traditional lateral cephalograms and panoramic radiographs [17]. However, this point of view is not shared by the AAOMR, and in their positional statement justified the use of CBCT on a case-by-case basis. The majority of individuals treated in orthodontics fall into an age group of high susceptibility to ionizing radiation. As per the ALARA principle, only situations where CBCT imaging provides a justifiable benefit over traditional radiographic modalities should it be prescribed [12]. Scenarios in literature that supported a limited FOV CBCT exposure include ectopically erupting teeth and dental impactions, orthognathic surgery, and TMD [12, 14–16].

A practical concern associated with comprehensive orthodontic care is the development of periodontal recession. Particularly, in Class II dental camouflage, mandibular incisors may be moved beyond their anatomical boundaries, predisposing the overlying periodontium towards bony dehiscences, fenestrations, and gingival recession [7, 27]. Some have proposed diagnostic advantages associated with CBCT imaging in order to better understand such scenarios [19, 20]. However, most of these studies were performed *in-vitro* with limited clinical applicability. In fact, the relationship between orthodontics and iatrogenically-induced gingival recession has been controversial. A survey of literature reveals early animal studies and clinical trials with results contradictory to one another

(refer to Section 1.3). Recent systematic reviews showed no direct relationship between the amount of incisor proclination - or labial movement of the incisors - and the width of attached gingival tissue. Admittedly, the studies included in these reviews presented low levels of evidence because of their methodological limitations associated with questionable outcome measures [42, 43]. Studies employing CBCT methodologies reported evidence of pre-existing bony defects, which included dehiscences and fenestrations, prior to orthodontic treatment (refer to Section 1.4.1). There appeared to be a relationship associated with different vertical facial patterns, such as short faces presenting with lower prevalence of bony defects compared with normal and long faces [67, 68]. Single slice analysis, which usually consisted of selecting one or several slices best representing the mandibular symphysis as a whole, was employed in these studies (Figure 1.8).

The primary goal of this study aimed to assess changes in the bony alveolus around the mandibular incisors in response to Class II orthodontic camouflage. With this goal in mind, volumetric change around these teeth was used as a proxy for alveolar response. Appliance type, facial height, and incisor inclination, three factors which have been suggested in literature to be prognostic indicators for gingival recession, were also assessed. This study also presented the opportunity to measure mandibular incisor inclinations independently from one another in 3-dimensional space, comparing their response to two different Class II correctors: Forsus™ and Xbow®.

5.2 General Discussion

As previously stated, the goal of this thesis was to study the alveolar response of the mandibular symphysis to orthodontic movements of the lower incisors. Volumetric measurements were chosen as a proxy to describe the changes in bony response over linear measurements for the following reasons:

1. CBCT offers distinct advantages over 2-dimensional imaging methods because it allows for study and analysis of 3-dimensional realities. Volume is more meaningful compared to linear measurements in quantification of 3-dimensional objects.

2. Many previous studies have selected one or a few slices which best represents the ROI as a whole. This process is subjective and hard to replicate within and between investigators. For example, the mandibular symphysis may consists of over 100 sagittal slices, and the selection of a few slices may not reflect the realities of the whole.

3. Pre- and post-treatment changes would be harder to quantify if linear measurements were to be used. This is due to increased chances for methodological error. The same pre- and post-treatment slices would need to be used in order to visualize change, which may not be appropriate if growth of the ROI is expected. In addition, any errors in landmarking and measurements may significantly affect the results.

In the context of the reasons presented above, careful consideration for exposing the participants to increasing levels of ionizing radiation compared with conventional radiography was balanced by the need to obtain data. Records required for comprehensive orthodontic care, which included lateral cephalograms and orthopantomograms, were constructed from the CBCT images. This negated the need for additional radiographic records. Every effort to reasonably minimize risk to the patients were taken, which included the prescription of a low resolution protocol.

In order to quantify the volume of the alveolar housing supporting the mandibular incisors, the first logical step was to define its boundaries using stable landmarks. Three points were chosen based on their proximity to the ROI, as well as their relative stability over time. The left and right mental foramen were chosen to define the lateral boundaries based on the work of de Oliveira Ruellas et al. [76], who showed that the body of the mandible could be used for superimposition. Lagravère et al. [99] also demonstrated that the distance between the left and right mental foramen only increased by 0.5mm during the peak of growth. B-point was chosen to define the inferior boundary of the alveolus given its proximity to the boundary between the basal and alveolar bone. It is also routinely used in cephalometric measurements and thus was a convenient landmark. Figure 2.11 represents the migration of B-point during growth from childhood to adolescence. Based on serial lateral cephalometric studies,Buschang et al. [100] found that B-point migrated superiorly by 0.5mm per year and lingually by 0.3mm during the pubertal growth spurt. Considering an average treatment time of 24 months, these increases may not be clinically significant.

Intra- and inter-examiner reliability of the proposed method was good with lower-bound ICC values above 0.75 (Table 2.8) for both quantification of the alveolar volume (V_{alv}) and incisor inclination ($\overline{IC}$). This can be visualized when measurements of the two investigators are plotted against each other and compared to a 45° line (Figure 2.9). Nevertheless, a large variation in volume measurement errors was seen ranging from as low as 1.5% to 12%. More precision was seen with incisor inclination measurements, with a range between 0.07% and 8.25% (Table 2.5, 2.7).

Applying the new method to a clinical sample showed that the alveolar volume increased by 4.55% after orthodontic treatment, in response to an average proclination of mandibular incisors by 9°. With this result, and assuming that the lateral boundaries remain stable between T_1 and T_2, it can be concluded that bony deposition occurred as the incisors were displaced forwards. It could also imply an adaptive mechanism, allowing bone to be maintained labial to the incisors as they were being pushed forwards. This supported an early theory proposed by Edwards [6]. However, given the uncertainty in the measurement, drawing this conclusion was too assumptive and premature.

It was also interesting to note that no differences in proclination were found between individual incisors, as well as between Forsus™ and Crossbow® treatment groups. This made sense as the four incisors were connected to one another by a continuous archwire. It

also supported the conclusion drawn by Miller et al. [46], which showed no differences in incisor inclination between the two fixed Class II correctors as measured on conventional lateral cephalograms. Interpreting these results in the context of Class II camouflage, it appeared that the lower dentition moved anteriorly while the maxillary dentition moved posteriorly a similar amount, irrespective of the appliance used. This observation may be due to the antero-posterior mechanism of force, as both appliances employed similar use of the Forsus™ springs.

Incisor proclination ($\overline{\Delta IC}$) was the only factor found to have been predictive of alveolar volume change ($\%\Delta V_{alv}$), albeit with a moderate level of evidence. Incisor proclination could only account for 11% of the variation observed. An inverse linear relationship was seen where increasing incisor proclination resulted in a diminishing increases in alveolar volume. More clinically relevant was to establish the degree of incisor proclination that resulted in alveolar volume loss. It was determined that if the mandibular incisors were proclined more than 11°, there was a good chance that the alveolar bone would lose volume, potentially resulting in dehiscences or fenestrations. This was based on the lower bound of a 95% confidence interval (Figure 4.1). The use of incisor inclination as prognostic indicators for bony response has clinical implications. It calls into question the justification for routine prescription of CBCTs to predict unwanted responses of the periodontium, especially in the area of the mandibular symphysis. In this study, there was much uncertainty as to the quantity of bone labial to the mandibular incisors, especially at the parameters with which the CBCTs were prescribed.

5.3 Limitations

Limitations of this study will be reported in 3 sections: methodological, instrumental, and limitations on generalisability. Methodological limitations include those sources of bias which stem from trial design. Instrumental limitations mainly entail constraints imposed by issues related to CBCT imaging techniques. These constraints include artifacts, noise, and resolution. Generalisability is important to consider in the context of applying the results clinically, especially in the context of study limitations.

5.3.1 Methodological Limitations

The sample size calculation, as covered in Chapter 3, was initially set on detecting a 5° change in mandibular incisor inclination based on previous results employing conventional methodologies [46]. Given that data was collected retrospectively, and that the outcome measures differed from the initial goals of the clinical trial, the low sample size may have increased the chances of making a Type I error. This is evident because of the large measurement uncertainty, increased measurement error, and overall large standard deviations (Tables 2.5, 4.1). An inadequate sample size may also have contributed to a low

R^2 value as seen in Figure 4.1. Factors such as oral hygiene, traumatic occlusion, eccentric tooth positions, pre-existing bony defects, gingival biotype, and the ambiguity associated with imaging artifacts may better account for the variation seen in $\%\Delta V_{alv}$.

The instability of the chosen landmarks, left and right MF, LiA, LIT, and ptB could have also contributed to a biased result. The two treatment groups were equal in all of the considered factors (Section 4.3.1) prior to treatment, although this study did not account for variances in natural growth. One solution to this problem would have been to include a non-treated control group, where age-matched controls were selected from a historical sample [45] . To date, there is no data where a series of CBCT records were taken on non-treated individuals over time to assess growth. Although the alveolar volume increased by a 4.55%, it was unknown whether this change was due to natural growth. More specifically, the study could not account for whether these changes were in the transverse, anteroposterior, or vertical dimensions. There have been recent developments in the field of computing sciences, especially in 3-dimensional shape analysis and correspondence [134]. Initial papers applying shape analysis to orthognathic surgery and TMD have already been published [135, 136]. This could provide further insight into where additional volume is being distributed, or where bone resorption is occurring. Although the results of this study attempts to quantify the response of the alveolus to Class II correction, it does not provide any spatial information. A recent study published in *Angle* used shape analysis techniques to determine how the morphology of the anterior alveolus changed with incisor retraction in bimaxillary dental protrusion cases [137]. Vertical bone loss was noted on the lingual surfaces in both jaws; however, it was more pronounced in the mandible. The alveolus labial to the lingually displaced mandibular incisor demonstrated lingual "bending" with no appreciable migration of the crestal bone.

One of the most significant limitations, as well as an assumption that was made throughout, was that the clinical response of the periodontium was somehow correlated to the change in bony volume. Although it may be true that the negative volume changes in the alveolus corresponded with the development of bony dehiscences and fenestrations, this may be clinically insignificant. As was previously discussed in Section 1.3, bony defects do not necessarily result in gingival recession. In fact, pre-existing bony defects have been documented in literature prior to orthodontic treatment, with no apparent recession noted [62, 71]. Perhaps a more clinically significant relationship would be to determine whether an association exists between the aforementioned factors and clinical gingival recession. Nevertheless, quantification of gingival recession and root exposure may be subject to inconsistencies and subjectivity, as it still depends on investigator experience, or may not be practical in a clinical orthodontic setting [42].

Finally, another source of methodological bias was the number of participants lost to follow-up, as reported in Chapter 3. An intention to treat analysis was not performed, due to missing records or their inadequate quality.

5.3.2 Instrumental Limitations

Outcome uncertainty in this study was evident given the large measurement error (Tables 2.5, 2.7), standard deviation (Table 4.1), and low R^2 value (Figure 4.1). This could be explained by the ambiguity in image interpretation and segmentation. Although the automated active-contouring algorithm reduces investigator error [138], semi-automated segmentation still required a great deal of manual refinement. This was subject to investigator interpretation and experience. Figure 4.4 depicts a typical case where the same patient at the same time point was measured twice, 1 week apart and yielded different volumes. For example, there was a significant difference in outcome, with Figure 4.4a demonstrating no bony defects, and Figure 4.4b depicting the opposite.

Image quality can be influenced by contrast resolution, spatial resolution, noise and image artifacts [127]. Contrast resolution - the ability to discern two adjacent objects based on their differences in grey values - as well as spatial resolution - the minimum distance needed to distinguish two objects - is influenced by the physical parameters and limitations of the technology. Parameter and limitations include beam geometry, radiation scatter, tube output, and detector specifications [24, 127]. In general terms, some image artifacts can be reduced by increasing tube output and exposure time. However, this increased exposure to ionizing radiation, especially in a vulnerable population, cannot be justified. Spatial resolution, which is related to the voxel size and is set by the manufacturer, has a significant impact on distinguishing structures and demarcating boundaries [5]. In a study looking at commercially available CBCT machines, Ballrick et al. [109] found that the effective voxel size was always larger than the specified voxel size. Using a classic iCAT (ISI, Hatfield, PA), the authors found that a 0.2mm voxel scan had an effective resolution of 0.4mm voxel, even when a line pair phantom was used. Even in the best case scenario, with the smallest specified voxel size, the effective spatial resolution will always be lower.

Partial volume averaging is a phenomenon that has a significant influence on spatial resolution. When an object or a boundary of differing densities (grey values) is less than the size of the voxel, the adjacent densities are averaged and displayed. This effectively reduces spatial resolution and makes boundaries hard to discern (Figure 1.6) [24, 127]. Given that the periodontal ligament can be as narrow as 0.3mm, its boundaries were hard to distinguish. In turn exacerbated the ambiguity in separating the cementum from the adjacent alveolar bone. Patcas et al. [106] illustrated this in a cadaver study. At a voxel size of 0.4mm, bone labial to the mandibular incisors could not be detected accurately. In fact, it overestimated bone loss by as much as 2mm if the overlying bone was less than 1mm in the bucco-lingual dimension [57].

Noise is caused by unwanted photons hitting the detector, which causes clouding of the the image and a decreased spatial resolution. CBCTs are prone to scatter, especially compared to medical CT. CBCTs have approximately 15 times higher in scatter levels than medical CT [125]. In order to reduce noise due to scatter, reducing the FOV is beneficial

[24]. However, if the ROI is only the mandibular symphysis and the labial alveolar bone height, CBCT imaging would not be useful for general orthodontic diagnostic purposes. A traditional panorex and lateral cephalogram would still be required, calling into question the need for additional CBCT imaging in the first place, especially given the reasons previously discussed.

The impact of patient motion during CBCT acquisition on image quality cannot be understated. Many of the previous investigations exploring the accuracy and reliability of using CBCT to detect bony defects were all *in-vitro* studies and therefore not susceptible to this artifact. Clinically, patient motion, which decreases spatial resolution, is unavoidable. One way to minimize the effects of motion is to reduce scan time. The trade off is undersampling, which makes resolving fine detail difficult [127].

5.3.3 Generalisability

The presented arguments are not meant to be antagonistic towards the use of CBCT in orthodontic applications. It would be prudent, and in patients' best interest, for the clinician to first understand the practical limitations of CBCT technology. There are clear benefits associated with its use including localization of impacted canines, TMD, and orthognathic surgical treatment planning. There are clear limitations with routine full FOV CBCT imaging, especially when fine details need to be resolved. In these cases, perhaps a small FOV methodology may be more practical when combined with traditional imaging modalities. Nevertheless, the treating clinician needs to assess the risks and benefits in order to determine whether the use of CBCT is justified, particulary in the context of increased radiation dose. Limitations associated with the study of the thin alveolar housing around the mandibular incisors cannot be resolved adequately with a large FOV CBCT.

The reported degree of incisor proclination was similar to results reported in past studies employing conventional 2D radiography [46]. Perhaps justifications for the use of CBCTs based on the measurement of incisor inclination alone may not enough, especially given no apparent advantage over traditional means.

An important consideration is to interpret the conclusions within the context of this study, and much care should be exercised when inferring the results of this study to the orthodontic population. Participants were only selected from the clinical patient pool at the University of Alberta's Graduate Orthodontic Clinic, which arguably has more stringent CBCT exposure protocols than private practice. It maybe prudent to note that, as part of treatment rendered in the university setting, patient specific factors and the care provider's preference and goals may not accurately represent private practice.

The conclusion of this study related to proclination of lower incisors does not take into account patients with retroclined incisors prior to the start of treatment. A reasonable assumption to make is that the probability for adverse periodontal events in those with retroclined incisors are less than those with normally inclined, or proclined incisors.

Future studies should attempt to reduce the limitations by using small FOV scans. However, this may be hard to justify ethically given the low levels of evidence associated with orthodontic movement and periodontal status. There will also be temporal and monetary costs associated with purchasing and learning how to use software, as well as adapting the presented methodology to their own research interests. Given that the developed method only requires the anterior half of the mandible, should future studies choose to incorporate it, a small FOV scan can be considered to reduce radiation burden.

5.4 Conclusions

The following conclusions presented should be considered in the context of this study and its appreciable set of limitations. The inference of these results to the clinical population is also limited given the demographics of the study sample. Therefore, these conclusions are presented in the context of an adolescent population in Edmonton, Alberta, Canada presenting with a mild to moderate Class II malocclusion, with no syndromes, and no extreme vertical facial types. The results do not take into account natural craniofacial growth, nor does it explain the response of the alveolar housing to orthodontic approaches other than Forsus™ or Xbow® appliances.

1. There was a median increase in alveolar volume of 4.55% after camouflage of a mild to moderate Class II malocclusion. Where this volume was distributed in the alveolar housing was unknown.

2. The type of appliance and the vertical face height was not found to be predictive of the alveolar response as it had been suggested in literature. However, incisor proclination showed a weak inverse linear relationship with alveolar volume ($R^2 = 0.11$). There was evidence that if the proclination exceeded approximately 11°, a loss of volume was likely (95% confidence interval).

3. The study did not show any relationship between volume of the alveolar housing and clinical periodontal manifestations, which were not measured in this study.

4. In support of previous studies in literature [46], there was no difference in incisor proclination between Forsus™ and Xbow® appliances when considered in 3-dimensions. Similarly, there was no difference in the amount of proclination experienced by each of the mandibular incisors.

5. Given the limitations discussed in this study, clinicians should be cautious to justify routine CBCT imaging based on incisor position and the potential for iatrogenic development of bony defects.

References

[1] J. B. Ludlow and M. Ivanovic. Comparative dosimetry of dental CBCT devices and 64-slice CT for oral and maxillofacial radiology. *Oral Surgery, Oral Medicine, Oral Pathology, Oral Radiology, and Endodontology*, 106(1):106–114, (2008). doi:10.1016/j.tripleo.2008.03.018.

[2] C. Angelopoulos, W. C. Scarfe, and A. G. Farman. A comparison of maxillofacial CBCT and medical CT. *Atlas of the oral and maxillofacial surgery clinics of North America*, 20(1):1–17, (2012).

[3] R. Pauwels, K. Araki, J. H. Siewerdsen, and S. S. Thongvigitmanee. Technical aspects of dental CBCT: State of the art. *Dentomaxillofacial Radiology*, 44(1):20140224, (2015).

[4] W. C. Scarfe and C. Angelopoulos. *Maxillofacial Cone Beam Computed Tomography: Principles, Techniques and Clinical Applications*. Springer, (2018). ISBN 3-319-62061-4.

[5] D. Brüllmann and R. K. W. Schulze. Spatial resolution in CBCT machines for dental/maxillofacial applications—what do we know today? *Dentomaxillofacial Radiology*, 44(1):20140204, (2014). doi:10.1259/dmfr.20140204.

[6] J. G. Edwards. A study of the anterior portion of the palate as it relates to orthodontic therapy. *American Journal of Orthodontics*, 69(3):249–273, (1976). doi:10.1016/0002-9416(76)90075-0.

[7] W. R. Proffit, H. W. Fields Jr, and D. M. Sarver. *Contemporary Orthodontics*. Elsevier Health Sciences, Philadelphia, PA, sixth edition, (2019). ISBN 978-0-323-54387-3.

[8] A. Khanum. Extraction vs Non Extraction Controversy: A Review. 14(01):9, (2018).

[9] L. W. Graber, R. L. Vanarsdall, K. W. Vig, and G. J. Huang. *Orthodontics-E-Book: Current Principles and Techniques*. Elsevier Health Sciences, (2016). ISBN 0-323-44432-6.

[10] I. Joss-Vassalli, C. Grebenstein, N. Topouzelis, A. Sculean, and C. Katsaros. Orthodontic therapy and gingival recession: A systematic review. *Orthodontics & Craniofacial Research*, 13(3):127–141, (2010). doi:10.1111/j.1601-6343.2010.01491.x.

[11] L. H. Cevidanes, A. C. Ruellas, and W. C. Scarfe. Orthodontic and Orthognathic Surgery Planning and Simulation Software. In *Maxillofacial Cone Beam Computed Tomography*, pages 715–743. Springer, (2018).

[12] Clinical recommendations regarding use of cone beam computed tomography in orthodontics. Position statement by the American Academy of Oral and Maxillofacial Radiology. *Oral Surgery, Oral Medicine, Oral Pathology and Oral Radiology*, 116(2): 238–257, (2013). doi:10.1016/j.oooo.2013.06.002.

[13] A. Becker, S. Chaushu, and N. Casap-Caspi. Cone-beam computed tomography and the orthosurgical management of impacted teeth. *The Journal of the American Dental Association*, 141:14S–18S, (2010).

[14] D. Tamimi and K. ElSaid. Cone beam computed tomography in the assessment of dental impactions. In *Seminars in Orthodontics*, volume 15, pages 57–62. Elsevier, (2009). ISBN 1073-8746.

[15] J. Treil, J. Braga, and A. A. Aït. 3D representation of skull and soft tissues. Usefulness in orthodontic and orthognathic surgery. *Journal de radiologie*, 90(5 Pt 2):634–641, (2009).

[16] L. M. J. Helenius, D. Hallikainen, I. Helenius, J. H. Meurman, M. Könönen, M. Leirisalo-Repo, and C. Lindqvist. Clinical and radiographic findings of the temporomandibular joint in patients with various rheumatic diseases. A case-control study. *Oral Surgery, Oral Medicine, Oral Pathology, Oral Radiology, and Endodontology*, 99(4):455–463, (2005).

[17] B. E. Larson. Cone-beam computed tomography is the imaging technique of choice for comprehensive orthodontic assessment. *American Journal of Orthodontics and Dentofacial Orthopedics*, 141(4):402–410, (2012). doi:10.1016/j.ajodo.2012.02.009.

[18] K. A. Misch, E. S. Yi, and D. P. Sarment. Accuracy of cone beam computed tomography for periodontal defect measurements. *Journal of Periodontology*, 77(7):1261–1266, (2006). doi:10.1902/jop.2006.050367.

[19] A. Mol and A. Balasundaram. In vitro cone beam computed tomography imaging of periodontal bone. *Dentomaxillofacial Radiology*, 37(6):319–324, (2008).

[20] B. Vandenberghe, R. Jacobs, and J. Yang. Detection of periodontal bone loss using digital intraoral and cone beam computed tomography images: An in vitro assessment of bony and/or infrabony defects. *Dentomaxillofacial Radiology*, 37(5):252–260, (2008).

[21] C.-S. Chen, C.-Y. Hsu, S.-K. Chen, C.-J. Lin, C.-H. Hsieh, and Y.-H. Liu. Image correction for cone-beam computed tomography simulator using neural network corrector. *Advances in Mechanical Engineering*, 9:168781401769047, (2017). doi:10.1177/1687814017690476.

[22] J. Hsieh. *Computed Tomography: Principles, Design, Artifacts, and Recent Advances*, volume 114. SPIE press, (2003). ISBN 0-8194-4425-1.

[23] D. W. Chakeres. Clinical significance of partial volume averaging of the temporal bone. *American journal of neuroradiology*, 5(3):297–302, (1984).

[24] A. D. Molen. Considerations in the use of cone-beam computed tomography for buccal bone measurements. *American journal of orthodontics and dentofacial orthopedics*, 137(4):S130–S135, (2010).

[25] T. N. Hangartner and V. Gilsanz. Evaluation of cortical bone by computed tomography. *Journal of bone and mineral research*, 11(10):1518–1525, (1996).

[26] H. S. Dorfman. Mucogingival changes resulting from mandibular incisor tooth movement. *American journal of orthodontics*, 74(3):286–297, (1978).

[27] S. D. Kapila and J. M. Nervina. Alveolar Boundary Conditions in Orthodontic Diagnosis and Treatment Planning. In *Cone Beam Computed Tomography in Orthodontics: Indications, Insights, and Innovations*, pages 293–316. John Wiley & Sons, Ltd, (2014). ISBN 978-1-118-67488-8. doi:10.1002/9781118674888.ch14.

[28] J. L. Wennström, J. Lindhe, F. Sinclair, and B. Thilander. Some periodontal tissue reactions to orthodontic tooth movement in monkeys. *Journal of Clinical Periodontology*, 14(3):121–129, (1987). doi:10.1111/j.1600-051X.1987.tb00954.x.

[29] B. Thilander, S. Nyman, T. Karring, and I. Magnusson. Bone regeneration in alveolar bone dehiscences related to orthodontic tooth movements. *The European Journal of Orthodontics*, 5(2):105–114, (1983).

[30] J. L. Wennström, B. L. Stokland, S. Nyman, and B. Thilander. Periodontal tissue response to orthodontic movement of teeth with infrabony pockets. *American Journal of Orthodontics and Dentofacial Orthopedics*, 103(4):313–319, (1993). doi:10.1016/0889-5406(93)70011-C.

[31] K. F. Batenhorst, G. M. Bowers, and J. E. Williams Jr. Tissue changes resulting from facial tipping and extrusion of incisors in monkeys. *Journal of periodontology*, 45(9): 660–668, (1974).

[32] G. G. Steiner, J. K. Pearson, and J. Ainamo. Changes of the Marginal Periodontium as a Result of Labial Tooth Movement in Monkeys. *Journal of Periodontology*, 52(6): 314–320, (1981). doi:10.1902/jop.1981.52.6.314.

[33] C. E. Wingard and G. M. Bowers. The effects of facial bone from facial tipping of incisors in monkeys. *Journal of periodontology*, 47(8):450–454, (1976).

[34] I. Ericsson and B. Thilander. Orthodontic forces and recurrence of periodontal disease: An experimental study in the dog. *American Journal of Orthodontics*, 74(1): 41–50, (1978).

[35] L. Hollender, A. Rönnerman, and B. Thilander. Root resorption, marginal bone support and clinical crown length in orthodontically treated patients. *The European Journal of Orthodontics*, 2(4):197–205, (1980).

[36] J. Årtun and O. Krogstad. Periodontal status of mandibular incisors following excessive proclination A study in adults with surgically treated mandibular prognathism. *American Journal of Orthodontics and Dentofacial Orthopedics*, 91(3):225–232, (1987). doi:10.1016/0889-5406(87)90450-1.

[37] S. Ruf, K. Hansen, and H. Pancherz. Does orthodontic proclination of lower incisors in children and adolescents cause gingival recession? *American Journal of Orthodontics and Dentofacial Orthopedics*, 114(1):100–106, (1998). doi:10.1016/S0889-5406(98)70244-6.

[38] G. Djeu, C. Hayes, and S. Zawaideh. Correlation between mandibular central incisor proclination and gingival recession during fixed appliance therapy. *The Angle Orthodontist*, 72(3):238–245, (2002).

[39] J. Årtun and D. Grobéty. Periodontal status of mandibular incisors after pronounced orthodontic advancement during adolescence: A follow-up evaluation. *American Journal of Orthodontics and Dentofacial Orthopedics*, 119(1):2–10, (2001).

[40] B. Melsen and D. Allais. Factors of importance for the development of dehiscences during labial movement of mandibular incisors: A retrospective study of adult orthodontic patients. *American Journal of Orthodontics and Dentofacial Orthopedics*, 127 (5):552–561, (2005). doi:10.1016/j.ajodo.2003.12.026.

[41] A.-M. Renkema, Z. Navratilova, K. Mazurova, C. Katsaros, and P. S. Fudalej. Gingival labial recessions and the post-treatment proclination of mandibular incisors. *European journal of orthodontics*, 37(5):508–513, (2015).

[42] T. Aziz and C. Flores-Mir. A systematic review of the association between appliance-induced labial movement of mandibular incisors and gingival recession. *Australian orthodontic journal*, 27(1):33–39, (2011).

[43] I. Joss-Vassalli, C. Grebenstein, N. Topouzelis, A. Sculean, and C. Katsaros. Orthodontic therapy and gingival recession: A systematic review. *Orthodontics & Craniofacial Research*, 13(3):127–141, (2010). doi:10.1111/j.1601-6343.2010.01491.x.

[44] S. Kapila, R. S. Conley, and W. E. Harrell. The current status of cone beam computed tomography imaging in orthodontics. *Dentomaxillofacial Radiology*, 40(1):24–34, (2011). doi:10.1259/dmfr/12615645.

[45] C. Flores-Mir, G. Barnett, D. W. Higgins, G. Heo, and P. W. Major. Short-term skeletal and dental effects of the Xbow appliance as measured on lateral cephalograms. *American Journal of Orthodontics and Dentofacial Orthopedics*, 136(6):822–832, (2009). doi:10.1016/j.ajodo.2008.01.021.

[46] R. A. Miller, L. Tieu, and C. Flores-Mir. Incisor inclination changes produced by two compliance-free Class II correction protocols for the treatment of mild to moderate Class II malocclusions. *The Angle Orthodontist*, 83(3):431–436, (2012).

[47] C. Flores-Mir, A. Ayeh, A. Goswani, and S. Charkhandeh. Skeletal and Dental Changes in Class II division 1 Malocclusions Treated with Splint-Type Herbst Appliances. *The Angle Orthodontist*, 77(2):376–381, (2007). doi:10.2319/0003-3219(2007)077[0376:SADCIC]2.0.CO;2.

[48] G. A. Barnett, D. W. Higgins, P. W. Major, and C. Flores-Mir. Immediate Skeletal and Dentoalveolar Effects of the Crown- or Banded Type Herbst Appliance on Class II division 1 Malocclusion. *The Angle Orthodontist*, 78(2):361–369, (2008). doi:10.2319/031107-123.1.

[49] K. O'brien, J. Wright, F. Conboy, Y. Sanjie, N. Mandall, S. Chadwick, I. Connolly, P. Cook, D. Birnie, and M. Hammond. Effectiveness of treatment for Class II malocclusion with the Herbst or twin-block appliances: A randomized, controlled trial. *American Journal of Orthodontics and Dentofacial Orthopedics*, 124(2):128–137, (2003).

[50] H. Pancherz and U. Fackel. The skeletofacial growth pattern pre-and post-dentofacial orthopaedics. A long-term study of Class II malocclusions treated with the Herbst appliance. *The European Journal of Orthodontics*, 12(2):209–218, (1990).

[51] J. C. Tulloch, W. R. Proffit, and C. Phillips. Outcomes in a 2-phase randomized clinical trial of early Class II treatment. *American Journal of Orthodontics and Dentofacial Orthopedics*, 125(6):657–667, (2004).

[52] K. O'Brien, J. Wright, F. Conboy, Y. Sanjie, N. Mandall, S. Chadwick, I. Connolly, P. Cook, D. Birnie, and M. Hammond. Effectiveness of early orthodontic treatment with the Twin-block appliance: A multicenter, randomized, controlled trial. Part 1: Dental and skeletal effects. *American journal of orthodontics and dentofacial orthopedics*, 124(3):234–243, (2003).

[53] M. O. Lagravère, J. Carey, R. W. Toogood, and P. W. Major. Three-dimensional accuracy of measurements made with software on cone-beam computed tomography

images. *American Journal of Orthodontics and Dentofacial Orthopedics*, 134(1):112–116, (2008).

[54] J. Kim, G. Heo, and M. O. Lagravère. Accuracy of laser-scanned models compared to plaster models and cone-beam computed tomography. *The Angle orthodontist*, 84 (3):443–450, (2014).

[55] P. Naji, N. A. Alsufyani, and M. O. Lagravère. Reliability of anatomic structures as landmarks in three-dimensional cephalometric analysis using CBCT. *The Angle Orthodontist*, 84(5):762–772, (2013). doi:10.2319/090413-652.1.

[56] C. C. Leung, L. Palomo, R. Griffith, and M. G. Hans. Accuracy and reliability of cone-beam computed tomography for measuring alveolar bone height and detecting bony dehiscences and fenestrations. *American Journal of Orthodontics and Dentofacial Orthopedics*, 137(4):S109–S119, (2010).

[57] Z. Sun, T. Smith, S. Kortam, D.-G. Kim, B. C. Tee, and H. Fields. Effect of bone thickness on alveolar bone-height measurements from cone-beam computed tomography images. *American Journal of Orthodontics and Dentofacial Orthopedics*, 139(2):e117–e127, (2011). doi:10.1016/j.ajodo.2010.08.016.

[58] A. M. Timock, V. Cook, T. McDonald, M. C. Leo, J. Crowe, B. L. Benninger, and D. A. Covell. Accuracy and reliability of buccal bone height and thickness measurements from cone-beam computed tomography imaging. *American Journal of Orthodontics and Dentofacial Orthopedics*, 140(5):734–744, (2011). doi:10.1016/j.ajodo.2011.06.021.

[59] H. M. Pinsky, S. Dyda, R. W. Pinsky, K. A. Misch, and D. P. Sarment. Accuracy of three-dimensional measurements using cone-beam CT. *Dentomaxillofacial Radiology*, 35(6):410–416, (2006).

[60] J. B. Chaison, C. S. K. Chen, S. W. Herring, and A.-M. Bollen. Bone volume, tooth volume, and incisor relapse: A 3-dimensional analysis of orthodontic stability. *American Journal of Orthodontics and Dentofacial Orthopedics*, 138(6):778–786, (2010). doi:10.1016/j.ajodo.2009.02.032.

[61] C.-x. Zhang, G. Shen, Y.-j. Ning, H. Liu, Y. Zhao, and D.-x. Liu. Effects of Twin-block vs sagittal-guidance Twin-block appliance on alveolar bone around mandibular incisors in growing patients with Class II Division 1 malocclusion. *American Journal of Orthodontics and Dentofacial Orthopedics*, 157(3):329–339, (2020).

[62] K. Evangelista, K. de Faria Vasconcelos, A. Bumann, E. Hirsch, M. Nitka, and M. A. G. Silva. Dehiscence and fenestration in patients with Class I and Class II Division 1 malocclusion assessed with cone-beam computed tomography. *American Journal of Orthodontics and Dentofacial Orthopedics*, 138(2):133. e1–133. e7, (2010).

[63] C. S. Handelman. The anterior alveolus: Its importance in limiting orthodontic treatment and its influence on the occurrence of iatrogenic sequelae. *The Angle Orthodontist*, 66(2):95–110, (1996). doi:10.1043/0003-3219(1996)066<0095:TAAIII>2.3.CO;2.

[64] H. Wehrbein, W. Bauer, and P. Diedrich. Mandibular incisors, alveolar bone, and symphysis afterorthodontic treatment. A retrospective study. *American Journal of Orthodontics and Dentofacial Orthopedics*, 110(3):239–246, (1996). doi:10.1016/S0889-5406(96)80006-0.

[65] A. Gracco, L. Luca, M. C. Bongiorno, and G. Siciliani. Computed tomography evaluation of mandibular incisor bony support in untreated patients. *American Journal of Orthodontics and Dentofacial Orthopedics*, 138(2):179–187, (2010). doi:10.1016/j.ajodo.2008.09.030.

[66] S. Lee, S. Hwang, W. Jang, Y. J. Choi, C. J. Chung, and K.-H. Kim. Assessment of lower incisor alveolar bone width using cone-beam computed tomography images in skeletal Class III adults of different vertical patterns. *The korean journal of orthodontics*, 48(6):349–356, (2018).

[67] S. Enhos, T. Uysal, A. Yagci, İ. Veli, F. I. Ucar, and T. Ozer. Dehiscence and fenestration in patients with different vertical growth patterns assessed with cone-beam computed tomography. *The Angle Orthodontist*, 82(5):868–874, (2012).

[68] N. Hoang, G. Nelson, D. Hatcher, and S. Oberoi. Evaluation of mandibular anterior alveolus in different skeletal patterns. *Progress in Orthodontics*, 17(1):22, (2016). doi:10.1186/s40510-016-0135-z.

[69] K. Mazurova, J.-B. Kopp, A. M. Renkema, N. Pandis, C. Katsaros, and P. S. Fudalej. Gingival recession in mandibular incisors and symphysis morphology—a retrospective cohort study. *European Journal of Orthodontics*, 40(2):185–192, (2018). doi:10.1093/ejo/cjx046.

[70] K. Mazurova, A.-M. Renkema, Z. Navratilova, C. Katsaros, and P. S. Fudalej. No association between gingival labial recession and facial type. *European journal of orthodontics*, 38(3):286–291, (2016).

[71] A. Yagci, İ. Veli, T. Uysal, F. I. Ucar, T. Ozer, and S. Enhos. Dehiscence and fenestration in skeletal Class I, II, and III malocclusions assessed with cone-beam computed tomography. *The Angle Orthodontist*, 82(1):67–74, (2011). doi:10.2319/040811-250.1.

[72] P. A. Yushkevich, J. Piven, H. C. Hazlett, R. G. Smith, S. Ho, J. C. Gee, and G. Gerig. User-guided 3D active contour segmentation of anatomical structures: Significantly improved efficiency and reliability. *Neuroimage*, 31(3):1116–1128, (2006).

[73] L. H. S. Cevidanes, A.-K. Hajati, B. Paniagua, P. F. Lim, D. G. Walker, G. Palconet, A. G. Nackley, M. Styner, J. B. Ludlow, and H. Zhu. Quantification of condylar resorption in temporomandibular joint osteoarthritis. *Oral Surgery, Oral Medicine, Oral Pathology, Oral Radiology, and Endodontology*, 110(1):110–117, (2010).

[74] L. H. Cevidanes, L. J. Bailey, G. R. Tucker Jr, M. A. Styner, A. Mol, C. L. Phillips, W. R. Proffit, and T. Turvey. Superimposition of 3D cone-beam CT models of orthognathic surgery patients. *Dentomaxillofacial Radiology*, 34(6):369–375, (2005).

[75] L. H. Cevidanes, J. B. L'Tanya, S. F. Tucker, M. A. Styner, A. Mol, C. L. Phillips, W. R. Proffit, and T. Turvey. Three-dimensional cone-beam computed tomography for assessment of mandibular changes after orthognathic surgery. *American journal of orthodontics and dentofacial orthopedics*, 131(1):44–50, (2007).

[76] A. C. de Oliveira Ruellas, M. S. Yatabe, B. Q. Souki, E. Benavides, T. Nguyen, R. R. Luiz, L. Franchi, and L. H. S. Cevidanes. 3D mandibular superimposition: Comparison of regions of reference for voxel-based registration. *PLoS One*, 11(6): e0157625, (2016).

[77] A. Fedorov, R. Beichel, J. Kalpathy-Cramer, J. Finet, J.-C. Fillion-Robin, S. Pujol, C. Bauer, D. Jennings, F. Fennessy, and M. Sonka. 3D Slicer as an image computing platform for the Quantitative Imaging Network. *Magnetic resonance imaging*, 30(9): 1323–1341, (2012).

[78] D. Forst, S. Nijjar, C. Flores-Mir, J. Carey, M. Secanell, and M. Lagravere. Comparison of in vivo 3D cone-beam computed tomography tooth volume measurement protocols. *Progress in orthodontics*, 15(1):69, (2014).

[79] C. A. Ahlbrecht, A. C. de Oliveira Ruellas, B. Paniagua, J. A. Schilling, J. A. McNamara Jr, and L. H. S. Cevidanes. Three-dimensional characterization of root morphology for maxillary incisors. *PloS one*, 12(6):e0178728, (2017).

[80] A. Fedorov, R. Beichel, J. Kalpathy-Cramer, J. Finet, J.-C. Fillion-Robin, S. Pujol, C. Bauer, D. Jennings, F. Fennessy, and M. Sonka. 3D Slicer as an image computing platform for the Quantitative Imaging Network. *Magnetic resonance imaging*, 30(9): 1323–1341, (2012).

[81] R. Kikinis, S. D. Pieper, and K. G. Vosburgh. 3D Slicer: A platform for subject-specific image analysis, visualization, and clinical support. In *Intraoperative Imaging and Image-Guided Therapy*, pages 277–289. Springer, (2014).

[82] L. H. Cevidanes, M. A. Styner, and W. R. Proffit. Image analysis and superimposition of 3-dimensional cone-beam computed tomography models. *American journal of orthodontics and dentofacial orthopedics*, 129(5):611–618, (2006).

[83] C. A. Ahlbrecht, A. C. de Oliveira Ruellas, B. Paniagua, J. A. Schilling, J. A. McNamara Jr, and L. H. S. Cevidanes. Three-dimensional characterization of root morphology for maxillary incisors. *PloS one*, 12(6):e0178728, (2017).

[84] L. E. Arriola-Guillén, Y. A. Rodríguez-Cárdenas, G. A. Ruíz-Mora, A. Aliaga-Del Castillo, J. Schilling, and H. L. Dias-Da Silveira. Three-dimensional evaluation of the root resorption of maxillary incisors after the orthodontic traction of bicortically impacted canines. *Progress in orthodontics*, 20(1):13, (2019).

[85] A. Weissheimer, L. M. Menezes, L. Koerich, J. Pham, and L. H. S. Cevidanes. Fast three-dimensional superimposition of cone beam computed tomography for orthopaedics and orthognathic surgery evaluation. *International journal of oral and maxillofacial surgery*, 44(9):1188–1196, (2015).

[86] L. H. Cevidanes, S. Tucker, M. Styner, H. Kim, J. Chapuis, M. Reyes, W. Proffit, T. Turvey, and M. Jaskolka. Three-dimensional surgical simulation. *American journal of orthodontics and dentofacial orthopedics*, 138(3):361–371, (2010).

[87] F. Maes, A. Collignon, D. Vandermeulen, G. Marchal, and P. Suetens. Multimodality image registration by maximization of mutual information. *IEEE transactions on Medical Imaging*, 16(2):187–198, (1997).

[88] S. Padala, B. C. Tee, F. M. Beck, K. Elias, D.-G. Kim, and Z. Sun. The usefulness of cone-beam computed tomography gray values for alveolar bone linear measurements. *The Angle Orthodontist*, 88(2):227–232, (2018).

[89] W. C. Scarfe, Z. Li, W. Aboelmaaty, S. A. Scott, and A. G. Farman. Maxillofacial cone beam computed tomography: Essence, elements and steps to interpretation. *Australian Dental Journal*, 57(s1):46–60, (2012). doi:10.1111/j.1834-7819.2011.01657.x.

[90] Y. Liu, R. Olszewski, E. S. Alexandroni, R. Enciso, T. Xu, and J. K. Mah. The validity of in vivo tooth volume determinations from cone-beam computed tomography. *The Angle orthodontist*, 80(1):160–166, (2010).

[91] G. Lemieux, J. P. Carey, C. Flores-Mir, M. Secanell, A. Hart, and M. O. Lagravère. Precision and accuracy of suggested maxillary and mandibular landmarks with cone-beam computed tomography for regional superimpositions: An in vitro study. *American Journal of Orthodontics and Dentofacial Orthopedics*, 149(1):67–75, (2016).

[92] M. O. Lagravère, C. Low, C. Flores-Mir, R. Chung, J. P. Carey, G. Heo, and P. W. Major. Intraexaminer and interexaminer reliabilities of landmark identification on digitized lateral cephalograms and formatted 3-dimensional cone-beam computerized tomography images. *American Journal of Orthodontics and Dentofacial Orthopedics*, 137(5):598–604, (2010).

[93] A. Björk and V. Skieller. Normal and abnormal growth of the mandible. A synthesis of longitudinal cephalometric implant studies over a period of 25 years. *European Journal of Orthodontics*, 5(1):1–46, (1983). doi:10.1093/ejo/5.1.1.

[94] S. Krarup, T. A. Darvann, P. Larsen, J. L. Marsh, and S. Kreiborg. Three-dimensional analysis of mandibular growth and tooth eruption. *Journal of Anatomy*, 207(5):669–682, (2005). doi:10.1111/j.1469-7580.2005.00479.x.

[95] S. D. Springate and A. G. Jones. The validity of two methods of mandibular superimposition: A comparison with tantalum implants. *American Journal of Orthodontics and Dentofacial Orthopedics*, 113(3):263–270, (1998). doi:10.1016/S0889-5406(98)70295-1.

[96] D. M. Wagner and C.-H. Chung. Transverse growth of the maxilla and mandible in untreated girls with low, average, and high MP-SN angles: A longitudinal study. *American journal of orthodontics and dentofacial orthopedics*, 128(6):716–723, (2005).

[97] R. M. Ricketts. *Orthodontic Diagnosis and Planning:–Their Roles in Preventive and Rehabilitative Dentistry*, volume 2. Rocky Mountain/Orthodontics, (1982).

[98] L. G. Gandini Jr and P. H. Buschang. Maxillary and mandibular width changes studied using metallic implants. *American Journal of Orthodontics and Dentofacial Orthopedics*, 117(1):75–80, (2000).

[99] M. O. Lagravère, J. Carey, G. Heo, R. W. Toogood, and P. W. Major. Transverse, vertical, and anteroposterior changes from bone-anchored maxillary expansion vs traditional rapid maxillary expansion: A randomized clinical trial. *American Journal of Orthodontics and Dentofacial Orthopedics*, 137(3):304. e1–304. e12, (2010).

[100] P. H. Buschang, K. Julien, R. Sachdeva, and A. Demirjian. Childhood and pubertal growth changes of the human symphysis. *The Angle Orthodontist*, 62(3):203–210, (1992).

[101] P. H. Buschang and L. G. Gandini Jr. Mandibular skeletal growth and modelling between 10 and 15 years of age. *The European Journal of Orthodontics*, 24(1):69–79, (2002).

[102] T. Aki, R. S. Nanda, G. F. Currier, and S. K. Nanda. Assessment of symphysis morphology as a predictorof the direction of mandibular growth. *American Journal of Orthodontics and Dentofacial Orthopedics*, 106(1):60–69, (1994).

[103] R. Al-Abdwani, D. R. Moles, and J. H. Noar. Change of incisor inclination effects on points A and B. *The Angle Orthodontist*, 79(3):462–467, (2009).

[104] L. G. Portney and M. P. Watkins. *Foundations of Clinical Research: Applications to Practice*, volume 892. Pearson/Prentice Hall Upper Saddle River, NJ, (2009).

[105] R. Wood, Z. Sun, J. Chaudhry, B. C. Tee, D.-G. Kim, B. Leblebicioglu, and G. England. Factors affecting the accuracy of buccal alveolar bone height measurements from cone-beam computed tomography images. *American Journal of Orthodontics and Dentofacial Orthopedics*, 143(3):353–363, (2013). doi:10.1016/j.ajodo.2012.10.019.

[106] R. Patcas, L. Müller, O. Ullrich, and T. Peltomäki. Accuracy of cone-beam computed tomography at different resolutions assessed on the bony covering of the mandibular anterior teeth. *American journal of orthodontics and dentofacial orthopedics*, 141(1):41–50, (2012).

[107] S. Lennon, S. Patel, F. Foschi, R. Wilson, J. Davies, and F. Mannocci. Diagnostic accuracy of limited-volume cone-beam computed tomography in the detection of periapical bone loss: 360° scans versus 180° scans. *International Endodontic Journal*, 44 (12):1118–1127, (2011). doi:10.1111/j.1365-2591.2011.01930.x.

[108] R. Schulze, U. Heil, D. Groβ, D. D. Bruellmann, E. Dranischnikow, U. Schwanecke, and E. Schoemer. Artefacts in CBCT: A review. *Dentomaxillofacial Radiology*, 40(5): 265–273, (2011).

[109] J. W. Ballrick, J. M. Palomo, E. Ruch, B. D. Amberman, and M. G. Hans. Image distortion and spatial resolution of a commercially available cone-beam computed tomography machine. *American Journal of Orthodontics and Dentofacial Orthopedics*, 134(4):573–582, (2008). doi:10.1016/j.ajodo.2007.11.025.

[110] T. Kimpe and T. Tuytschaever. Increasing the number of gray shades in medical display systems—how much is enough? *Journal of digital imaging*, 20(4):422–432, (2007).

[111] D. Moher, S. Hopewell, K. F. Schulz, V. Montori, P. C. Gøtzsche, P. J. Devereaux, D. Elbourne, M. Egger, and D. G. Altman. CONSORT 2010 explanation and elaboration: Updated guidelines for reporting parallel group randomised trials. *International Journal of Surgery*, 10(1):28–55, (2012). doi:10.1016/j.ijsu.2011.10.001.

[112] N. Pandis, P. S. Fleming, S. Hopewell, and D. G. Altman. The CONSORT Statement: Application within and adaptations for orthodontic trials. *American Journal of Orthodontics and Dentofacial Orthopedics*, 147(6):663–679, (2015). doi:10.1016/j.ajodo.2015.03.014.

[113] N. Pandis, L. Shamseer, V. G. Kokich, P. S. Fleming, and D. Moher. Active implementation strategy of CONSORT adherence by a dental specialty journal improved randomized clinical trial reporting. *Journal of Clinical Epidemiology*, 67(9):1044–1048, (2014). doi:10.1016/j.jclinepi.2014.04.001.

[114] J. Hennessy, T. Garvey, and E. A. Al-Awadhi. A randomized clinical trial comparing mandibular incisor proclination produced by fixed labial appliances and clear aligners. *The Angle Orthodontist*, 86(5):706–712, (2016). doi:10.2319/101415-686.1.

[115] R. A. Miller, L. Tieu, and C. Flores-Mir. Incisor inclination changes produced by two compliance-free Class II correction protocols for the treatment of mild to moderate Class II malocclusions. *The Angle Orthodontist*, 83(3):431–436, (2013).

[116] T. Aziz, U. Nassar, and C. Flores-Mir. Prediction of lower incisor proclination during Xbow treatment based on initial cephalometric variables. *The Angle Orthodontist*, 82 (3):472–479, (2011). doi:10.2319/072311-465.1.

[117] V. D'Antò, R. Bucci, L. Franchi, R. Rongo, A. Michelotti, and R. Martina. Class II functional orthopaedic treatment: A systematic review of systematic reviews. *Journal of Oral Rehabilitation*, 42(8):624–642, (2015). doi:10.1111/joor.12295.

[118] C. S. Handelman. The anterior alveolus: Its importance in limiting orthodontic treatment and its influence on the occurrence of iatrogenic sequelae. *The Angle Orthodontist*, 66(2):95–110, (1996). doi:10.1043/0003-3219(1996)066<0095:TAAIII>2.3.CO;2.

[119] L. L. Dantas, P. P. Ferreira, L. Oliveira, F. S. Neves, P. S. F. Campos, W. C. Scarfe, and I. Crusoe-Rebello. Cone beam computed tomography devices in the evaluation of buccal bone in anterior teeth. *Australian Dental Journal*, 64(2):161–166, (2019). doi:10.1111/adj.12685.

[120] M. Sendyk, J. B. de Paiva, J. Abrão, and J. Rino Neto. Correlation between buccolingual tooth inclination and alveolar bone thickness in subjects with Class III dentofacial deformities. *American Journal of Orthodontics and Dentofacial Orthopedics*, 152(1):66–79, (2017). doi:10.1016/j.ajodo.2016.12.014.

[121] F. Zhang, S.-C. Lee, J.-B. Lee, and K.-M. Lee. Geometric analysis of alveolar bone around the incisors after anterior retraction following premolar extraction. *The Angle Orthodontist*, (2019). doi:10.2319/041419-266.1.

[122] J. O. Agbaje, R. Jacobs, F. Maes, K. Michiels, and D. V. Steenberghe. Volumetric analysis of extraction sockets using cone beam computed tomography: A pilot study on ex vivo jaw bone. *Journal of Clinical Periodontology*, 34(11):985–990, (2007). doi:10.1111/j.1600-051X.2007.01134.x.

[123] K. F. G. Yared, E. G. Zenobio, and W. Pacheco. Periodontal status of mandibular central incisors after orthodontic proclination in adults. *American Journal of Orthodontics and Dentofacial Orthopedics*, 130(1):6. e1–6. e8, (2006).

[124] R. Fuhrmann. Three-dimensional interpretation of periodontal lesions and remodeling during orthodontic treatment. *Journal of Orofacial Orthopedics / Fortschritte der Kieferorthopädie*, 57(4):224–237, (1996). doi:10.1007/BF02190235.

[125] W. C. Scarfe and C. Angelopoulos. *Maxillofacial Cone Beam Computed Tomography: Principles, Techniques and Clinical Applications*. Springer, (2018). ISBN 3-319-62061-4.

[126] W. C. Scarfe, Z. Li, W. Aboelmaaty, S. A. Scott, and A. G. Farman. Maxillofacial cone beam computed tomography: Essence, elements and steps to interpretation. *Australian dental journal*, 57:46–60, (2012).

[127] W. C. Scarfe, A. G. Farman, M. D. Levin, and D. Gane. Essentials of maxillofacial cone beam computed tomography. *The Alpha omegan*, 103(2):62–67, (2010).

[128] W. C. Scarfe, B. Azevedo, L. R. Pinheiro, M. Priaminiarti, and M. A. O. Sales. The emerging role of maxillofacial radiology in the diagnosis and management of patients with complex periodontitis. *Periodontology 2000*, 74(1):116–139, (2017). doi:10.1111/prd.12193.

[129] T. L. Slovis. Children, computed tomography radiation dose, and the As Low As Reasonably Achievable (ALARA) concept. *Pediatrics*, 112(4):971–972, (2003).

[130] Y. Liu, R. Olszewski, E. S. Alexandroni, R. Enciso, T. Xu, and J. K. Mah. The validity of in vivo tooth volume determinations from cone-beam computed tomography. *The Angle orthodontist*, 80(1):160–166, (2010).

[131] V. García-Sanz, C. Bellot-Arcís, V. Hernández, P. Serrano-Sánchez, J. Guarinos, and V. Paredes-Gallardo. Accuracy and reliability of Cone-Beam Computed Tomography for linear and volumetric mandibular condyle measurements. A human cadaver study. *Scientific reports*, 7(1):1–8, (2017).

[132] M. Bayram, S. Kayipmaz, Ö. S. Sezgin, and M. Küçük. Volumetric analysis of the mandibular condyle using cone beam computed tomography. *European journal of radiology*, 81(8):1812–1816, (2012).

[133] N. D. Kravitz, B. Kusnoto, E. BeGole, A. Obrez, and B. Agran. How well does Invisalign work? A prospective clinical study evaluating the efficacy of tooth movement with Invisalign. *American Journal of Orthodontics and Dentofacial Orthopedics*, 135(1):27–35, (2009).

[134] M. Styner, I. Oguz, S. Xu, C. Brechbühler, D. Pantazis, J. J. Levitt, M. E. Shenton, and G. Gerig. Framework for the statistical shape analysis of brain structures using SPHARM-PDM. *The insight journal*, (1071):242, (2006).

[135] B. Paniagua, L. Cevidanes, D. Walker, H. Zhu, R. Guo, and M. Styner. Clinical application of SPHARM-PDM to quantify temporomandibular joint osteoarthritis. *Computerized Medical Imaging and Graphics*, 35(5):345–352, (2011).

[136] B. Paniagua, L. Cevidanes, H. Zhu, and M. Styner. Outcome quantification using SPHARM-PDM toolbox in orthognathic surgery. *International journal of computer assisted radiology and surgery*, 6(5):617–626, (2011).

[137] F. Zhang, S.-C. Lee, J.-B. Lee, and K.-M. Lee. Geometric analysis of alveolar bone around the incisors after anterior retraction following premolar extraction. *The Angle Orthodontist*, 90(2):173–180, (2020). doi:10.2319/041419-266.1.

[138] P. A. Yushkevich, J. Piven, H. C. Hazlett, R. G. Smith, S. Ho, J. C. Gee, and G. Gerig. User-guided 3D active contour segmentation of anatomical structures: Significantly improved efficiency and reliability. *NeuroImage*, 31(3):1116–1128, (2006). doi:10.1016/j.neuroimage.2006.01.015.

Appendix A

Raw Data

A.1 Demographic Data and Treatment Specifics

Table A.1: A table of participant demographic data and treatment specifics. Age is given in years (yrs), the time in active treatment is given in months (mths), and the FMA is given in degrees (°).

Pt.#	Gender	Age	Time in Active Treatment	Appliance Type	FMA
1	Female	13.46	14.70	Forsus	18.0
2	Male	13.13	19.83	Forsus	24.2
3	Male	11.44	29.40	Crossbow	29.2
4	Female	14.93	31.73	Forsus	36.9
5	Female	12.09	31.73	Crossbow	27.8
6	Male	12.58	22.63	Crossbow	26.4
7	Female	13.23	27.77	Crossbow	19.8
8	Female	11.35	22.17	Forsus	27.3
9	Female	13.94	18.70	Forsus	18.7
10	Male	14.20	18.90	Crossbow	19.6
11	Male	12.85	26.83	Forsus	17.5
12	Male	15.85	26.37	Forsus	25.0
13	Female	14.40	22.63	Forsus	30.1
14	Female	13.85	17.30	Forsus	27.5
15	Male	15.25	18.90	Forsus	17.5

Table Continues.....

Pt.#	Gender	Age	Time in Active Treatment	Appliance Type	FMA
16	Female	11.83	14.93	Forsus	26.8
17	Female	12.52	26.83	Crossbow	25.7
18	Female	12.31	21.47	Crossbow	23.2
19	Female	14.29	20.33	Forsus	23.4
20	Male	12.53	24.27	Crossbow	21.5
21	Female	14.92	18.20	Forsus	19.4
22	Female	13.49	26.83	Crossbow	13.3
23	Female	14.16	27.00	Crossbow	7.8
24	Male	11.77	18.90	Forsus	16.8
26	Female	11.74	36.40	Crossbow	25.3
27	Male	13.96	32.67	Crossbow	11.9
28	Female	15.26	19.37	Forsus	12.1
29	Male	13.87	25.43	Forsus	10.8
30	Male	15.17	20.07	Forsus	24.1
31	Male	14.92	30.33	Crossbow	17.6
32	Female	12.84	22.87	Crossbow	14.4
33	Female	12.39	19.83	Forsus	26.1
34	Male	13.37	19.83	Crossbow	21.2
35	Male	14.52	32.20	Forsus	11.9
37	Female	13.06	30.10	Forsus	19.7
38	Male	13.07	38.03	Crossbow	9.4
39	Female	14.26	17.27	Forsus	14.8
40	Female	13.27	19.60	Crossbow	17.4
41	Male	13.17	19.63	Crossbow	19.4
42	Female	15.58	27.30	Forsus	15.7
43	Female	14.50	24.97	Crossbow	12.4
45	Female	13.78	20.77	Forsus	25.9
46	Female	12.62	43.63	Crossbow	27.4

A.2 Method Reliability Data

Table A.2: Reliability data of the measured alveolar volume (mm^3) in order to determine the reliability of the method. Investigator 1 was the author of the study (KC), and investigator 2 was the co-investigator (GCM).

		Investigator 1			Investigator 2
Pt.#	Time Point	1st Measure	2nd Measure	3rd Measure	Measurement
1	1	2206.91	2178.35	2234.66	2111.33
2	1	2194.55	2167.55	2259.68	2196.43
3	2	1317.87	1288.54	1317.05	1172.45
4	2	1723.67	1961.65	1642.52	1862.38
5	2	2522.97	2725.93	2345.86	2665.41
6	2	1727.91	1592.66	1621.77	1656.91

Table A.3: Reliability data of the measured incisor inclination (°) in 3-dimensions to determine the reliability of the method. Investigator 1 was the author of the study (KC), and investigator 2 was the co-investigator (GCM). These patients correspond to the same participants and time points in Table A.2.

		Investigator 1			Investigator 2
Pt.#	Tooth Number	1st Measure	2nd Measure	3rd Measure	Measurement
1	#3.2	131.61	132.17	132.73	131.86
	#3.1	140.27	140.42	140.27	139.47
	#4.1	138.15	139.29	139.81	139.03
	#4.2	131.38	131.29	133.44	132.18
2	#3.2	108.27	108.92	108.23	108.72
	#3.1	114.95	115.60	116.03	114.82
	#4.1	122.18	122.33	122.80	122.33
	#4.2	115.41	114.96	114.20	114.11
3	#3.2	126.32	124.38	125.33	127.12
	#3.1	131.20	130.65	131.27	131.94
	#4.1	130.83	131.49	131.66	132.78
	#4.2	127.38	127.69	128.87	127.59
4	#3.2	114.10	114.97	123.34	123.75
	#3.1	121.86	120.17	127.99	129.19
	#4.1	121.47	121.93	130.06	130.80
	#4.2	116.73	116.26	125.78	126.26
5	#3.2	125.51	129.90	129.26	128.32
	#3.1	134.20	136.98	135.95	138.61
	#4.1	131.03	132.72	132.69	134.63
	#4.2	121.89	125.06	125.31	125.20
6	#3.2	111.61	108.87	106.25	107.90
	#3.1	112.94	110.23	107.40	111.35
	#4.1	116.16	113.64	112.14	112.90
	#4.2	111.04	108.80	106.23	109.98

A.3 Measured Data

Table A.4: A complete table of the raw measurements for all the studied variables. The units of measurement for the volume of the alveolar housing (V_{alv}) was mm^3, and degrees (°) for FMA and incisor inclination.

			V_{alv}		Incisor Inclination T_1				Incisor Inclination T_2			
Pt.#	Appliance	FMA	T_1	T_2	3.2	3.1	4.1	4.2	3.2	3.1	4.1	4.2
1	Forsus	18.0	2178.35	2132.26	121.59	130.50	130.31	123.08	135.99	128.94	129.86	138.69
2	Forsus	24.2	2167.55	1982.75	108.57	115.12	123.41	114.72	120.14	129.66	133.35	131.75
3	Crossbow	29.2	1390.95	1288.54	102.82	113.42	107.03	105.87	124.99	129.69	130.82	126.49
4	Forsus	36.9	1876.27	1961.65	120.31	126.45	127.48	127.22	113.81	118.83	120.56	115.81
5	Crossbow	27.8	1837.72	2725.93	126.72	132.23	131.21	127.27	124.71	135.11	131.31	121.69
6	Crossbow	26.4	1403.66	1592.66	118.42	123.49	123.66	120.45	108.50	109.60	113.00	108.09
7	Crossbow	19.8	1377.26	1605.05	137.90	136.42	131.42	135.90	149.04	147.33	147.69	152.79
8	Forsus	27.3	1368.21	1382.53	116.29	118.58	123.00	114.50	119.75	123.23	125.20	125.40
9	Forsus	18.7	1642.38	1860.37	142.13	144.54	145.40	141.91	140.46	142.36	144.32	145.83
10	Crossbow	19.6	2013.79	2239.77	124.00	133.35	131.76	126.68	127.17	132.50	133.57	129.44
11	Forsus	17.5	1166.12	1279.39	139.36	147.74	147.46	138.26	143.63	146.40	148.45	144.11
12	Forsus	25.0	1555.55	1267.86	125.58	127.68	128.60	126.20	135.23	139.31	138.84	134.79
13	Forsus	30.1	2490.38	2337.20	131.19	135.77	136.16	132.69	139.48	138.51	139.75	138.24
14	Forsus	27.5	3460.99	3056.73	131.61	135.70	135.64	130.80	140.19	145.44	145.50	143.15

Table Continues.....

			V_{alv}		Incisor Inclination T_1				Incisor Inclination T_2			
Pt.#	Appliance	FMA	T_1	T_2	3.2	3.1	4.1	4.2	3.2	3.1	4.1	4.2
15	Forsus	17.5	1531.45	1558.52	132.39	141.31	134.56	135.99	149.94	153.76	155.29	146.82
16	Forsus	26.8	1280.62	1449.49	125.02	118.24	122.38	116.33	138.06	145.18	144.02	139.35
17	Crossbow	25.7	1787.44	1908.13	145.90	148.08	148.63	146.15	153.45	155.02	155.39	151.73
18	Crossbow	23.2	1478.94	1958.05	148.02	154.17	155.14	148.20	156.11	161.36	160.56	155.60
19	Forsus	23.4	1412.33	1481.25	142.48	142.80	142.03	144.46	148.72	146.14	147.97	151.11
20	Crossbow	21.5	2203.60	2413.81	99.21	105.45	104.38	103.28	103.76	108.12	108.11	108.13
21	Forsus	19.4	2533.68	2579.84	110.07	111.32	114.06	107.97	127.86	129.71	133.22	132.76
22	Crossbow	13.3	1900.68	1759.29	130.76	130.55	131.01	129.51	138.97	139.35	138.58	138.13
23	Crossbow	7.8	1083.15	1147.05	128.23	127.43	129.22	126.09	134.80	133.35	133.85	133.66
24	Forsus	16.8	1213.87	1457.77	122.69	125.09	127.43	120.79	118.73	120.79	121.00	117.02
26	Crossbow	25.3	2541.06	2893.16	122.83	129.65	127.35	126.33	150.11	156.12	157.57	151.37
27	Crossbow	11.9	1829.01	1892.64	141.53	142.35	143.61	142.11	150.16	150.12	151.23	147.14
28	Forsus	12.1	1140.89	1178.43	140.44	147.40	149.35	140.46	148.15	149.38	151.58	147.72
29	Forsus	10.8	2734.20	2214.37	127.47	134.27	134.38	133.79	145.35	152.30	150.07	147.72
30	Forsus	24.1	4518.44	4600.27	109.44	115.78	116.87	108.00	128.28	131.83	130.75	126.91
31	Crossbow	17.6	2797.41	3030.67	135.26	140.53	140.62	136.85	139.77	142.83	146.84	138.76
32	Crossbow	14.4	1491.86	1966.19	140.34	148.24	149.17	143.18	149.71	153.56	153.76	151.67
33	Forsus	26.1	1238.54	1354.05	126.53	129.79	129.15	120.13	138.78	141.12	142.26	137.29

Table Continues.....

			V_{alv}		Incisor Inclination T_1				Incisor Inclination T_2			
Pt.#	Appliance	FMA	T_1	T_2	3.2	3.1	4.1	4.2	3.2	3.1	4.1	4.2
34	Crossbow	21.2	2331.27	2460.40	120.33	121.77	122.62	120.26	127.85	127.68	130.30	128.29
35	Forsus	11.9	1365.31	1225.78	138.36	142.68	140.25	139.42	150.98	159.11	158.64	150.49
37	Forsus	19.7	1608.82	1608.44	113.78	121.88	129.14	113.33	148.09	151.69	148.76	146.96
38	Crossbow	9.4	984.75	1089.74	132.55	141.31	139.92	133.05	126.32	131.19	133.33	130.23
39	Forsus	14.8	2263.29	2091.77	126.69	133.36	136.61	131.16	141.03	148.66	150.28	149.25
40	Crossbow	17.4	1552.13	1556.42	140.74	146.47	148.09	143.10	152.56	154.91	151.19	150.74
41	Crossbow	19.4	1445.94	1513.05	130.72	135.03	130.58	127.27	142.72	143.81	139.75	141.06
42	Forsus	15.7	2007.21	2118.86	134.73	135.00	138.31	137.60	150.25	152.88	157.05	153.62
43	Crossbow	12.4	1981.74	1828.00	146.96	150.58	149.01	147.82	153.09	156.34	156.21	153.53
45	Forsus	25.9	1792.36	1829.65	117.21	119.44	114.91	117.52	127.94	131.69	126.19	129.32
46	Crossbow	27.4	2326.26	2358.60	107.32	116.16	116.82	110.37	131.94	133.93	134.29	127.35

Appendix B

Hypothesis Testing

There were 3 explanatory variables: 1 nominal (appliance type), 2 continuous both (FMA and $\overline{\Delta IC}$ expressed in °), and 1 response variable, % volume change of the alveolar housing (refer to Equation (4.2)). Given that the initial volume of the bony housing varies between individuals, expressing volume changes as a proportion instead of absolute values were more clinically relevant. For example, a given absolute change in bony volume might be less significant in individuals with larger symphysis but more significant in those with smaller mandibles.

The significance level was set at $\alpha = 0.05$ for all statistical analyses performed except for the t-test on individual regression coefficients which was set at $\alpha = 0.10$.

B.1 Baseline Comparisons

B.1.1 Comparison of Pre-treatment Factors

In order to ensure that the groups, Forsus™ and Xbow®, were homogenous at T_1, a MANOVA omnibus test was used. Descriptives for the baseline data can be found in Table 4.1. The following hypothesis was tested:

H_0**:** Jointly, there was no difference in the means of age, FMA, $\overline{IC}_{T_1}$, and $V_{alv_{T_1}}$ between Forsus™and Xbrow® groups.

H_a**:** Jointly, there was at least one difference in the means of age, FMA, $\overline{IC}_{T_1}$, and $V_{alv_{T_1}}$ between Forsus™and Xbrow® groups.

Checking the assumptions for MANOVA, the independent sampling requirement was fulfilled as the sampling of one participants was not influenced by the selection of another. Visual inspection of the bivariate plot of all factors revealed approximately a linear relationship between pairs of all variables (Figure B.1). Using Mahalanobis distances, the data showed multivariate normality. However, the Box's test of equality of variance-covariance matrices revealed a $p < 0.05$ and thus this assumption was violated. MANOVA

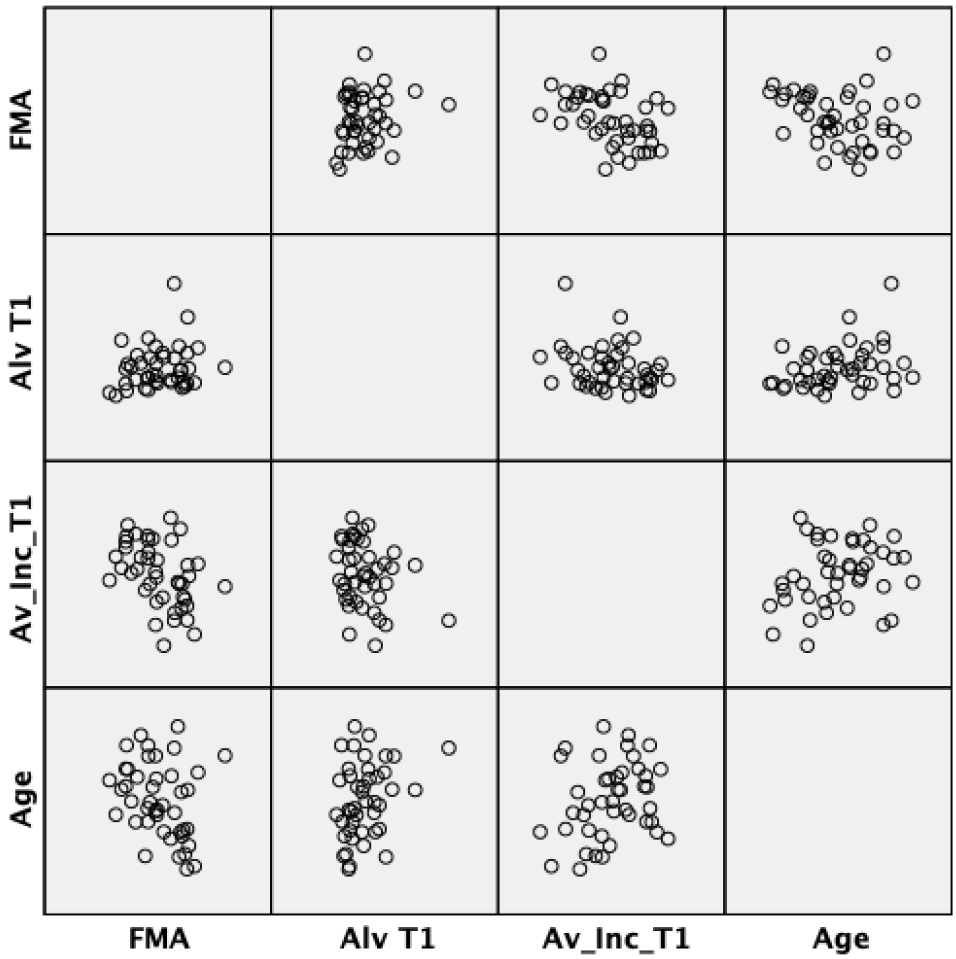

Figure B.1: A bivariate plot of all the baseline factors in order to verify the assumption that all pairs of variables are linearly related. "Av_Inc_T1" represents the average incisor inclination, and "Alv T1" is the alveolar volume at baseline. Visual inspection of the bivariate scatter plots reveals approximate linear relationships.

is robust to violations of both normality and equality of variance-covariance matrices if the sample size is large and equal. Because the sample sizes for both Forsus™ and Xbow® were approximately equal, hypothesis testing with MANOVA could proceed. The results of the MANOVA showed that there were no differences between the Forsus™ and Xbow® groups in all the pre-treatment factors combined, $F(4, 38) = 2.46, p = 0.062 > 0.05; Wilks' \Lambda = 0.794; partial\eta^2 = 0.206$. Therefore, there was no evidence against the null hypothesis.

B.2 Response in Incisor Inclination

For descriptive statistics of the mandibular incisor response, refer to Table 4.3. Box plots of ΔIC of each incisor type can be found in Figure B.2.

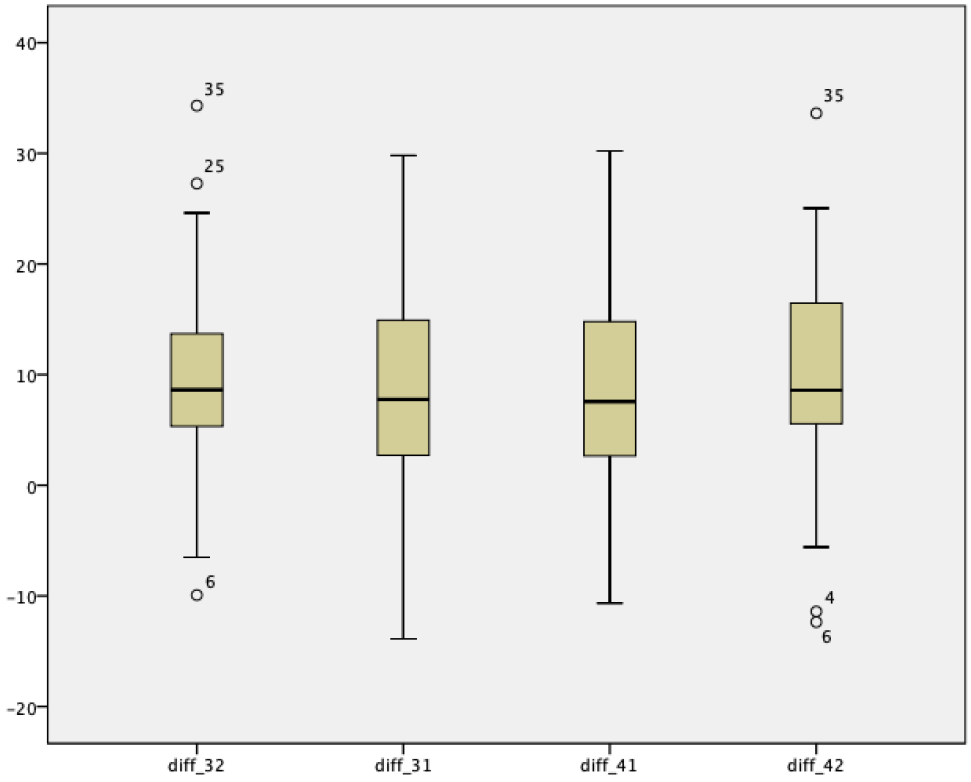

Figure B.2: Boxplots of the change in incisor inclination (proclination) from pre- to post-treatment. Central incisors 3.1 and 4.1 demonstrate an approximate normal distribution. Violations of normality were seen in teeth 3.2 and 4.2.

Response of Each Incisor Pre- to Post-treatment

Incisors 3.1 and 4.1 demonstrated approximate normality and the independent sampling assumption was also met. One sample t-tests were used to determine whether there were significant changes in inclination between T_1 and T_2. The results of the t-test can be found in Table B.1. A Wilcoxon Signed-Rank Test was used to determine whether proclination of the mandibular lateral incisors were significant. The distribution of the differences for both 3.2 and 4.2 were approximately symmetric (Figure B.3) which satisfied the assumption for this test. The results showed that the median change in inclination was significant for both lateral incisors (Section 4.3.2). Based on these results, the alternative hypothesis was accepted: $H_a : \Delta IC_{32} \& \Delta IC_{31} \& \Delta IC_{41} \& \Delta IC_{42} \neq 0$

Differences in ΔIC between Mandibular Incisors

An ANOVA was then used to determine whether the changes in incisor proclination between each of the incisors were different from each other. The following hypotheses were therefore tested:

H_0: ΔIC_{32} - ΔIC_{31} - ΔIC_{41} - $\Delta IC_{42} = 0$

Table B.1: T-test results for changes in incisor inclination from pre- to post-treatment. This test was used only on 3.1 and 4.1 as they demonstrated normality and the equal variances assumption had been met based on the rule of thumb. Test value = 0.

					95% Confidence Interval	
Tooth	t-stat	df	p-val	Mean Diff.(°)	Lower Bound (°)	Upper Bound(°)
ΔIC_{31}	5.70	42	<0.001	8.18	5.28	11.08
ΔIC_{41}	6.17	42	<0.001	8.42	5.67	11.18

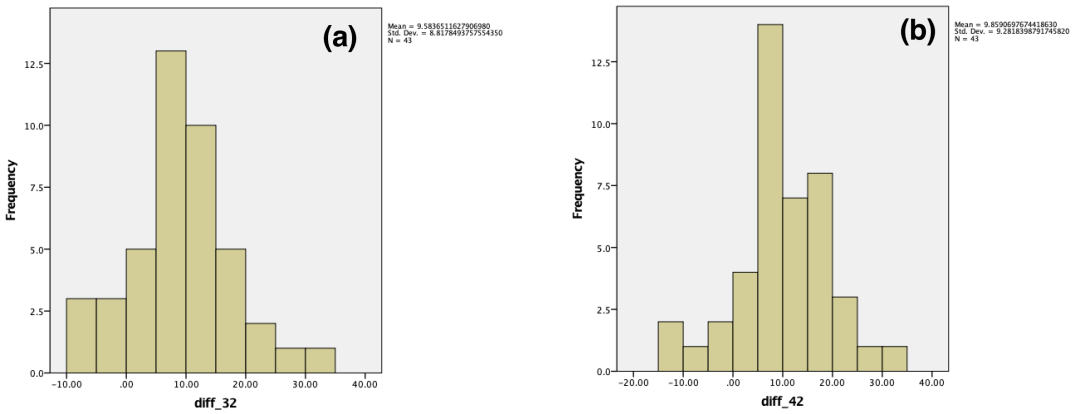

Figure B.3: Histogram of ΔIC_{32} and ΔIC_{42}. Both (a) and (b) show approximate symmetric distributions which satisfy the assumption for the Wilcoxon Signed-Rank Test.

Table B.2: The result of the ANOVA to determine whether there were any differences between the changes in incisor inclination between any of the mandibular incisors.

	F-Statistic	Degrees of Freedom	p-value
Incisor	0.360	3	0.782
Error		168	

H_a: $\Delta IC_{32} - \Delta IC_{31} - \Delta IC_{41} - \Delta IC_{42} \neq 0$

Although violations of normality were seen in ΔIC_{32} and ΔIC_{42} (Figure B.2), ANOVA are robust against departures from normality provided that the sample sizes are large (n>20) and approximately equal. Equal variances assumption was met using the rule of thumb which states that the the variances between each group can be considered equal if the standard deviations are no more than two times the smallest standard deviation (Table 4.3). The result of the ANOVA can be found in Table B.2. There was no evidence against the null hypothesis and therefore no difference in incisor proclination amongst any of the mandibular incisors.

Difference in $\overline{\Delta IC}$ between Forsus™ and Crossbow®

Because there was no difference found in incisor proclination amongst the mandibular incisors, the average change in incisor inclination between all the mandibular incisors was calculated for each participant and used in subsequent analyses. Descriptive statistics can also be found in Table 4.3, in the last row labelled "$\overline{\Delta IC_{32,31,41,42}}$". Box plots of the data can be found in Figure B.4, which demonstrates violations of normality. Because t-tests are sensitive to deviations in normality, a non-parametric Mann-Whitney U test was chosen. The hypotheses that were tested were the following:

H_0: $\text{median}(\Delta IC_{\text{Forsus}}) = \text{median}(\Delta IC_{\text{Xbow}})$

H_a: $\text{median}(\Delta IC_{\text{Forsus}}) \neq \text{median}(\Delta IC_{\text{Xbow}})$

There was no evidence against the null hypothesis ($U = 281, p = 0.214 > 0.05$), and thus no difference in incisor proclination between the two groups.

B.3 Alveolar Volume Response

Refer to Table B.3 for descriptive statistics of the alveolar housing response.. The mean percent alveolar change was $4.89\% \pm 12.80\%$. Figure B.5 is a visual representation of the data, and inspection reveals 5 outliers with one extreme outlier. As such, the data followed a non-normal right skewed distribution which violated the normality assumption of a one-sample t-test. The independent sampling assumption was not violated as the selection

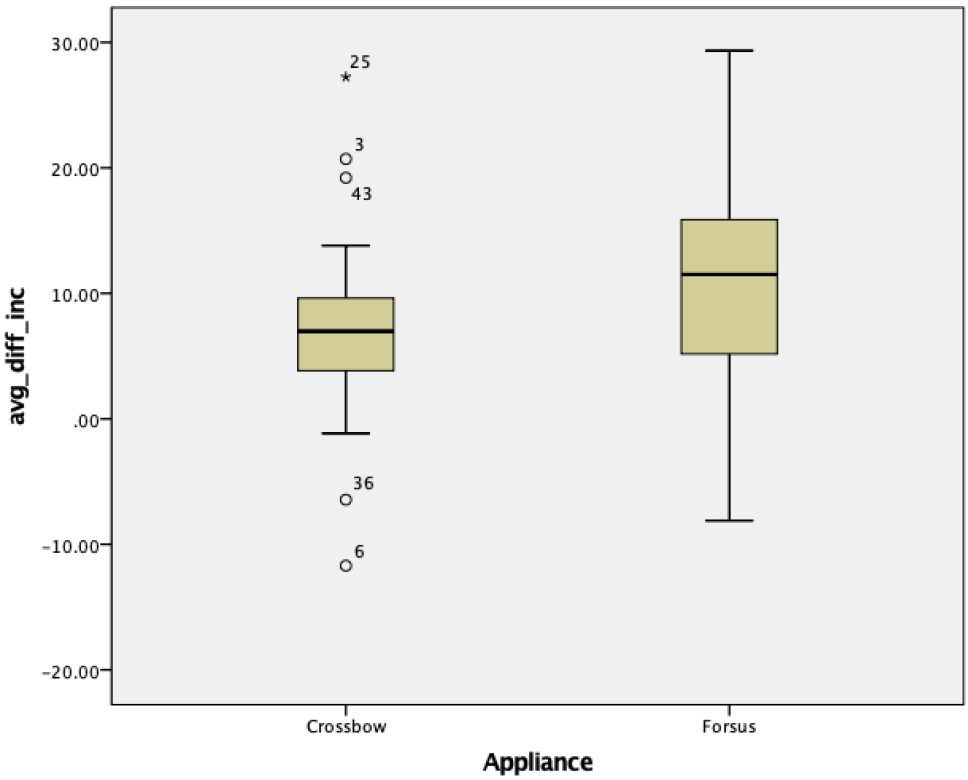

Figure B.4: Boxplots of the $\overline{\Delta IC}$ for Forsus™ and Xbow® groups.

Table B.3: Descriptive statistics of the alveolar response as expressed in volume (mm^3). Log transformed data was included in an attempt to use parametric hypothesis testing. Due to departures from normality, a non-parametric test was chosen instead.

Variable	Mean	Median	SD	N
Alveolar Volume T_1	1867.57	1787.44	677.70	43
Alveolar Volume T_2	1935.73	1860.37	663.94	43
$\Delta V_{alv}(T2 - T1)$	68.16	67.11	235.98	43
$\%\Delta V_{alv}$	4.89	4.55	12.80	43
$\ln V_a lv(T1)$	7.48	7.49	0.32	43
$\ln V_a lv(T2)$	7.52	7.53	0.31	43

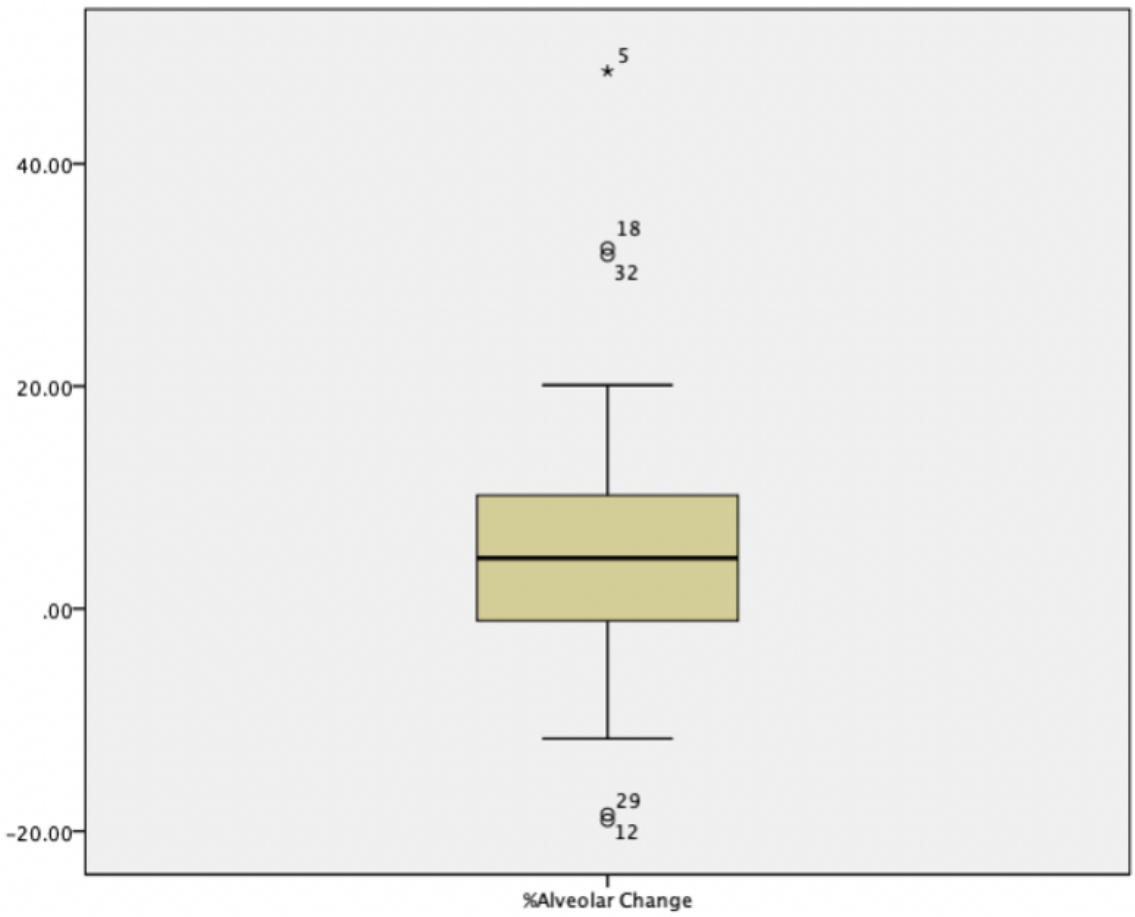

Figure B.5: Box plot of % alveolar volume change ($\%\Delta V_{alv}$). 5 outliers with one extreme outlier (patient 5) identified.

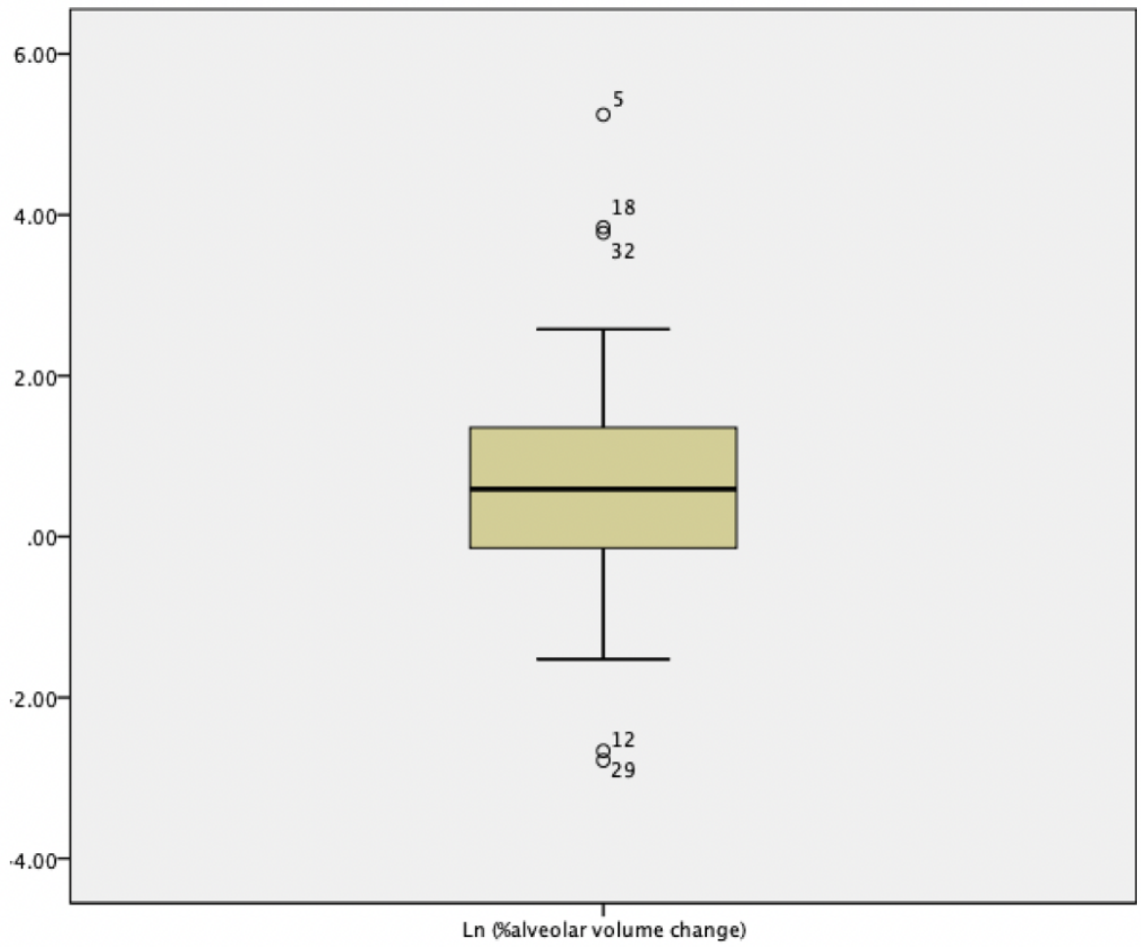

Figure B.6: Box plot of logarithm transformed % alveolar volume change ($\ln \%\Delta V_{alv}$). Note the y-axis scale is smaller compared to Figure B.5 as it is a logarithmic.

of one patient was not dependent on the other. Visual inspection of the log transformed data (Figure B.6) still revealed right skewness and violation of normality.

In order to determine whether the extreme outlier can be ignored, hypothesis testing with and without the extreme outlier was performed. The result of the t-test was t(42)=2.503, $p = 0.016$ with a mean difference of 4.89% [0.95%, 8.83%]. Removing the extreme outlier resulted in $t(41) = 2.272$, $p = 0.028$ with a mean difference of 3.85% [0.43%, 7.28%] (Table B.4). Because the p-value and confidence intervals changed, parametric testing was not suitable and a non-parametric method such as the Wilcoxon Signed-Rank Test was used for this paired dataset. The following hypotheses were tested:

$\mathbf{H_0}$ There was no median percent alveolar volume change.

$\mathbf{H_a}$ There was a change in median percent alveolar volume change.

Figure B.7 demonstrates the distribution of the volume differences between pre- and post-treatment. It is approximately symmetric which, in addition to independent sampling,

Table B.4: Results of the t-test with outliers included and excluded. The 95% confidence interval (C.I.) is presented in square brackets.

	t-statistic	df	*p*-value (2-tailed)	Mean Difference (%)	95% C.I.
All sample data	2.503	42	0.016	4.89	[0.95,8.83]
Outlier Excluded	2.272	41	0.028	3.85	[0.43, 7.28]

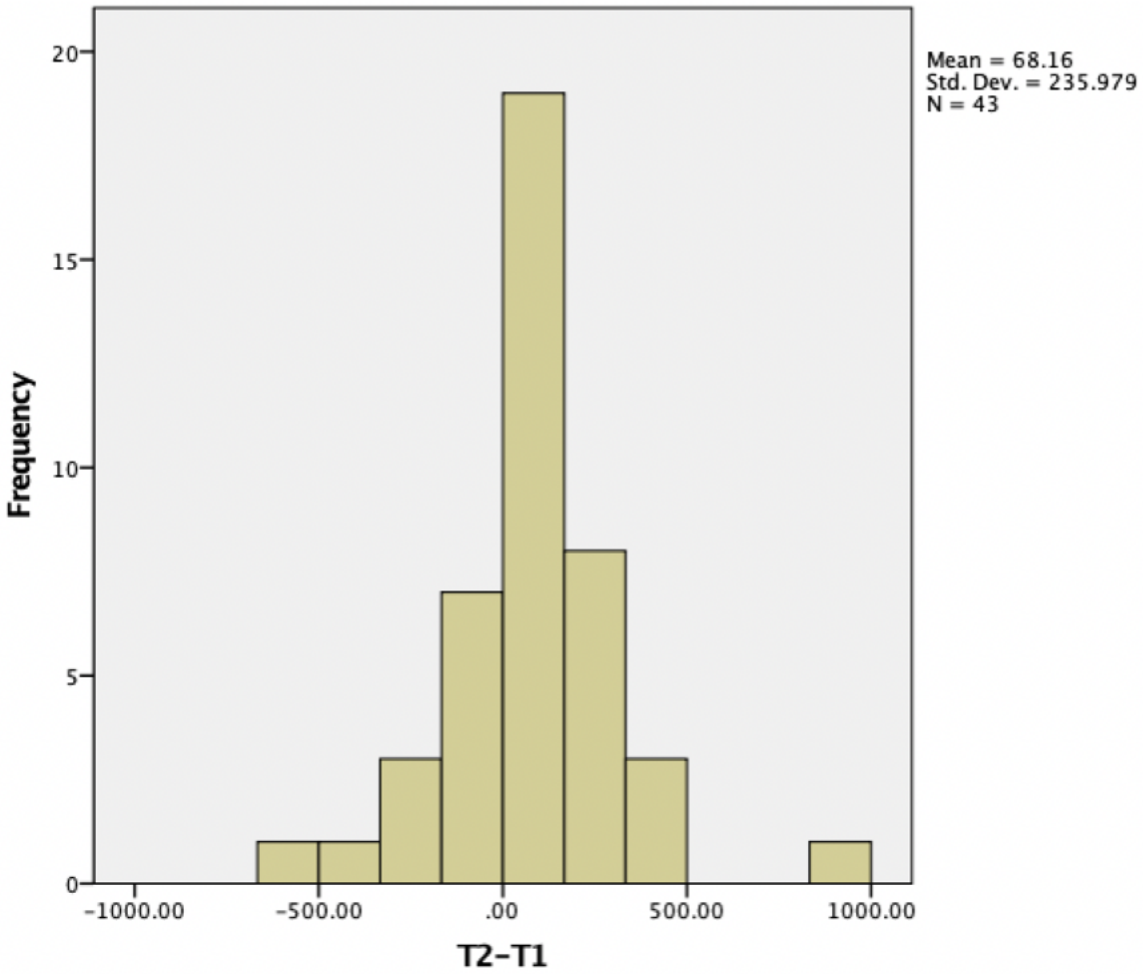

Figure B.7: A distribution of the difference in alveolar volume measured between pre- and post-treatment. Note the approximate symmetric distribution of the resulting figure.

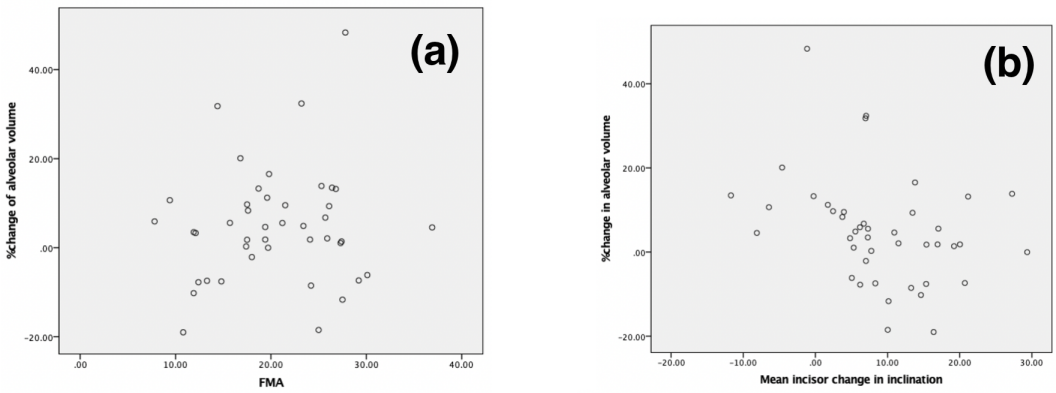

Figure B.8: Scatterplots to check the linearity assumption required by multiple linear regression analysis. (a) is a plot of the FMA values against $\%\Delta V_{alv}$ and a positive linear relationship was assumed. (b) is a plot of the $\overline{\Delta IC}$ values against $\%\Delta V_{alv}$. A negative linear relationship was assumed.

satisfies the assumptions of the Wilcoxon Signed-Rank Test. Of the 43 patients included in this study, 31 had increased alveolar volume and 12 had decreased volume. There was moderate evidence that the median alveolar volume increased by 67.11 mm^3 ($z = -2.11, p = 0.035$) with median pre-treatment median volume of 1787.44 mm^3 and post-treatment median volume 1860.37 mm^3 (Table B.3). It was more useful to express the result in percentage, and there was a 4.55% increase in median alveolar volume with a similar mean increase of 4.89%.

B.4 Prognostic Factors for Alveolar Response

Descriptives statistics of the following data are presented in Table 4.2. A multiple regression analysis was chosen because both the response and two of the explanatory variable are continuous. The following model assumptions were verified to determine feasibility of multiple regression analysis. The independent sampling assumption was fulfilled. Figure B.8 are scatter plots of the explanatory variables against $\%\Delta V_{alv}$, and both plots approximated linearity. Based on the residual plot, homoscedasticity assumption was not violated. Finally, the P-P plot of the residuals also revealed approximate normal distribution of each of the subpopulations (Figure B.9). The null hypothesis of the regression analysis was that all coefficients of the multiple regression equation was simultaneously zero. In other words, the $\%\Delta V_{alv}$ was not a function of appliance type, FMA, $\overline{\Delta IC}$, and all of their interactions. The alternate hypothesis was that there was at least one factor that was predictive of $\%\Delta V_{alv}$.

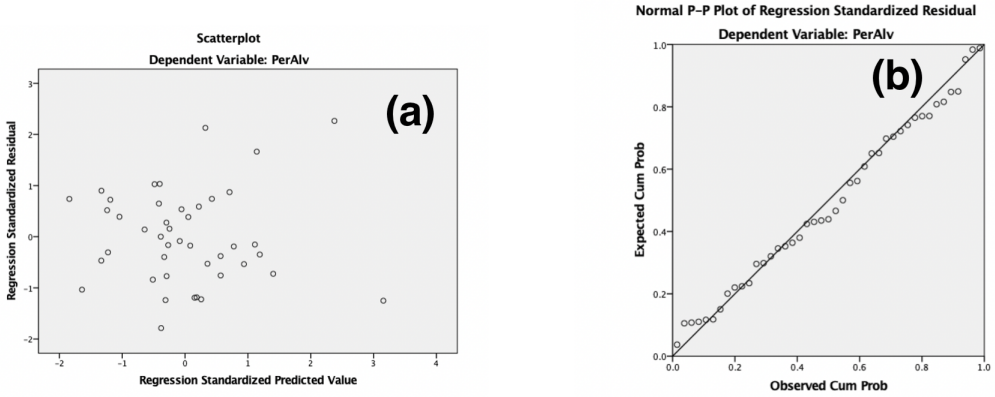

Figure B.9: Visual checking of the homoscedasticity and normality assumptions. (a) is a plot of the predicted value against the residual. Homoscedasticity was assumed given no clear visual pattern noted. (b) is a P-P plot of the residuals. Distribution normality of each of the subpopulations was assumed given that the points approximated linearity.

B.4.1 Determining a Linear Regression Model

The results of the regression model considering all the explanatory variables and their interactions can be found in Tables B.5,B.6. There was moderate evidence against the null for the overall test, and thus there was at least one explanatory variable which could be used to predict the average % volume change, F(7,35)=2.398, p=0.04. The variables that had moderate evidence against the null was $\overline{\Delta \text{IC}}(p = 0.096)$ and the interaction between appliance type and FMA ($p = 0.069$). All other factors and interactions were considered not significant. In the context of the research questions however, this model was considered complex. Therefore a "by-hand" sequential elimination method was used to determine the most appropriate model, starting with the most complex non-significant interaction, appliance type x FMA x $\overline{\Delta \text{IC}}$. The p-value for the overall test did not change significantly $F(6, 36) = 2.426, p = 0.045$ (Tables B.7,B.8). The next most insignificant interaction was appliance type x $\overline{\Delta \text{IC}}(p = 0.51)$ however given that this interaction was potentially interesting, the interaction between FMA x $\overline{\Delta \text{IC}}(p = 0.47)$ was removed instead which resulted in another model (Tables B.9,B.10). The problem with this model became apparent as according to the overall ANOVA, there was moderate evidence that at least one of the coefficients $\neq 0, F(5, 37) = 2.837, p = 0.029$. However, none of the coefficients were significant in the individual tests (p>0.10). This may have been due to issues with multicollinearity. A tolerance<0.1 or VIF>10 may lead to problems with multicollinearity. Both appliance type and appliance type X FMA had potential issues with multicollinearity. The interaction between appliance type x $\overline{\Delta \text{IC}}$ was removed as it had the highest p value.

Table B.5: The overall ANOVA of the first MLR model. All factors and interactions were included. The response variable was $\%\Delta V_{alv}$. The explanatory variables were appliance type, FMA, and $\overline{\Delta IC}$. Interactions between explanatory variables included: appliance type x FMA, appliance type x $\overline{\Delta IC}$, FMA x $\overline{\Delta IC}$, and appliance type x $\overline{\Delta IC}$ x FMA. $R^2 = 0.324$

Model	Sum of Squares	D. of Freedom	F-statistic	p-value
Regression	2231.94	7	2.398	0.041
Residual	4654.03	35		
Total	6885.96	42		

Table B.6: Coefficient results of the first MLR model. All factors and interactions were included. The response variable was $\%\Delta V_{alv}$. The explanatory variables were appliance type, FMA, and $\overline{\Delta IC}$. Interactions between explanatory variables included: appliance type x FMA, appliance type x $\overline{\Delta IC}$, FMA x $\overline{\Delta IC}$, and appliance type x $\overline{\Delta IC}$ x FMA. B is the coefficient of each variable inside the multiple linear regression equation.

				95% Confidence Interval	
Variables	B	Std. Error	p-value	Lower Bound	Upper Bound
(Constant)	12.935	11.803	0.281	-11.026	36.896
Appliance Type	-17.572	15.840	0.275	-49.729	14.585
FMA	-0.352	0.466	0.455	-1.299	0.594
$\overline{\Delta IC}$	-1.588	0.928	0.096	-3.473	0.296
Appliance x FMA	1.288	0.687	0.069	-0.107	2.683
Appliance x $\overline{\Delta IC}$	1.882	1.645	0.260	-1.458	5.222
FMA x $\overline{\Delta IC}$	0.055	0.039	0.168	-0.024	0.135
App. x FMA x $\overline{\Delta IC}$	-0.092	0.067	0.180	-0.228	0.044

The final model resulted in a convincing evidence against the null hypothesis $F(4, 38) = 3.531, p = 0.015$ which means that there was at least one explanatory variable that was predictive of the $\%\Delta V_{alv}$ (Table B.11). Refer to Equation (4.3) for the equation of the final model based on Table 4.4. This model could explain 27% of the variance seen in $\%\Delta V_{alv}$ ($R^2 = 0.271$).

B.4.2 Simplified MLR Model

It is beneficial for the practising clinician to determine the threshold at which lower incisors can procline until loss of alveolar volume is experienced. In the final model (Table 4.4), the only factor that was significant was $\overline{\Delta IC}$. The regression model was simplified to clarify the relationship between incisor proclination and the change in alveolar volume (Equation (4.4)). Approximately 10% of the variance can be explained by this model which confirmed that the final model selected was more suitable, $R^2 = 0.271$. Figure 4.1 is a scatter plot with

Table B.7: The overall ANOVA of the second MLR model. The response variable was $\%\Delta V_{alv}$. The 3-way interaction, appliance type x $\overline{\Delta IC}$ x FMA, was removed. $R^2 = 0.288$

Model	Sum of Squares	D. of Freedom	F-statistic	p-value
Regression	1982.63	6	2.426	0.045
Residual	4903.33	36		
Total	6885.96	42		

Table B.8: Coefficient results of the second MLR model. All factors and interactions were included. The response variable was $\%\Delta V_{alv}$. The 3-way interaction, appliance type x $\overline{\Delta IC}$ x FMA, was removed. B is the coefficient of each variable inside the multiple linear regression equation.

				95% Confidence Interval	
Variables	B	Std. Error	p-value	Lower Bound	Upper Bound
(Constant)	7.799	11.326	0.496	-15.171	30.768
Appliance Type	-5.395	13.266	0.687	-32.3	21.51
FMA	-0.148	0.447	0.742	-1.055	0.758
$\overline{\Delta IC}$	-0.881	0.781	0.266	-2.464	0.702
Appliance x FMA	0.787	0.588	0.189	-0.406	1.98
Appliance x $\overline{\Delta IC}$	-0.291	0.441	0.514	-1.184	0.603
FMA x $\overline{\Delta IC}$	0.024	0.032	0.465	-0.042	0.089

Table B.9: The overall ANOVA of the third MLR model. The response variable was $\%\Delta V_{alv}$. The 3-way interaction, appliance type x $\overline{\Delta IC}$ x FMA, was removed along with FMA x $\overline{\Delta IC}$. $R^2 = 0.277$

Model	Sum of Squares	D. of Freedom	F-statistic	p-value
Regression	1908.46	5	2.837	0.029
Residual	4977.5	37		
Total	6885.96	42		

Table B.10: Coefficient results of the third MLR model. All factors and interactions were included. The response variable was $\%\Delta V_{alv}$. The 3-way interaction, appliance type x $\overline{\Delta IC}$ x FMA, was removed along with FMA x $\overline{\Delta IC}$. B is the coefficient of each variable inside the multiple linear regression equation.

				95% Confidence Interval	
Variables	B	Std. Error	p-value	Lower Bound	Upper Bound
(Constant)	3.935	9.981	0.696	-16.288	24.157
Appliance Type	-4.315	13.104	0.744	-30.867	22.236
FMA	0.005	0.393	0.990	-0.792	0.802
$\overline{\Delta IC}$	-0.349	0.297	0.247	-0.950	0.252
Appliance x FMA	0.751	0.583	0.205	-0.430	1.932
Appliance x $\overline{\Delta IC}$	-0.243	0.433	0.578	-1.121	0.635

Table B.11: The overall ANOVA of the final MLR model. The response variable was $\%\Delta V_{alv}$. The 3-way interaction, appliance type x $\overline{\Delta IC}$ x FMA, was removed along with FMA x $\overline{\Delta IC}$ and appliance type x $\overline{\Delta IC}$. $R^2 = 0.271$

Model	Sum of Squares	D. of Freedom	F-statistic	p-value
Regression	1866.01	4	3.531	0.015
Residual	5019.95	38		
Total	6885.96	42		

the regression line and confidence bands drawn. The estimated mean and 95% confidence intervals were calculated for each $\overline{\Delta IC}$. At $\overline{\Delta IC} = 10.93°$, the mean volume of the alveolus increased by 3.96%[0.1%, 7.82%]. At $\overline{\Delta IC}$=11.51°, the estimated mean was 3.68% with a 95% confidence interval of [-0.24%, 7.6%]. In conclusion, as long as the average lower incisors do not procline more than 11 degrees, there will be no loss of alveolar volume.